学位申請論文

Translational Diffusion of Photoreaction Intermediate Radicals in Organic, Aqueous, and Micellar Solutions

（光反応中間体ラジカルの有機溶液，
水溶液，及びミセル溶液中での並進拡散）

京都大学 大学院
理学研究科　化学専攻

岡本　晃一

Translational Diffusion of PhotoReaction Intermediate Radicals in Organic, Aqueous, and Micellar Solutions

Doctoral Thesis

Koichi Okamoto

Division of Chemical Physics,
Department of Chemistry,
Graduate School of Science,
Kyoto University

December 1997, Kyoto

Contents

Chapter 1

INTRODUCTION

A translational diffusion process in solution is one of fundamental and important processes in chemistry and physics and has attracted many investigators for a long time. Therefore, the diffusion constants (D) have been measured by many methods (capirally method, NMR spin echo, dynamic light scattering, Tayler dispersion method, etc.). [1-3] The diffusion is the flow of substance to achieve the equilibrium condition from a macroscopic point of view. According to the Fick's low, the amount of the flowing matter is proportional to the gradient of the concentration (strictly, of chemical potential), and this proportional constant is the diffusion constants (D). [4] Such the flow of the substance are described by the hyrododynamic theory by using the macroscopic parameter of solvents (melting point, boiling point, density, dielectric constant, or viscosity, etc.). [5] On the other hand, the diffusion is also described as the movement of molecules by the random force from surrounding molecules from a microscopic point of view. Such the behavior is expressed by the statistical theory by using the microscopic parameter (molecular structure, location, or intermolecular interaction, etc.,). [6] On the basis of the statistical theory, diffusion constant is often obtained by the molecular dynamics (MD) simulation. [1-2, 6] However, obtaining D of the solute molecules in solution by the simulation are generally difficult and obtained values of D are hardly reproduce the experimental one.

In many case, D are treated by the hydrodynamic theory because it is simple and convenient. Simply, according to the hydrodynamic theory, D is given by the Stokes-Einstein (SE) formula with the radius of the solute molecule (r), the viscosity of the solvent (η), and the temperature (T). [1-3, 5] However, in many cases, the calculated D by the SE equation cannot reproduce the

experimentally observed D. The discrepancy may come from several factors. For example, the SE equation is based on some assumptions such that the solvent is treated as a continuous fluid, the form of the solute molecule is spherical, and solute-solvent and/or solute-solute interactions are disregarded. Perrin proposed a method for correcting the deviation from the spherical shape.[7] Spernol and Wiltz modified the SE equation in terms of a molecular interaction semiempirically.[8] Many empirical equations have been proposed so far.[9-12] By using these modified equations, the calculated D, in many case, can reproduce the experimental D.

An interesting case will arise, when there is a strong intermolecular interaction among the molecules. In such a case, these calculated D no longer agrees with the experimental D. For example, ions [13] or ion radicals [14] have strong interactions with solvents by the Coulombic potentials and this electrostatic interaction influences the diffusion process. This effect should be taken into account in the diffusion theories. For example, Zwanzig,[15] Hubbord and Onsager,[16] and Bagchi[17] have proposed dielectric friction models. The influence of the solute-solvent interaction through the hydrogen bonding was reported by Chan and Chan [18a], and Tominaga et al. [18b] recently. The hydrogen bonding between the -OH or $-NH_2$ group of a solute molecule and protic solvents makes the diffusion process very slow. Naturally, this effect was not observed in non-polar solvents. As shown from these examples, it is apparent that D is very sensitive to the environment around the solute molecule.

In this respect, it is very interesting and important to examine the diffusion process of the intermediate radicals from the following view points. First, the diffusion processes of radicals are essential for understanding the reaction mechanisms because most of chemical reactions are controlled by the diffusion processes of intermediate radicals. [19] Therefore, we have to know the diffusion of the intermediate radicals for understanding the rate constant, yield, and activation energy, etc., of the chemical reaction. Second, radical diffusion also influences the chemically induced dynamic electron (nuclear) polarization (CIDEP, CIDNP) and magnetic field effect on the reactions. [20] For example, mutual diffusion of radicals in a radical pair governs the electron spin dynamics through the electron-electron interaction and, then, the spin dynamics control the recombination probability of the radicals as well as the magnitude of the electron or nuclear spin

polarization.[20] Third, it is important to know the relationship between the intermolecular interaction and the molecular dynamics in solution. Since radicals have unpaired electrons and the chemical reactivities of radicals are generally high, we expect that the molecular interaction of radicals is quite different from those of stable molecules and ionic species. Fourth, it is interesting to study the microscopic structure or microscopic aggregation around chemically active molecules. The solvation and aggregation in solution are important processes especially, in aqueous solutions. Since D is very sensitive to the environment around the solute molecule, information of the solvation structure and the existence of microscopic aggregation, etc. of radicals may be extracted from the studies of the diffusion process.

However, only a few attempts have so far been made to measure D of transient radicals mainly because of the experimental difficulties. Most of the traditional methods require relatively long times for measurements. Naturally such methods cannot be applied to transient radicals that appear during chemical reaction for just short periods. Usually concentrations of the radicals are not very high unless very strong light intensity is used to produce radicals. Even if such a high radical concentration can be established, it will induce undesirable side reactions and will not be suitable for the study on the diffusion. Therefore, D of radicals are often assumed to be similar to those of the non-radical molecules with similar molecule volumes.[21] Such an assumption seems to be reasonable because D is governed by only three parameters, r, η, and T, from the SE relation. However, when there is a strong intermolecular interaction among the molecules, D no longer can be treated only by the hydrodynamic models. Then, there is no a priori reason why D of the radicals should be similar to that of the non-radical molecules.

In spite of these difficulties, there have been several reports on the measurement of D of the transient species. For example, Burkhart et al. have measured D of the some alkyl radicals using the photochemical space intermittency (PCSI) method,[22] which was developed by Noyes.[23] They have shown that alkyl radicals diffuse more slowly compared with the parent molecules even though the molecular sizes are similar.[22] However, probably because of the difficulties in the procedures and relatively large uncertainties,[24] the application of this method has been limited. Nickel and co-workers have developed a method for measuring D of transient species by modifying

the PCSI method with an interference pattern between two laser beams. [25] They have detected delayed florescence and succeeded in determining D of several aromatic molecules in the triplet states with high accuracy. Although, potentially this method could be applied to photochemical reaction system, the sample is limited to a molecule that shows luminescence. More recently, Levin et al. suggested slow diffusion of a benzophenone ketyl radical created by the photoinduced hydrogen abstraction reaction in glycerin on the basis of the magnetic field effect on the disappearing rate of the radical. [26] However, this method is not a direct detection of the diffusive motion in solution.

The laser induced transient grating (TG) method is another method to measure D of photochromic molecules. In the TG experiment, a sinusoidal pattern is created by the interference of two excitation beams. If the sample contains photochemically active molecules, these molecules are converted to other species in the bright region but not in the dark region. This site-selective excitation induces a spatially modulated distribution of the chemical species and it causes a spatially modulated refractive index and/or absorbance. This modulation (grating) diffracts another probe beam entering in this region. The signal decays as the modulation smears out by the diffusion. Therefore, the decay of the TG signal reflects the diffusion process of the probe molecules. Since this method has the advantage that it detects the diffusion in a short distance (~μm), the measurement time is dramatically reduced. Also because of the high sensitivity of this method, the concentration of the probe molecules can be low enough not to perturb the solution dynamics. On the basis of these advantages, the TG method has been applied to measure the D of dye molecules not only in organic solutions [27] but also in polymer solutions, [28] polymer glasses, [29] a gel, [30] and liquid crystals. [31] The diffusion processes in such mediums are too slow to measure D by the traditional methods.

In this thesis, I describe the measurements of D of transient radicals in solution. In chapter 2, the theory and the experimental set up for the TG method are described. [32] In chapter 3, measurements of D of the transient radicals created by the photoinduced hydrogen abstraction reactions are discussed.[33] Anomalously slow diffusion processes of such the radicals were found. [33] In chapter 4, the solvent viscosity, [34] solute size, [35] and temperature [36] dependences of

radical's D were investigated to know the factors which control the diffusion process. In chapter 5, diffusion process of the benzyl radical created by the photodissociation is compared with those of the hydrogen abstracted radicals.[37] In chapter 6, D of anion radicals are compared with D of the electrically neutral radicals to know the charge effect.[38] The radical diffusion in the aqueous solution[39] and the micellar solution[40] are shown in chapter 7 and 8, respectively.

References to Chapter 1

1. E. L. Cussler, *Diffusion* (Cambridge University, Cambridge, 1984).

2. H. J. V Tyrrell, and K. R. Harris, *Diffusion in Liquid* (Butterworths, London, 1984).

3. *Landolt-Bornstein Tabellen* (Springer, Berlin, 1961), 6 Aufl., Bd. II.

4. A. Fick, Prog. Annln, 94, 59 (1855).

5. V. G. Levich, *Physicochemical Hydrodynamics* (Prentice-Hall, Canada, 1982).

6. D. A. McQuarrie, *Statistical Mechanics* (Indiana University, New York, 1976).

7. F. Perrin, J. Phys. Radium., 7, 1 (1936).

8. A. Spernol, K. Wirtz, Naturforsch., 8a, 352 *ibid* 522 (1953).

9. E. G. Scheibel, Indu. Eng. Chem., 46, 2007 (1954).

10. C. R. Wilke, P. C. Chang, Am. Inst. Chem. Eng. J., 1, 264 (1955).

11. C. J. King, L. Hsueh, K. W. Mao, J. Chem. Eng, Data., 10, 348 (1965).

12. (a) H. T. Davis, T. Tominaga, D. F. Evans, AIChE J., 26, 313 (1980). (b) D. F. Evans,H. T. Davis, T. Tominaga, J. Chem. Phys., 74, 1298 (1981). (c) S. H. Chen, H. T. Davis, D. F. Evans, J. Chem. Phys., 77, 2540 (1982).

13. (a) D. F. Evans, C. Chen, B. C. Lamartine, J. Am. Chem. Soc., 99, 6492 (1977). (b) D. F. Evans, T. Tominaga, C. Chen, J. Solution Chem., 8, 461 (1978).

14. (a) S. S. Sam, G. R. Freeman, J. Chem. Phys., 70, 1538 (1979). (b) S. K. Lim, M. E. Burba, A. C. Albrecht, J. Phys. Chem., 98, 9665 (1994).

15. R. Zwanzig, J. Chem. Phys., 38 (1963). *ibid.* 52, 3625 (1970).

16. (a) J. B. Hubbard, L. Onsager, J. Chem. Phys., 67, 4850 (1977). (b) J. B. Hubbard, J. Chem. Phys., 68, 1649 (1978).

17. R. Biswas, S. Roy, B. Bagchi, Phys. Rev. Lett., 75, 1098 (1995).

18. (a) M. L. Chan and T. C. Chan, J. Phys. Chem., 99, 5765 (1995); (b) T. Tominaga, S. Tenma, and H. Watanabe, J. Chem. Soc. Faraday Trans., 92, 1863 (1996).

19. (a) H-H. Schuh and H. Fischer, Helv. Chim. Acta, 61, 2130 (1978).; Int. J. Chem. Kint., 8, 341 (1976).; (b) M. Lehni, H. Schuh, and H. Fischer, *ibid.*,11, 705 (1979).; (c) M. Sitarski, *ibid.*, 13, 125 (1981).; (d) M. Lehni and H. Fischer, *ibid.*, 15, 733 (1983).

20. (a) F. J. Adrian, J. Chem. Phys., 54, 3918 (1971).; (b) J. B. Pedersen, and J.H. Freed, *ibid.*, 58, 2746 (1973).; (c) H.J. Werner, Z. Schulten, and K. Schulten, *ibid.*, 67, 646 (1977).; (d) R. Kaptein, J. Am. Chem. Soc., 94, 6251 (1972).

21. (a) L. L. Jones and R. N. Schwartz, Mol. Phys. 43, 527 (1981).; (b) J. P. Hornak, J. K. Moscicki, D. J. Schneider, and J. H. Freed, J. Chem. Phys., 84, 3387 (1986).; (c) O. E. Yakimchenko, E. V. Gal'tseva, and Ya. S. Lebedev, Soc. J. Chem. Phys., 4, 2596 (1989).

22. (a) R. D. Burkhart, J. Phys. Chem., 73, 2703 (1969).; (b) R. D. Burkhart, R. F. Boynton, and J. C. Merrill, J. Am. Chem. Soc., 93, 5013 (1971).; (c) R. D. Burkhart, and R. J. Wong, ibid., 95, 7203 (1973).

23. (a) R.M. Noyes, J. Am. Chem. Soc., 81, 566, (1959).; (b) S.A. Levison, R.M. Noyes, J. Am. Chem. Soc., 86, 4525, (1964)

24. R.D. Burkhart, R.J. Wong, J. Am. Chem. Soc., 95, 7203, (1973).

25. (a) B. Nickel and H. Maxdorf, Chem. Phys. Lett. 9, 555 (1971), (b) E. G. Meyer and B. Nickel, *Lasers in Physical Chemistry and Biophysics*, editd by J. Joussot-Dubien (Elsevier, Amsterdam, 1975).; (c) Z. Naturforsh, Teil A, 35, 503 (1980).

26. P.P. Levin, I.V. Khudyakov, and V.A. Kuzumin, J, Phys, Chem., 93, 208 (1989).

27. M. Terazima, K.Okamoto, and N. Hirota, J. Phys. Chem., 97, 5188 (1993).

28. (a) J. L. Xia, S. S. Gong, C. H. Wang, J. Phys. Chem., 91, 5805, (1987); (b) J. A. Lee, T. P. Lodge, J. Phys. Chem., 91, 5546, (1987); (c) J. L. Xia, C. H. Wang, J. Chem. Phys., 88, 5211, (1988) *ibid* 92, 2603, (1990); (d) T. P. Loge, J. A. Lee, T. S. Frick, J. Polym. Sci., 28B, 2607, (1990); (e) C. H. Wang, J. L. Xia, J. Phys. Chem., 96, 190, (1992)

29. (a) S.S. Gong, D. Christensen, J. Zhang, C.H. Wang, J. Phys. Chem.,91, 4505, (1987); (b) J. Zang, B.K. Yu, C.H. Wang, J. Phys. Chem, 90, 1299, (1986)

30. J. H. Wesson, H. Takezoe, H. Yu, S.P. Chan, J. Appl. Phys, 53, 6513, (1982)

31. (a) H. Takezoe, S. Ichikawa, A. Fukuda, E. kuze, Jpn. J. Appl. Phys., 23, L78. 3594,(1987).; (b) M. Hara, H. Takezoe, A. Fukuda, Jpn. J. Appl. Phys. 23, 1420, (1984) *ibid* 25, 1756, (1986).

32. M. Terazima, N. Hirota, J. Chem. Phys., 95, 6490 (1991).

33. (a) M. Terazima, and N. Hirota, J. Chem. Phys., 98, 6257 (1993).; (b) M. Terazima, K.Okamoto, and N. Hirota, Laser Chem., 13, 169 (1994).

34. (a) M. Terazima, K.Okamoto, and N. Hirota, J. Phys. Chem., 97, 13387 (1993).; (b) K.Okamoto, N. Hirota, and M. Terazima, J. Phys. Chem. A, 101, 5380 (1997).

35. (a) M. Terazima, K.Okamoto, and N. Hirota, J. Chem. Phys., 102, 2506 (1995).; (b) M. Terazima, K. Okamoto, and N. Hirota, J. Mol. Liq., 65/66, 401 (1995).

36. K. Okamoto, M. Terazima, and N. Hirota, J. Chem. Phys., 103, 10445 (1995).

37. K. Okamoto, N. Hirota, and M. Terazima, J. Phys. Chem. A, 101, 5269 (1997).

38. K. Okamoto, N. Hirota, and M. Terazima, J. Chem. Soc. Faraday Trans., in press

39. K. Okamoto, N. Hirota, and M. Terazima, submitted for publication

40. K. Okamoto, N. Hirota, and M. Terazima, submitted for publication

Chapter 2

METHOD

2.1 Principle of the Transient Grating Method.

The transient grating (TG) method is one of third ordered nonlinear optical spectroscopy.[1-2] The fourth electromagnetic wave (TG signal) is created by the mixing from the three electromagnetic waves (two excitation beams and a probe beam). Such a nonlinear effect of the TG method is interpreted by the diffraction of the probe beam from grating created by the two excitation beams.[3] First, a sinusoidal bright-dark pattern in the sample solution is created by crossing two coherent beams (optical grating). Solute molecules in the cell were excited by the interference pattern. The excited molecules release the heat by non-radiative relaxation and the temperature of the sample is modulated (thermal grating). The excited molecules partly react and the concentrations of the reactant and product are also modulated (species grating). The optical properties (refractive index and /or absorbance) of the sample solution are spatially modulated by the spatially periodic distributions of the temperature and the concentration of reactants and products. Therefore, a probe beam is partly diffracted by the grating when the phase matching condition was satisfied. The diffracted probe light intensity (the TG signal) is related to the magnitude of these modulations.

The modulated light intensity for the optical grating is obtained by superposition of two monotony plane waves and given by

$$I(x) = I_0/2\,(1+\cos qx) \qquad (2\text{-}2)$$

where $I_o/2$ is the light intensity of the excitation beams. q is the magnitude of grating vector and described by the difference of the direction vector of two excitation beams ($\mathbf{k}_1$ and $\mathbf{k}_2$).

$$q = k_1 - k_2 \tag{2-3}$$

The relationship between the magnitude of **q** and the fringe spacing Λ is given by

$$q = 2\pi/\Lambda \tag{2-4}$$

Λ is obtained from the intrusion angle θ_e and the wavelength λ_e of the excitation beams by

$$\Lambda = \frac{\lambda_e}{2\sin\theta_e} \tag{2-5}$$

If the angle θ_p and the wavelength λ_p of the probe beam are satisfied the following Bragg condition, the TG signal is created.

$$\frac{\sin\theta_e}{\sin\theta_p} = \frac{\lambda_e}{\lambda_p} \tag{2-6}$$

This condition is illustrated in Fig. 2-1.

Kogelnik calculated the diffraction efficiency [the ratio of the intensity of the TG signal (I_{TG}) to that of the probe beam (I_{probe})] by solving the coupled wave equation with thin grating condition ($d > \Lambda^2/\lambda_p$, d; width of the grating). [4]

$$I_{TG}/I_{probe} = \exp\left(\frac{-k\,d}{\cos\frac{\theta_p}{2}}\right)\left(\sin^2\frac{\pi\Delta n\,d}{I_{probe}\cos\frac{\theta_p}{2}} + \sinh^2\frac{\Delta k\,d}{4\cos\frac{\theta_p}{2}}\right) \tag{2-7}$$

where Δn and Δk are the peak-null difference of the refractive index and absorbance, respectively, which induced by the thermal grating and species grating. When the diffraction efficiency is very

small (I_{TG}/I_{probe} <0.01), eq. (2-7) is rewritten by [4]

$$I_{TG}/I_{probe} = \left(\frac{\pi \Delta n\, d}{I_{probe}} \right)^2 + \left(\frac{\Delta k\, d}{4} \right)^2 \qquad (2\text{-}8)$$

Therefore, the intensity of the TG signals can be described by a sum of the square of the refractive index change and the absorbance change, both of which are induced by the optical grating.

2.2 Measurement of Diffusion Constants.

The thermal grating and the species grating are smeared out by the heat conduction and the mass diffusion between the fringes, respectively. Therefore, these processes can be measured from the time profile of the TG signal. In this section, we described the method of calculating D for reactants and products from the time dependence of the TG signals.

When the sample is excited by the optical grating described by eq. (2-2) and consequence non-radiative relaxation and photochemical reaction occur, the spatial distribution of the induced temperature change (ΔT) and concentration change (ΔC) of reactant (i) and product (j) are given by

$$T(x) = T^{O} + \Delta T(x) = T^{O} + \Delta T(0)/2\,(1+\cos qx) \qquad (2\text{-}9a)$$

$$C_j(x) = \Delta C_j(x) = \Delta C_j(0)/2\,(1+\cos qx) \qquad (2\text{-}9b)$$

$$C_i(x) = C_i^{O} + \Delta C_i(x) = C_i^{O} - \Delta C_j(0)/2\,(1+\cos qx) \qquad (2\text{-}9c)$$

where $\Delta C_j(0)$ is the initial concentration of the product created by the reaction. The modulation of the refractive index change (Δn) (phase grating) and absorbance change (Δk) (intensity grating) is given by

$$n(x,t) = n^{O} + \Delta n(x,t) = n^{O} + \Delta n_{th}(x,t) - \sum_i \Delta n_i(x,t) - \sum_j \Delta n_j(x,t) \qquad (2\text{-}10a)$$

$$k(x,t) = k^{O} + \Delta k(x,t) = k^{O} - \sum_i \Delta k_i(x,t) + \sum_j \Delta k_j(x,t) \qquad (2\text{-}10b)$$

where $\Delta n_{th}(x, t)$, $\Delta n_i(x, t)$, and $\Delta n_j(x, t)$ represent the refractive index change by the thermal grating, species grating of reactants and products. The refractive index becomes smaller with increasing the temperature. So, $\Delta n_{th}(x, t)$ is negative. On the other hand, since the absorbance of the sample is usually insensitive to the temperature, $\Delta k_{th}(x, t) = 0$. The refractive index change and the absorbance change relate to the temperature change and the concentration change as following.

$$\Delta n_{th}(x, t) = \left(\frac{dn}{dT}\right)\Delta T(x, t) \tag{2-11a}$$

$$\Delta n_{i,(j)}(x, t) = \left(\frac{dn}{dC_{i,(j)}}\right)\Delta C_{i,(j)}(x, t) \tag{2-11b}$$

$$\Delta k_{i,(j)}(x, t) = \left(\frac{dk}{dC_{i,(j)}}\right)\Delta C_{i,(j)}(x, t) \tag{2-11c}$$

where $\Delta T(x, t)$ and $\Delta C_{i,(j)}(x, t)$ are the space and time profile of the induced temperature change and concentration change, and these are described by the diffusion equation of Fourier and Fick, respectively. [5]

$$\frac{\partial \Delta T(x, t)}{\partial t} = D_{th}\frac{\partial^2 \Delta T(x, t)}{\partial x^2} \tag{2-12a}$$

$$\frac{\partial \Delta C_i(x, t)}{\partial t} = D_i\frac{\partial^2 \Delta C_i(x, t)}{\partial x^2} \tag{2-12b}$$

where D_{th} [$=\lambda_\omega/C_p\ \rho$ (λ_ω:thermal conductivity, C_p:heat capacity, ρ:density)] is the thermal diffusivity and D_i is the mass diffusion constant of reactant i. In the case of products, if the subsequence reaction process of the product is exist, $\Delta C_j(x, t)$ is given by the following diffusion-reaction couple equation.

$$\frac{\partial \Delta C_j(x, t)}{\partial t} = D_j\frac{\partial^2 \Delta C_j(x, t)}{\partial x^2} - f_j(x, t) \tag{2-13}$$

where $f_j(x, t)$ is the reaction velocities of the products. When the reaction is the first or the second

order, $f_j(x, t)=k_1\Delta C_j$ (x, t) and $f_j(x, t)=2k_2\Delta C_j$ (x, t)^2, respectively. The solution of the diffusion-reaction couple equation with the first and the second order reaction will describe later chapter (chapter 4). Now, we neglect the subsequence reaction [f(x, t)=0], then, eq. (2-13) is the same as eq. (2-12b). The time profiles of the concentration modulation are determined by only the diffusion process and the solution of eqs (2-12~13) are given by

$$\Delta \hat{T}\,(q, t) = \Delta \hat{T}\,(q, 0)\exp(-D_{th} q^2 t) \tag{2-14a}$$

$$\Delta \hat{C}_{i,(j)}(q, t) = \Delta \hat{C}_{i,(j)}(q, 0)\exp(-D_{i,(j)} q^2 t) \tag{2-14b}$$

where $\hat{C}_i$ (q, t) is the q-component of the Fourier transform of C_i (x, t). From eqs (2-10, 11, 14), the time dependence of the TG signal is given by

$$I_{TG}(t) = A\{\delta n_{th}^{\,o}\exp(-D_{th}q^2 t) - \sum_i \delta n_i^{\,o}\exp(-D_i q^2 t) + \sum_j \delta n_j^{\,o}\exp(-D_j q^2 t)\}^2$$

$$B\{-\sum_i \delta k_i^{\,o}\exp(-D_i q^2 t) + \sum_j \delta k_j^{\,o}\exp(-D_j q^2 t)\}^2 \tag{2-15}$$

where $(dn/dT)\Delta \hat{T}$ (q, 0), $(dn/dC_{i,(j)})\Delta \hat{C}_{i,(j)}$ (q, 0), and $(dk/dC_{i,(j)})\Delta \hat{C}_{i,(j)}$ (q, 0) are rewritten as $\delta n_{th}^{\,o}$, $\delta n_{i,(j)}^{\,o}$, and $\delta k_{i,(j)}^{\,o}$, respectively. A and B are the constants.

2.3 Experimental Setup of the TG Method.

The experimental setup for the TG measurements is shown in figure 2-2. [6] An excitation beam from an excimer laser [XeCl (308nm); Lumonics Hyper-400] was split to two beams by a beam splitter. The repetition rate of the excitation pulse was 1~3 Hz, the pulse width is about 20ns, and the beam size is 1~2mm. These beams crossed inside a 10-mm-path quartz sample cell and the interference pattern between these beams (optical grating) was created. The laser power at the crossing point was measured by a pyroelectric jouelemeter (Molectron J3-09) and it was typically ~0.3 mJ/cm^2. A probe beam from a He-Ne laser was partly diffracted by the grating when the

phase matching condition was satisfied. The TG signal was detected by a photomultiplier tube (Hamamatsu R-928) after isolation with a pinhole and a glass filter (Toshiba R-62) and recorded with a digital oscilloscope (Tektronix 2430A). The time profile of the TG signal was analyzed with a microcomputer. The signal was averaged by a digital oscilloscope and a microcomputer to improve the S/N ratio. The fringe spacing Λ was roughly estimated from the crossing angle θ and then calibrated by the decay rate of the thermal grating signal from a benzene solution containing a light absorbing solute and the reported thermal diffusion constant. [7]

Spectroscopic grade organic solvents, distilled water, and solute were purchased from Nacalai tesque Co. Benzoquinone and dibenzyl ketone were purified by recrystallization. Benzophenone, acetophenone, benzaldehyde, and aniline were purified by vacuum sublimation. The other solute and the solvent were used without further purification. Typical concentrations of the solutes were $\sim 10^{-2}$ M. Sample solutions were deoxygenated by the nitrogen bubbling method and flowed by a peristaltic pump (Atto SJ-1211) to avoid the effect of reaction products in the signal. The irradiated volume is so small (typically $\sim 4X10^{-3} cm^3$) compared with the entire volume of the sample solution ($\sim 4\ cm^3$) that the interference due to the reaction product in the signal is not serious during one measuring. The temperature of the sample solution was controlled (50 °C ~ -50 °C) by flowing temperature-regulated methanol around a cell holder with a temperature control system (Lauda RSD6D).

For a transient absorption (TA) measurement, the sample was excited by the excimer laser light ($1 \sim 5\ mJ/cm^2$) and probed by light from a 100W Xe lamp. The probe light was monochromated with a Spex model 1704 and detected by a photomultiplier. The TA measurements were carried out at room temperature (~20 °C).

An EPR spectrum was measured by same spectrometer with 100kHz field modulation under the laser light irradiation (repetition rate=20 Hz). For the decay measurement, the signal from the spectrometer was averaged by the digital oscilloscope with a slower repetition rate (3 Hz). The response time of the spectrometer is several milliseconds. CIDEP spectra of the time resolved EPR were measured by the same spectrometer as reported previously. [8] The EPR measurements were carried out at room temperature (~20 °C).

Pulsed field gradient spin-echo (PGSE) measurements [NMR spectrometer (JEOL JNM-EX270-W)] were made to independently measure D of stable molecules. [9] The PGSE measurements were carried out at 30 ^{o}C.

The van der Waals volumes V_w of the molecules were obtained from the atomic increments method given by Edward. [10] The radii of the molecules r were calculated from V_w using the relation; $r = (3V_w/4\pi)^{1/3}$. The values of r/ Å in this study are as following. benzophenone (3.43), acetone (2.46), acetaldehyde (2.25), benzaldehyde (2.88), acetophenone (3.04), benzoquinone (2.67), α-naphthoquinone (3.19), β-naphthoquinone (3.19), xanthone (3.40), 1,4-chrysenequinone (3.66), pyrazine (2.59), quinoline (3.05), quinoxaline (3.01), acridine (3.38), phenazine (3.34), octahydrophenazine (3.54), and 2,2-biquinoline (3.78).

Reference to Chapter 2

1. Y. R. Shen, *The Principles of Nonlinear Optics* (University of California, Berkeley, 1984).

2. R. W. Boyd, *Nonlinear Optics* (University of Rochester, New York, 1992).

3. H. J. Eichler, P. Gunter, and D. W. Pohl, *Laser-Induced Dynamic Grating* (Springer, Berlin, 1986).

4. (a) H .Kogelmik, Bell. Syst. Tech, J, 48, 2909 (1969).; (b) T. K. Gaylord, M. G. Moharam, Appl. Phys., B28, 1 (1982).

5. A. Fick, Prog. Annln, 94, 59 (1855).

6. M. Terazima, N. Hirota, J. Chem. Phys., 95, 6490 (1991).

7. M. Terazima, K.Okamoto, and N. Hirota, J. Phys. Chem., 97, 5188 (1993).

8. S. Yamauchi, N. Hirota, J. Phys. Chem., 88, 4631 (1984).

9. (a) M. Nakahara, C. Wakai, Y. Yoshimoto, and N. Matubayasi, J. Phys. Chem., 100, 1345 (1996).; (b) P. Stillbs, Prog. Nucl. Magn. Reson. Spectrasc., 19,1 (1987).

10. J. T. Edward, J. Chem. Edc., 47 , 261, (1970)

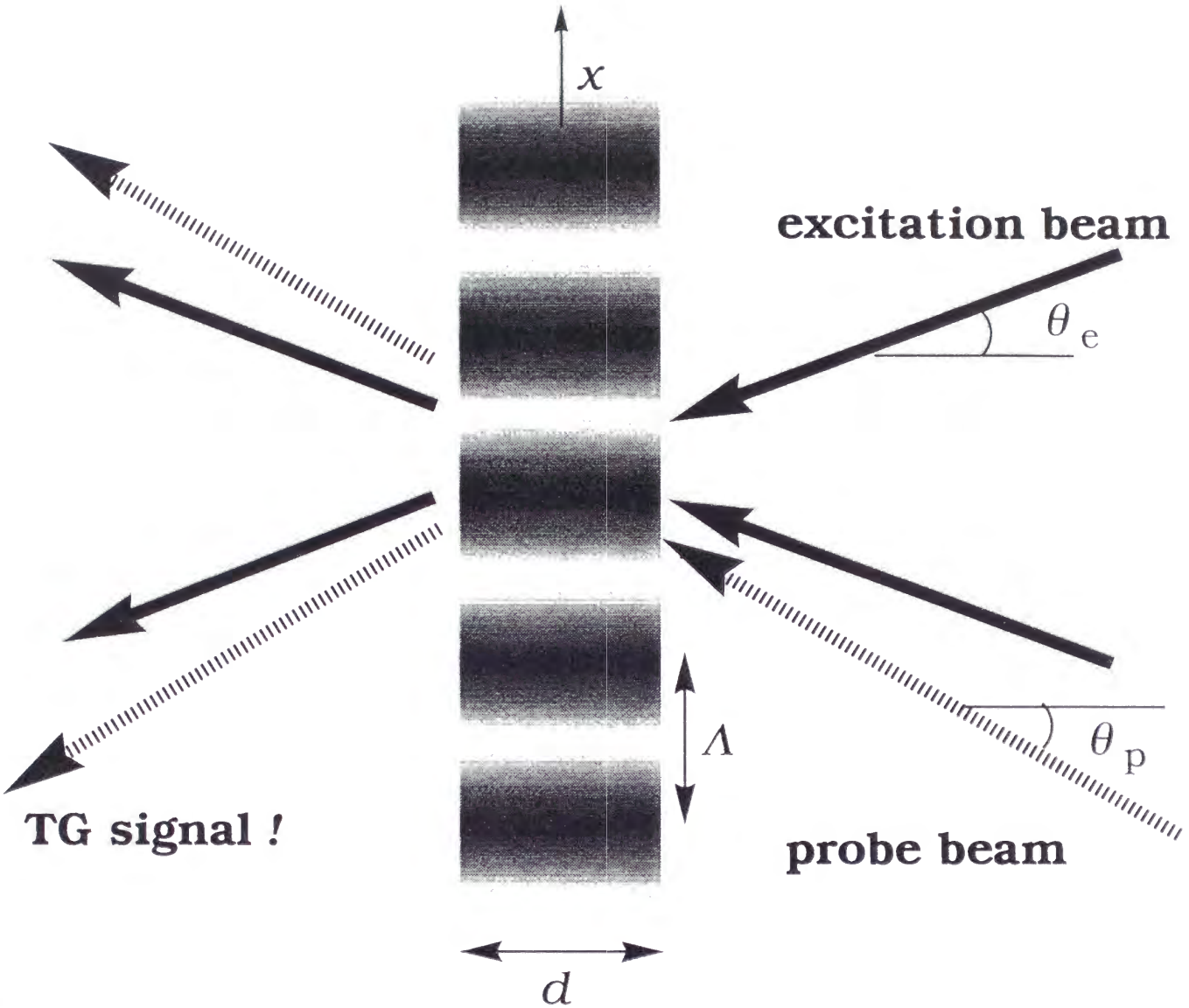

Fig. 2-1 The configuration of the excitation and probe beams for the TG method.

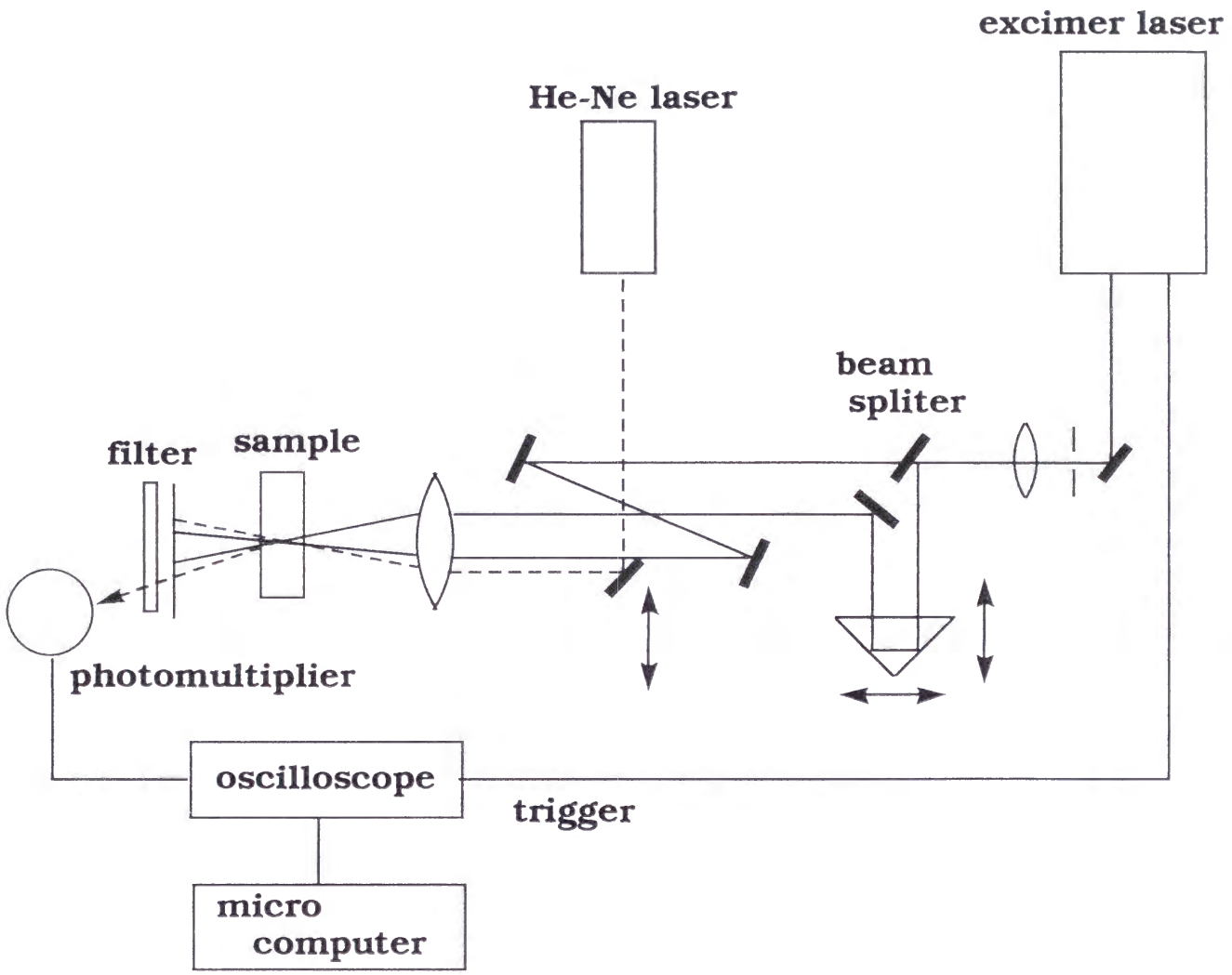

Fig. 2-2 Experimental setup for the TG measurement.

Chapter 3

DIFFUSION OF THE RADICALS CREATED BY HYDROGEN ABSTRACTION

3.1 Photochemical Reaction of Hydrogen Abstraction.

In this chapter, the diffusion processes of the intermediate radicals created by the photoinduced hydrogen abstraction of carbonyl, quinones, and azaromatic compounds are investigated. [1-6] Based on previous studies, the hydrogen abstraction reaction scheme of carbonyl, quinones, and azaromatic compounds (M) from alcohol and alkane (RH) are described by the scheme 3-1. [7] The ground state of the solute molecule (M) are excited to the higher excited singlet states ($^1M^{**}$) by the UV irradiation (process a) and relaxed to the lowest excited singlet (S_1) states ($^1M^*$) (process b) by the internal conversion. The lowest excited triplet (T_1) state ($^3M^*$) is created by the intersystem crossing from the lowest S_1 state (process c). process a~c are completed within an excitation laser pulse (~20ns). The hydrogen abstracted radical ($MH^{\cdot}$) are created from T_1 state by the hydrogen abstraction from the solvent (process d). The recombination reaction of the two radicals is a dominant subsequent reaction (process e).

We used benzoquinone (BQ), pyrazine (Py), and benzophenone (BP) as the reactant in 2-propanol. The hydrogen abstraction reactions of these molecules are shown in scheme 3-2. Benzosemiquinone radical (BQH), pyrazinyl radical (PyH), and BP ketyl radical (BPK) are created from BQ, Py, and BP, respectively.

3.2 Time Profile of the TG Signals.

Figure 3-1 shows that the time dependence of the TG signal after the photo excitation of BQ

(0.01M) in 2-propanol at the room temperature. This signal consists of a strong signal which decays in a few microseconds and a subsequent slowly developing one. The spike-like signal in Fig. 3-1 originates from the thermal grating created by the non-radiative transitions of the photoexcited molecules. The decay of the thermal grating signal is determined by the heat conduction process. After the thermal grating signal decays to the baseline completely, another signal appears and then decays again with a lifetime of millisecond order. The time development of this component reflects the spatial movement of several chemical species and, from this profile, D of each species can be measured.

The time profile of the root square of the TG signal $[I_{TG}(t)^{1/2}]$ can be fitted well with a sum of three exponential functions.

$$I_{TG}(t)^{1/2} = -a_1 \exp(-k_1 t) - a_2 \exp(-k_2 t) + a_3 \exp(-k_3 t) \qquad (3\text{-}1)$$

where, $k_1 > k_2 > k_3 > 0$ are the decay constants and $a_1 > a_2 > a_3 > 0$ are the pre-exponential factors. The solid line in Fig. 1a is the line fitted by using the non-linear least-squares method with eq. (3-1) and the profiles of the three components are shown in Fig. 1b. Similar signals are observed from Py in 2-propanol and BP in 2-propanol (Fig. 3-2), which are also fitted by eq. (3-1).

Analytically, the intensity of the TG signals can be described by a sum of the square of the refractive index changes and the absorption changes [eq. (2-8)], both of which are induced by the optical grating.[8] In this reaction system, absorption bands of any species are on the far blue side from the probe wavelength (633nm).[9-12] Thus, the TG intensity is proportional to only the square of the refractive index change. The thermal effect (thermal grating) and the creation or depletion of chemical species (species grating) can contribute to the refractive index change. The time profiles of the signals due to the thermal grating and the species grating are given by solving the Fourier's thermal diffusion equation and Fick's reaction-diffusion equation, respectively [eq. (2-15)].[13] Since in the observation time range of the TG signal, the creation and termination reaction of the radicals can be neglected as shown later, the time dependence of the TG signal is

given by the following equation [eq. (2-15) with B=0].

$$I_{TG}(t)^{1/2} = \delta n_{th}^{o} \exp(-D_{th} q^2 t) - \sum_{P} \delta n_{P}^{o} \exp(-D_{P} q^2 t) + \sum_{R} \delta n_{R}^{o} \exp(-D_{R} q^2 t) \quad (3\text{-}2)$$

where δn_P^o and δn_R^o are the initial refractive index changes by the species grating of the parent molecules and the radicals, respectively. D_P and D_R are the diffusion constants of the parent molecules and the radicals, respectively. Comparing eq. (3-2) with eq. (3-1), D_{th} is given by $k_1 = D_{th} q^2$. D_{th} from the TG signal agrees well with the calculated one from $D_{th} = \lambda_\omega / C_p \rho$ (λ_ω:thermal conductivity, C_P:heat capacity ρ:density) within ~10%. [14]

As both the parent molecules and the radicals in this system have the absorption bands at shorter wavelengths than that of the probe beam, both δn_P^o, δn_R^o are expected to be positive from Kramers-Kronig relationship. Therefore, the sign of the second term of eq. (3-2) is negative, which is the same as the sign of the fiest term. On the basis of this reason, component 2 in the TG signal (Fig. 3-1b) is assigned to the signal due to the parent molecule. On the other hand, the third term should be positive. Component 3 in Fig. 3-1b should be due to the radical. It has been reported that the BQH radical is created by photoexcitation of BQ in a pure alcoholic solvent. [9] In this reaction system, four chemical species (BQ, BQH, 2-propanol, 2hydroxypropyl radical) could contribute to the signal. However, since the absorption coefficient of 2-propanol and 2hydroxypropyl radical [12] are smaller than those of BQ and the BQH radical, [9] the refractive index changes of 2-propanol and 2hydroxypropyl radical [12] should be smaller than those of BQ and the BQH radical. Therefore, the TG signal due to 2-propanol and 2hydroxypropyl radical could not be detected. We assign component 2 to the species grating of BQ and component 3 to that of the BQH radical. Then, D_P, D_R are the diffusion constants of BQ and the BQH radical, respectively. The time profiles of the TG signal of Py/2-PrOH and BP/2-PrOH (Fig. 3-2) are also analyzed in a similar manner.

3.3 Anomalous Slow Diffusion of Radicals.

The decay rate constants k_2, k_3 obtained by the fitting of the TG signals at various fringe spacing are plotted against the square of the grating vector q in Fig. 3-3. Based on the assignment given above and from eqs. (3-1) and (3-2), the following relationships are obtained.

$$k_2 = D_p \ q^2 \tag{3-3a}$$

$$k_3 = D_R \ q^2 \tag{3-3b}$$

The TG signal decays not only by the diffusion process but also by any reaction processes. In this case, the decay rate of the TG signal is accelerated by the reaction, and more detailed consideration is necessary for the analysis as we will mention in chapter 4. However, the good linear relationship between the decay rate constants and q^2 with small intercepts with the ordinate indicates that the intrinsic lifetimes of transient radicals are negligible in the observation time scale. Therefore, D of each species can be determined from the slope of the plot. The obtained D of the parent molecule and the radicals are listed in table 3-1.

Comparing D of the radicals with those of the parent molecules, we found that the intermediate radicals created by photoinduced hydrogen abstraction reactions diffuse much more slowly than the stable parent molecules, even though the radical and the parent molecule possess nearly the same size and the same shape. Such an anomalously slow diffusion of the radicals suggests a strong intermolecular interaction between the radicals and the surround molecules. This fact points out that D of a transient radical should not be simply substituted by that of a stable molecule with a similar molecular volume in an analysis of chemical reaction dynamics. It is very important to explain the exact origin of the slow diffusion of the radicals.

3.4 Support from TA, EPR, and NMR Measurement.

We investigated the reaction and the kinetics by the TA, EPR, and NMR methods to support the result of the TG measurement. Until now, TA and EPR have been used to detect the transient radicals and the TA and EPR spectra have been reported about several radicals. Fig. 3-4 shows the

observed TA spectra of (a) BQ, (b) Py, and (c) BP in 2-propanol. These observed spectra are similar to the reported spectra of transient radicals of BQH, [9] PyH, [10] and BPK, [11] respectively. These TA signals are detected with a stronger laser power (~5 mJ/cm^2) because the TA signals were too weak to be detected with the same excitation laser power as in the TG experiment (~0.3 mJ/cm^2). The decay of the TA signal of BQH is shown in Fig. 3-5. This decay is expressed by the second-order decay and the half-lifetime ($\tau_{1/2}$) is ~ 10ms under our experimental conditions. The decay of the TA signal of BPK and PyH are also expressed by the second-order decay and $\tau_{1/2}$ is also a few tens millisecond. This fact is reasonable because the termination reactions of these radicals are due to the collision of the two radicals. [15] The intensities of these TA signals are nearly constant in the time range of our TG experiment. Therefore the neglecting of the subsequence reaction processes in the analysis of the TG signals is reasonable.

Figure 3-6 shows the cw EPR spectrum of BQ/2-propanol measured under the irradiation by laser pulse with a 20 Hz repetition rate. The spectrum is unambiguously assigned to BQH. There is no other detectable EPR signal. This fact gives conclusive evidence that the transient radical seen in the TG signal is BQH. Furthermore, the fact that the signal can be detected under the cw operation of EPR with the pulse excitation indicates that the lifetime of BQH is sufficiently long in the millisecond time range. Indeed, the decay of the EPR signal could be detected at few-tens-millisecond order (Fig. 3-6). The half-lifetime of this decay is ~20ms under the excitation laser power of ~2 mJ/cm^2.

Using the TG method, one can measure D of both the transient radicals and the parent molecules at the same time. Therefore D of the radicals can be compared with D of the parent molecules at the same conditions. D of the transient radicals have never been detected by the traditional methods. However, D of the parent molecules can be measured by such the method. We measured D of BQ, BP and Py in 2-propanol by using the pulsed field gradient spin-echo (PGSE) method of NMR spectroscopy and compared with that for the TG method (Table 3-1). All of the D measured by the PGSE method are very close to D of the parent molecules rather than D of the radicals obtained by the TG method. This fact supports the assignment of the TG signals.

Recently, Donkers and Leaist reported D of carbonyl, quinones, and azaromatic compounds

by using the Taylar dispersion (TD) method. [16] They found that D of several stable molecules obtained by the TD method are slight different from those determined by the TG method. Compared with the rather simple and stable setup of the TD method, D from the TG method have to be determined by taking account of several factors, and the accuracy is not generally as good as that from the TD method. [3] The fitting of the double-exponential function for the time profile of the TG signals leads to some uncertainties. In particular, since the time profile due to the parent molecule is superimposed on the decay of the radical signal, the error in D of parent molecules is more serious than D of the radicals. We also listed the reported D of BQ, BP and Py in 2-propanol by TD method in Table 3-1. Considering the different method and experimental conditions for TG and TD, we think that the D from the TG method agree reasonably with those from the TD method within the error range.

3.5 Comparison of Experimental D with the Calculated D.

In this section, we compare D obtained by the TG method with the calculated D from several method. Since the diffusion process of molecules in solution is one of fundamental and important processes, diffusion constants (D) have been measured by various methods and theoretically treated in many ways.[13] Simply, according to the hydrodynamic theory, D is given by the Stokes-Einstein (SE) formula: [13]

$$D_{SE} = \frac{k_B T}{f \pi r \eta} \qquad (3\text{-}4)$$

where r, η, and T are the radius of the solute, the viscosity of the solution, and the temperature, respectively. f is a constant which depends on the boundary condition between the solute-solvent molecules; f=4 (slip) ~ 6 (stick). When the solute size becomes much larger than the solvent size, f obtained from experimental D becomes closer to 6 (stick boundary). However, in many case, f have to be much smaller than 4 (slip) to reproduce experimental D by eq (3-4). Generally, D_{SE} gives the under estimation. The discrepancy may come from two factors, mainly. First is the non-hydrodynamics effect, which is due to the breakdown of the some approximation of the SE

equation, e.g., the solvent is treated as a continuous fluid or the shape of the solute molecule is treated as a spherical form. Second is the intermolecular interaction effect. In SE equation, solute-solvent and/or solute-solute interactions are disregarded. If the special solute-solute and/or solute-solvent interaction exist, the friction of the solute molecule becomes larger and D becomes smaller. The slow diffusion of ions, hydrogen bonded molecules, and transient radicals are classified to this effect. Many groups proposed equations to estimate the non-hydrodynamic effect. For example, Perrin proposed a method for correcting the deviation from the spherical shape. [17] Spernol and Wiltz modified the SE equation in terms of a molecular interaction semiempirically. [18] Scheibel proposed an empirical equation to reproduce the solute size dependence of D. [19] Wilke and Chang corrected the SE formula empirically by using the solute-solvent interaction factor. [20] King et al. corrected the SE formula empirically by the ratios of vapor enthalpy changes of the solutes to that of the solvents. [21] By using these modified equations, experimental determined D for molecules without any intermolecular interaction can be reproduced reasonably well. Especially, by using the modified equation proposed by Evans et al., [22-23] the calculated D can reproduce the experimental D in a wide range of the viscosity, solute size, and temperature. They empirically described $D/10^{-9} m^2 s^{-1}$ (D_{EV}) by [22]

$$D_{EV} = \frac{A\,T}{\eta^{p}} \qquad (3\text{-}5a)$$

where A is a constant, which is equivalent to $k_B/6\pi r$ in the SE equation with p=1. Evans et al. found that both A and p depend on the solute molecular size by measuring D of many solutes at variable temperatures. They proposed that A and p are given by [23]

$$A = \exp (a/r + b) \qquad (3\text{-}5b)$$

$$p = c/r + d \qquad (3\text{-}5c)$$

where a, b, c and d are constants and they are a=5.9734 Å, b=-7.3401, c=-0.86365 Å and d=1.0741. Equation (3-5b) indicates that D increases exponentially with increasing 1/r. Equation (3-5c) means that the effective viscosity of the solvent against the solute increases with increasing the solute molecular size. When r approaches infinity, η^p becomes η.

We compare the obtained D of the radicals (D_R) and the parent molecules (D_p) with D_{SE} under the stick condition and Evans et al. equation (D_{EV}) in Table 3-1. We found that D_p are close to D_{EV} rather than D_{SE}. D of the parent molecules are able to reproduce by the hydrodynamic theory with the non-hydrodynamic effect without intermolecular interaction effect (normal diffusion). On the other hand, D_R are close to D_{SE} rather than D_{EV}. This fact suggests that the diffusion processes of the transient radicals can be described by the simple hydrodynamic theory (anomalous diffusion). In this case, the intermolecular interaction effect which make D smaller may be compensate the non-hydrodynamic effect which make D larger. Then, D of the radicals can be reproduced by the simple hydrodynamic theory without both intermolecular interaction and non-hydrodynamic effect.

3.6 Molecular Size and Solvent dependence.

To understand the diffusion in solution, it is useful to investigate factors which control the diffusion process. According to the hydrodynamic theory, D is governed by three parameters; r, η, and T. [13] Therefore, for elucidating the diffusion mechanism of the radicals, the first step is to investigate the influence of these factors.

Firstly, we investigate the solvent dependence of D_R and D_P. We plotted D of BP and acetophenone (AP) against the viscosities of the protic polar solvents (mthanol, ethanol, 2-propanol, btanol, pentanol, hexanol, and ethyrenglycol), aprotic polar solvents (aceton, acetonitril, N,N-dimethylformamid, dimethylsulfoxide, benzene, and toluene), and non-polar solvents (hexane, cyclohexane, methylcyclohexane, decane, undecane, tetradecane, dodecane, hexadecane, and squarane) in Fig. 3-7. [2-4] D_R was found to be smaller than D_P in a variety of solvents regardless of the solvent properties, such as the polarity, the dipole moment and the protic (or aprotic) character of the solvent. From these observations, we have concluded that the hydrogen bonding between the radical and the solvent cannot be the essential origin of the slow diffusion.

Next, we investigate the molecular size (radius) dependence of D_R and D_P. [3-5] For the reactants, we choose carbonyls (benzaldehyde, acetophenone, benzophenone, xanthone), quinones (benzoquinone, 1,2-naphthoquinone, 1,4-naphthoquinone, 1,4-chrysenquinone), and azaromatics (pyrazine, quinoline, quinoxaline, acridine, phenazine, octahydrophenazine, 2,2-biquinonline) in ethanol and in 2-propanol. These molecules create the intermediate radicals by the photoinduced hydrogen abstraction reaction similar to BQ, BP, and Py. There are three aims in this study. First, measurements of various radicals will give us a clue to answer the question: whether or not the slower radical diffusion is a general phenomenon and if there is a characteristic behavior depending on the type of molecules (such as carbonyls, quinones, and azaromatic compounds). Second, D_R will provide valuable data for the analysis of many works on photochemical reactions. Third, the molecular size effect on D_R may give us an insight for understanding the movement of the radicals in solution. Figure 3-8 shows the molecular size dependence of D_R and D_P. It is found that D of all the radicals studies here are generally two to three times smaller than those of the parent molecules. Therefore, we conclude that the anomalous slow diffusion is the general property of hydrogen abstracted radicals. Moreover, this result suggests that the slow diffusion of radicals is not related to their detailed molecular structure and the type of molecules.

We also found that D_R are close to D_{SE} (straight line in Fig. 7, 8) although D_P are close to D_{EV} (curved line) in the wide range of $1/r$ and $1/\eta$. The reported D of the parent molecules by the TD method are also plotted in Fig. 3-7, 8. D of the parent molecules in this work are very close to the reported D within the error bar. We found that the ratios of D_R to D_P depend on the molecular size and solvent viscosities, and it becomes larger with decreasing the molecular size and increasing the solvent viscosities.

3.7 Temperature Dependence.

In this section, we focus our attention on the temperature dependence of D to obtain a further insight into the diffusion processes of the transient radicals in solution. [6] The temperature dependence of stable molecules have been studied extensively in liquids and solids so far. [13] Almost all results revealed that the logarithm of D is proportional to the reciprocal of T. This

Arrhenius-type expression of D is described as follows with a diffusion activation energy E_D and a pre-exponential factor D_o .

$$D=D_o \exp\left(-\frac{E_D}{k_B T}\right) \tag{3-6}$$

If the radical diffusion is governed solely by the molecular dynamics of the solvent, we expect that the temperature dependence of D should be expressed by this Arrhenius type expression and E_D should be close to that of the viscosity (E_η). However, when the solute interacts with the solvent rather strongly by a specific interaction such as hydrogen bonding and the interaction influences the diffusion process seriously, E_D should deviate from E_η. For example, E_D for hydrogen bonded molecules was found to be larger than E_η by about 2~4 kcal/mol because of the activation energy of the hydrogen bonding. [24] Or if the fraction of the hydrogen-bonded structure depends on the temperature, the Arrhenius plot of D would not be represented well by a single activation energy.[25] In other words, the specific intermolecular interaction between solutes and solvents like a hydrogen bonding can be manifested itself by a larger E_D than E_η and/or a deviation from a linear relation in the Arrhenius plot.

The D of BP and BPK in 2-propanol are plotted against the various temperatures in Fig. 3-9a and the Arrhenius-type plots are shown in Fig.3-9b. The logD vs. 1/T plots show a linear relationship. The linear Arrhenius plot suggest that the diffusion process is dominantly controlled by the hydrodynamic force of the solvent. The activation energies of BP (E_P) and BPK (E_R) obtained from the slopes are listed in table 3-2. By a similar manner, E_P and E_R of other solutes were obtained and also listed in table 3-2. An important point to be noticed from table 3-2 is the resemblance of E_D of the radicals and the parent molecules with the activation energy of the viscosity (E_η). Furthermore, although E_D of BPK and BP are similar, the small difference is beyond our experimental uncertainty. E_D of BPK is slightly smaller than that of BP. We will come back to this point in a later section.

Table 3-2 summarizes E_D of the radicals and their parent molecules in 2-propanol and in ethanol. As shown before in the BP case, E_D of the radical are slightly smaller than those of the

parent molecule in all the reaction systems. More importantly, although E_D in a solvent is close to that of E_η, there is a definitive variation depending on the solutes.

3.8 Activation Energy of Diffusion

According to the SE theory, D depends on r, η, and T. η depends on temperature and is frequently given by [26]

$$\eta = \eta_o T \exp\left(\frac{E_\eta}{k_B T} \right) \tag{3-7}$$

where E_η is the activation energy of viscosity η. The SE equation can be written with eq.(3-7) as

$$D_{SE} = \frac{k_B}{6 \pi r \eta_o} \exp\left(- \frac{E_\eta}{k_B T} \right) \tag{3-8}$$

When eq.(3-8) is compared with eq. (3-6), we obtain the following relationship

$$E_D = E_\eta$$

The temperature dependences of the viscosities of 2-propanol [27] and ethanol [28] have been already reported and from these values, we obtain E_η= 5.854 kcal/mol for 2-propanol and E_η= 3.957 kcal/mol for ethanol. The results in table 3-2 indeed show that the obtained E_D in 2-propanol and ethanol are close to these E_η. This resemblance would indicate that the diffusion process of the radicals as well as the parent molecules are mainly controlled by the solvent dynamics as stated before. Moreover, if the specific interaction such as the hydrogen bonding between the radical and the solvents dominantly control the diffusion process, the activation energy would not be close to E_η.

As stated previously, there is a difference between E_R and E_P, and the solute dependence of E_D is also noticeable. Before discussing the difference in E_D between the radicals and the parent molecules, we consider the dependence of E_D on the molecular size of the parent molecule. Figure

3-10 is the plotted E_D against the reciprocal of the solute radii r in 2-propanol and ethanol. From this figure, E_D seems to relate to 1/r. For simplicity, we assume that E_D is linear in 1/r,

$$E_D = -\frac{\alpha}{r} + E_\eta \tag{3-9}$$

where α is a constant. The relation ensures that if $r \sim \infty$, then $E_\eta = E_D$. Therefore, (eq.3-6) may be rewritten as the following.

$$D = D_o \exp\left(\frac{-\frac{\alpha}{r} + E_\eta}{k_B T}\right) \tag{3-10}$$

The size-dependence of E_D for stable molecules has been studied by Evans et al.[22-23] Equation (3-5b) indicates that D increases exponentially with the increase in 1/r. Equation (3-5c) means that the effective viscosity of the solvent against the solute increases with increase of the solute molecular size. When r approaches infinity, η^p becomes η.

Our experimentally observed relation [eq. (3-10)] is very close to the relation derived by Evans et al. Since the viscosity of the solvent is expressed by eq. (3-7), eq. (3-5b) can be described as follows.

$$D_{EV} = \frac{AT^{1-p}}{\eta_o^p} \exp\left[\frac{-E_\eta\left(\frac{c}{r} + d\right)}{k_B T}\right] \tag{3-11}$$

Therefore, when p is close to 1 the activation energy for diffusion is given by

$$E_D = E_\eta\left(\frac{c}{r} + d\right) \tag{3-12}$$

Comparing eq. (3-9) and eq. (3-12), we find that both equations become identical when $\alpha = -E_\eta c$, d=1. Indeed, the value of d obtained by Evans et. al. was 1.0741, which is sufficiently close to

unity. Therefore the molecular size dependence of E_D proposed for the parent molecule [eq. (3-9)] is almost equivalent to the previously proposed relation (Fig.3-10). Equation (3-10) is identical to eq. (3-11) when $AT^{1-p}/\eta_o^{p}=D_o$. The values of E_D calculated from eq. (3-12) with c=-0.85365, d=1 and E_η=5.854 kcal/mol in 2-PrOH, E_η=3.957 kcal/mol in EtOH are plotted in Fig. 3-10. Since this line agrees with experimental values fairly well.

The 1/r dependence of E_D can be explained by the breakdown of the continuous fluid approximation of the solvent in the theory of the hydrodynamics. The viscosity of the solvent is the macroscopic parameter and the hydrodynamic theory treats the solvent as continuous fluid. When the solute size is as small as the solvent molecular size, the solvent can be no longer treated as continuous fluid and the microscopic viscosity (local viscosity around the solute molecules) of the solvent is apparently reduced by the non-hydrodynamic effect. In such a solvent, the activation energy for diffusion is also reduced by similar effect. Contrary, when the solute molecules become larger, the solvent molecules can be treated as continuous fluid. If the solute molecule has a infinite size, the microscopic viscosity should coincide with the macroscopic viscosity η. Actually, Fig. 3-10 suggests that the values of E_D of the parent molecules are close to E_η (E_η=5.854 kcal/mol in 2-PrOH, E_η=3.957 kcal/mol in EtOH) when 1/r approaches zero; i.e. r approaches infinity.

3.9 The Excess Volume Model of Diffusion.

We will interpret the different E_D of radicals and parent molecules in terms of the previously proposed model of the radical diffusion. We considered that the transient radicals are surrounded by the solvent or solute molecules with an attractive intermolecular interaction, and the effect of the attractive interaction was treated as an increase of the effective molecular volume. Namely we have treated the small D of the radicals in terms of the apparent molecular size expansion (the excess volume model).

Assuming that the excess volume by the interaction is V_o, apparent radius of the radical (r *) is calculated from

$$r^{*} = \left(r^{3} + \frac{3 V_{o}}{4 \pi} \right)^{\frac{1}{3}} \qquad (3\text{-}13)$$

If we replace r in eq. (3-9) by r *, E_D of the radical is described by

$$E_D = - \frac{\alpha}{\left(r + \frac{3 V_{o}}{4 \pi} \right)^{\frac{1}{3}}} + E_{\eta} \qquad (3\text{-}14)$$

This equation reduces to eq. (3-9) when $r^3 >> 3V_o/4\pi$. In other words, E_D of the radical becomes closer to that of the parent molecule with increasing the molecular volume. When r becomes smaller, E_D of the radicals approaches a constant value. The curved lines in Fig.3-10 are fitted lines calculated from eq.(3-14) with $V_o = 8 \times 10^2$ Å^3 in 2-propanol and ethanol. They reproduce the observed molecular size dependence of E_D fairly well.

It should be noted that eq. (3-12) as well as eq. (3-14) predict that E_R and E_P should approach E_η as the molecular size increases. For the parent molecule, this tendency is consistent with the continuous model of the medium in the hydrodynamic theory. For the radicals, when the molecular size becomes large, the character of the radical (probably the spin density) is diluted and the diffusion process becomes similar to that of the parent molecule. Then the activation energy should be again close to E_η.

In the analysis in this section, we assume that the increase of the effective volume is a constant which is independent of the solute size and the temperature. If we assume that the volume expansion is the result of the aggregation of the solvent molecules around the radicals, the estimated volume $V_o = 8 \times 10^2$ Å^3 corresponds to about ten solvent molecules in 2-propanol or ethanol.

We try to reproduce the molecular size dependence of D_R [Fig. 3-8] by using the excess volume model. From eq. (3-5) and (3-13), diffusion constant from the excess volume model (D_V) is given by

$$D_V = T \exp \left[a/(r^3 + 3V_o/4\pi)^{1/3} + b \right] \eta^{\left[- c/(r^3 + 3V_o/4\pi)^{1/3} - d \right]} \qquad (3\text{-}15)$$

The plot of D_V vs. r is shown in Fig. 3-8. For calculating D_V, we fix the values a, b, c and d determined by Evans et al.[21] and use the increase of the molecular volume V_o as an adjustable parameter. The best fitted lines by eq.(3-15) are obtained using V_o=5 x 10^2 Å^3 as shown in Fig. 3-8. The calculated values of D_V are close to D_{SE} and the experimental D of radicals. The value V_o =5 x 10^2 Å^3 is close to V_o =8 x 10^2 Å^3 which obtained from the fitting of the size dependence of the activation energies in this section.

The attractive intermolecular interaction is recently supported by the time resolved transient Ramman spectroscopy by Terazima and Hamaguchi.[29] More recently, Terazima and co-workers investigated the diffusion of 2,2,5,5-tetramethyl-1-piperidinyloxy (TEMPO) or some other stable radicals by using the Taylar dispersion (TD) method.[30] They found that D of such stable radicals are not small but close to D of the analogous non-radicals molecules, and discussed in terms of the chemical stability. Therefore, the anomalous slow diffusion must be the character of the chemically unstable radicals created by the photoinduced hydrogen abstraction.

3.10 Conclusion.

We succeeded in measuring D of the short-lived radicals accurately by using the laser induced transient grating (TG) method, which requires only a short time (micro~millisecond) for the measurement of the diffusion constants (D). We have found that D of the radicals created by photoinduced hydrogen abstraction reactions of ketones, quinones, and azaromatic compounds from organic solvents are 2~3 times smaller than those of the parent molecules, even though the radicals and parent molecules possess nearly the same sizes and the same shapes. Such an anomalously slow diffusion of the radicals should be due to a strong intermolecular interaction between the radicals and the surround molecules. Extended researches was investigated, such as the solvent dependence, the solute size dependence, the temperature dependence. The differences in D between the radicals and the parent molecules become larger with increasing η, 1/r, or 1/T. These D are compared with the values calculated based on the Stokes-Einstein equation (D_{SE}) and the equation proposed by Evans et al. (D_{EV}). D of the parent molecules are close to D_{EV}, while D of the radicals are close to D_{SE} in wide ranges of solvent viscosities, solute size, and temperatures.

The temperature dependences of D of both the radicals and the parent molecules can be expressed by the Arrhenius relationship with one activation energy. The activation energies (E_D) for diffusion of the radicals are larger than those of the parent molecules and also they depend on the solute molecular size. When the solute molecular sizes become larger, the values of E_D become larger. The solute molecular size dependence of the parent molecule's E_D could be explained by the empirical formula obtained by Evans et. al.

Different values in E_D between the transient radicals and their parent molecules are interpreted in terms of the excess volume model; the radicals are surrounded by other molecules (solvent and/or parent molecules) in solution by an attractive interaction. The equation of E_D as a function of solute radii derived by assuming that the apparent volume increase of the radical is constant for all of the radicals can reproduce the molecular size dependence of E_D of the radicals. The results of this investigation will give us a clue to understand the anomalous slow diffusion process of transient radicals.

References to Chapter 3

1. (a) M. Terazima, and N. Hirota, J. Chem. Phys., 98, 6257 (1993).; (b) M. Terazima, K.Okamoto, and N. Hirota, Laser Chem., 13, 169 (1994).

2. M. Terazima, K.Okamoto, and N. Hirota, J. Phys. Chem., 97, 13387 (1993).

3. K. Okamoto, N. Hirota, and M. Terazima, J. Phys. Chem. A, 101, 5380 (1997).

4. M. Terazima, K. Okamoto, and N. Hirota, J. Mol. Liq., 65/66, 401 (1995).

5. M. Terazima, K. Okamoto, and N. Hirota, J. Chem. Phys., 102, 2506 (1995).

6. K. Okamoto, M. Terazima, and N. Hirota, J. Chem. Phys., 103, 10445 (1995).

7. Cadogan, J. I. G. *Principles of Free Radical Chemistry* (The Chemical Society Monographs For Teachers No. 24, **1973**).

8. H. J. Eichler, P. Gunter, and D. W. Pohl, *Laser-Induced Dynamic Grating* (Springer, Berlin, 1986).

9. (a) K. Kimura, K. Yoshinaga, H. Tsubomura, J. Phys. Chem. 71, 4485 (1967).; (b) G. E. Adams, B. D. Michel, B. D. Trans. Faraday Soc., 63, 1171 (1967).

10. D. V. Bent et al., Chen. Phys. Lett., 27, 544, (1974)

11. (a) V. Nagarajan and R. W. Fessenden, Chem. Phys. Lett., 112, 207 (1984).; (b) F. W. Deeg, J. Pinsl, and Chr. Brauchle, J. Phys. Chem., 90, 5710 (1986).; (c) Y. Kajii, M. Fujita, H. Hiratsuka, K. Obi, Y. Mori, and I. Tanaka, J. Phys. Chem., 91, 2791 (1987).; (d) P. P. Levin, L. F. Vieira Ferreira and Silvia M. B. Costa, Chem. Phys. Lett., 173, 277 (1990).

12. G. Porter, S. K. Dogra, R. O. Loutfy, S. E. Sugamori, R. W. Yip, J. Chem. Soc. Farad. Trans., 1, 1462 (1973).

13. (a) E. L. Cussler, *Diffusion* (Cambridge University, Cambridge, 1984).; (b) H. J. V Tyrrell, and K. R. Harris, *Diffusion in Liquid* (Butterworths, London, 1984).; (c) *Landolt-Bornstein Tabellen* (Springer, Berlin, 1961), 6 Aufl., Bd. II.

14. (a) Y. S. Touloukian, *Thermophysical Properties of Matter* (Plenum, New York, 1970), vol III.; (b) *International Critical Tables* (McGraw-Hill, New York, 1928), vol. III.; (c) *Landolt-Bornstein Tabellen* (Springer, Berlin, 1972), 6 Aufl., Bd. IV.

15. I. V. Khudyakov, L. L. Koroli, Chem. Phys. Lett., 103, 383 (1984).

16. L. R. Donkers and G. Leaist, J. Phys. Chem. B, 101, 304 (1997).

17. F. Perrin, J. Phys. Radium., 7, 1 (1936).

18. A. Spernol, K. Wirtz, Z. *Naturforsch.* , 8a, 352 *ibid* 522 (1953).

19. E. G. Scheibel, Indu. Eng. Chem., 46, 2007 (1954).

20. C. R Wilke, P. C. Chang,. Am. Inst. Chem. Eng. J, 1, 264 (1955).

21. C. J King, L. Hsueh, K. W. Mao, J. Chem. Eng, Data., 10, 348 (1965).

22. (a) D. F. Evans, C. Chen, and B. C. Lamartine, J. Am. Chem. Soc., 99, 6492 (1977).; (b) D. F. Evans, T. Tominaga, and C. Chan, J. Solution Chem., 8, 461 (1979).; (c) H. T. Davis, T. Tominaga, and D. F. Evans, AIChE J, 26, 313 (1980).; (d) D. F. Evans, H. T. Davis, and T. Tominaga, J. Chem. Phys., 74, 1298 (1981).

23. S. H. Chen, H. T. Davis, and D.F. Evans, J. Chem. Phys., 77, 2540 (1982).

24. (a) K. Mckeigue and E. Gulari, J. Phys. Chem.,88, 3472 (1984).

25. J. A. Roberts, X. Zhang, and Y. Zhang, J. Chem. Phys., 100, 1503 (1994).; (b) M. M. Marting, Chem. Phys. Lett., 43, 332 (1976).

26. (a) D. S. Viswanath, G. Natarajan, *Data book on the Viscosity of Liquids* (Hemisphere, New York ,1989).; (b) P. A. Egelstaff, *An Introduction to the Liquid Stat* (Academic, New York, 1976).

27. J. Timmermans and Y. Delcourt, J. Chem. Phys., 31, 85 (1934).

28. (a) S. Mizushima, Bull. Chem. Soc., (Japan) 1, 143 (1926).; (b) T. W. Phillips, K. P. Murphy, J. Chem. Eng. Data, 15, 304, (1970).; (c) M. A. Rauf, G. H. Stewart, and Farhataziz, J. Chem. Eng. Data, 28, 324 (1983).

29. M. Terazima, and H. Hamaguchi, J. Phys. Chem., 99, 7891 (1995)

30. M. Terazima, S. Tenma, H. Watanabe, and T. Tominaga, J. Chem. Soc. Faraday Trans., 92, 3057 (1996).

$$M \xrightarrow{\text{photoexcitation}} {}^1M^{**} \quad \text{(a)}$$

$${}^1M^{**} \xrightarrow{\text{internal conversion}} {}^1M^{*} \quad \text{(b)}$$

$${}^1M^{*} \xrightarrow{\text{intersystem crossing}} {}^3M^{*} \quad \text{(c)}$$

$${}^3M^{*} + RH \xrightarrow{\text{hydrogen abstraction}} MH^{\bullet} + R^{\bullet} \quad \text{(d)}$$

$$2MH^{\bullet} \xrightarrow{\text{recombination}} (MH)_2 \text{ or } M + MH_2 \quad \text{(e)}$$

Scheme 3-1

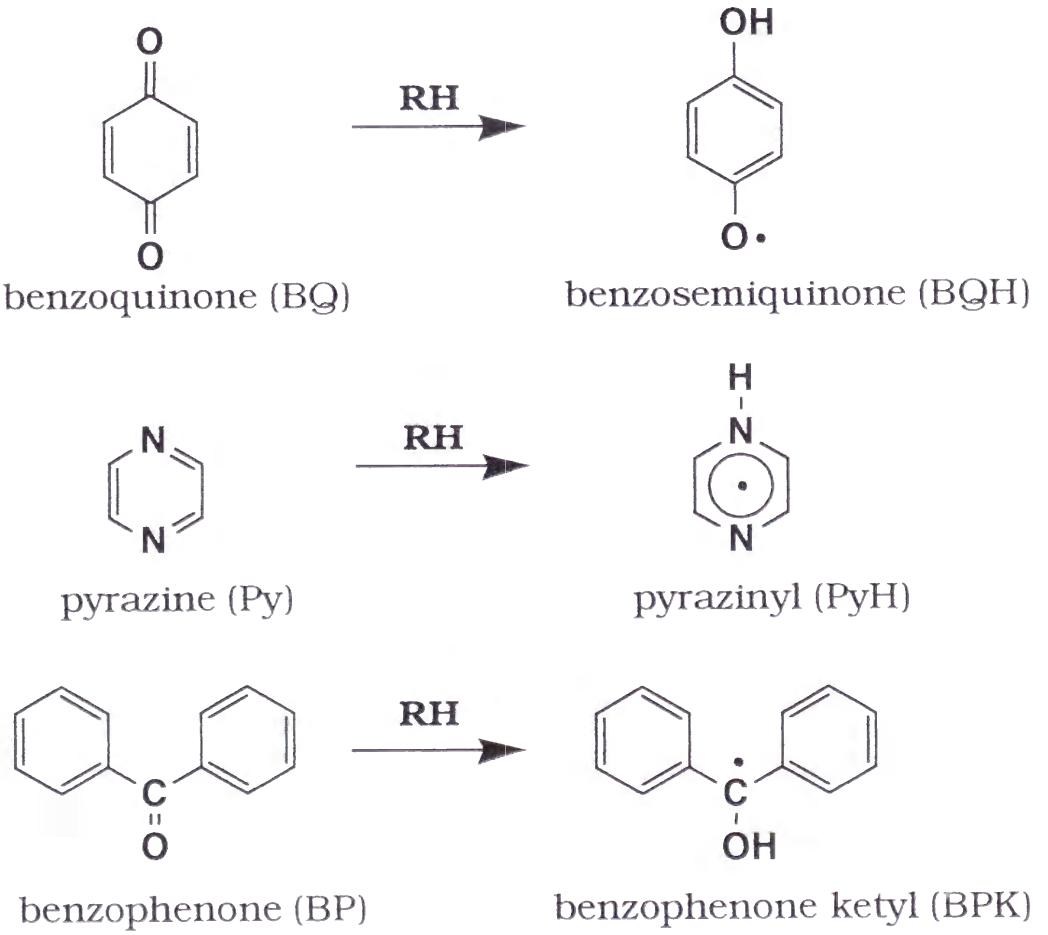

Scheme 3-2

Table 3-1 Diffusion constants (D) of the transient radicals (D_R) and parent molecules (D_P) obtained by the TG method in 2-propanol at ~23 °C. D_{SE} and D_{EV} are the calculated value from Stokes-Einstein and Evans et al. equation, respectively at ~20 °C. D_{PGSE} are D of the parent molecules obtained by the PGSE method at ~30 °C. D_{TG} are reported D of the parent molecules by the TD method at ~25 °C (ref. 16).

	Diffusion constants (10^{-9} m^2s^{-1})					
Solute	D_R	D_P	D_{SE}	D_{EV}	D_{PGSE}	D_{TD}
Benzoquinone	0.36±0.03	0.98±0.11	0.34	0.95	1.1	0.94
Benzophenone	0.33±0.02	0.68±0.13	0.26	0.54	0.65	0.57
Pyrazine	0.38±0.03	1.2±0.2	0.35	1.02	1.5	0.92

Table 3-2 The activation energies for diffusion of the transient radicals created by a photoinduced hydrogen abstraction reaction (E_R) and their parent molecules (E_P) in 2-propenol and ethanol. For comparison, the activation energy of solvent viscosity are E_η=5.854 kcal/mol in 2-PrOH, E_η=3.957 kcal/mol in EtOH.

solute	E_R	E_P	E_R	E_P
	(/ kcal mol-1 in 2-PrOH)		(/ kcal mol-1 in EtOH)	
acetone	4.85±0.20			
acetoaldehyde			3.23±0.31	
benzophenone	5.12±0.10	4.34±0.12	3.53±0.20	3.16±0.13
benzaldehyde	5.21±0.06	4.08±0.04	3.70±0.03	2.85±0.05
acetophenone	5.19±0.05	4.45±0.12	3.43±0.06	3.15±0.12
benzoquione	5.06±0.31	4.36±0.29	3.52±0.07	2.62±0.09
pyrazine	4.87±0.26	4.37±0.52	3.61±0.10	3.09±0.22
phenazine	5.16±0.15	4.17±0.27	3.44±0.13	3.07±0.26
xanthone	5.07±0.13	4.40±0.09	3.50±0.09	3.22±0.14
2.2.biquinoline	5.30±0.31	4.56±0.28	3.53±0.15	3.46±0.08

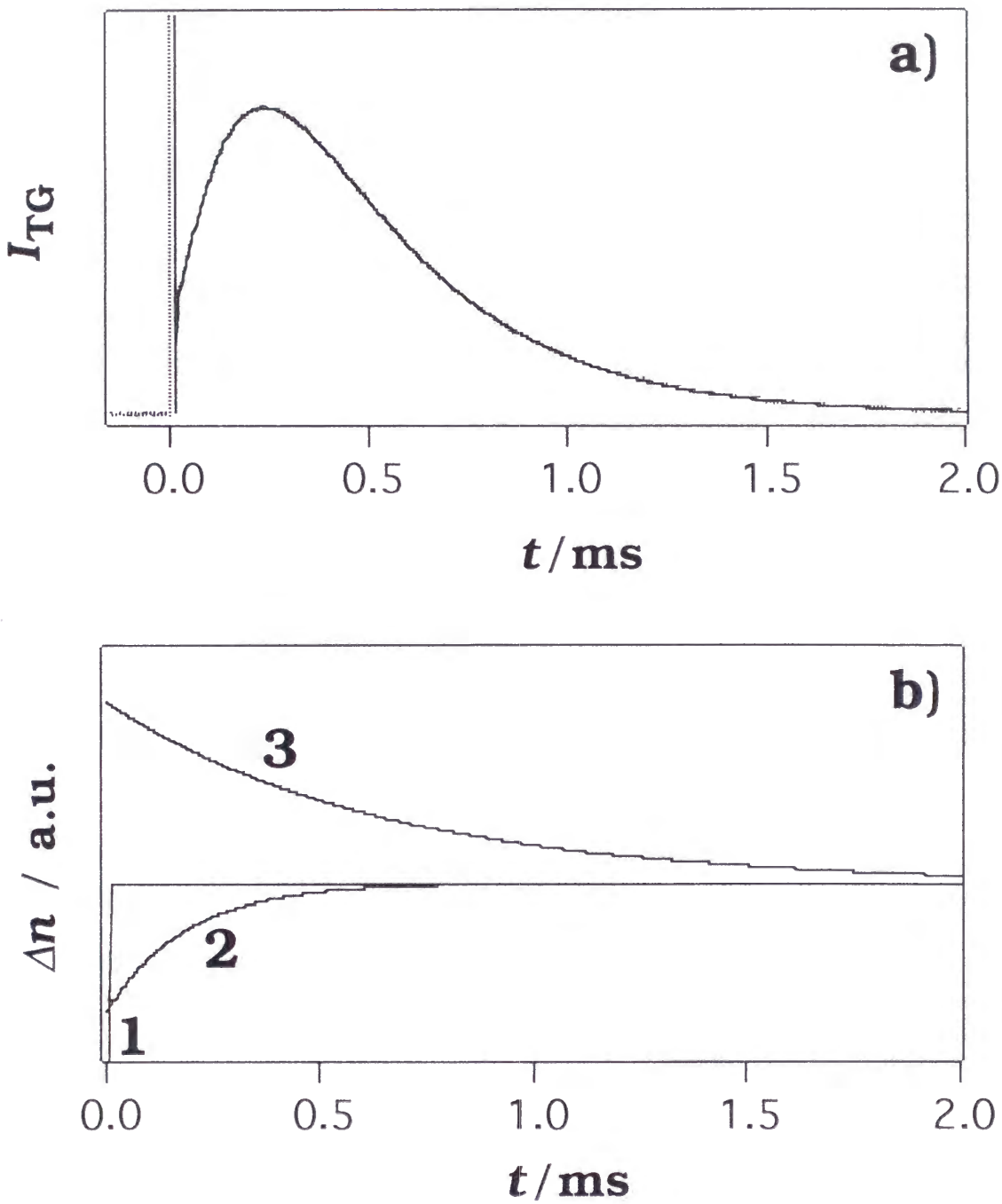

Fig. 3-1 (a) Typical temporal profile of the TG signal ($I_{TG}^{1/2}$) after the photoexcitation of benzoquinone in 2-propanol under the nitrogen-bubbled condition at room temperature (dotted line) and the best-fitted curve by eq. (3-1) (solid line). (b) Phase grating contributions to the signal in (a) as given by the fitting procedure described in the text. The assignments of these component are (1) the thermal grating, (2) the species grating of benzoquinone, and (3) the species grating of benzosemiquinone radical.

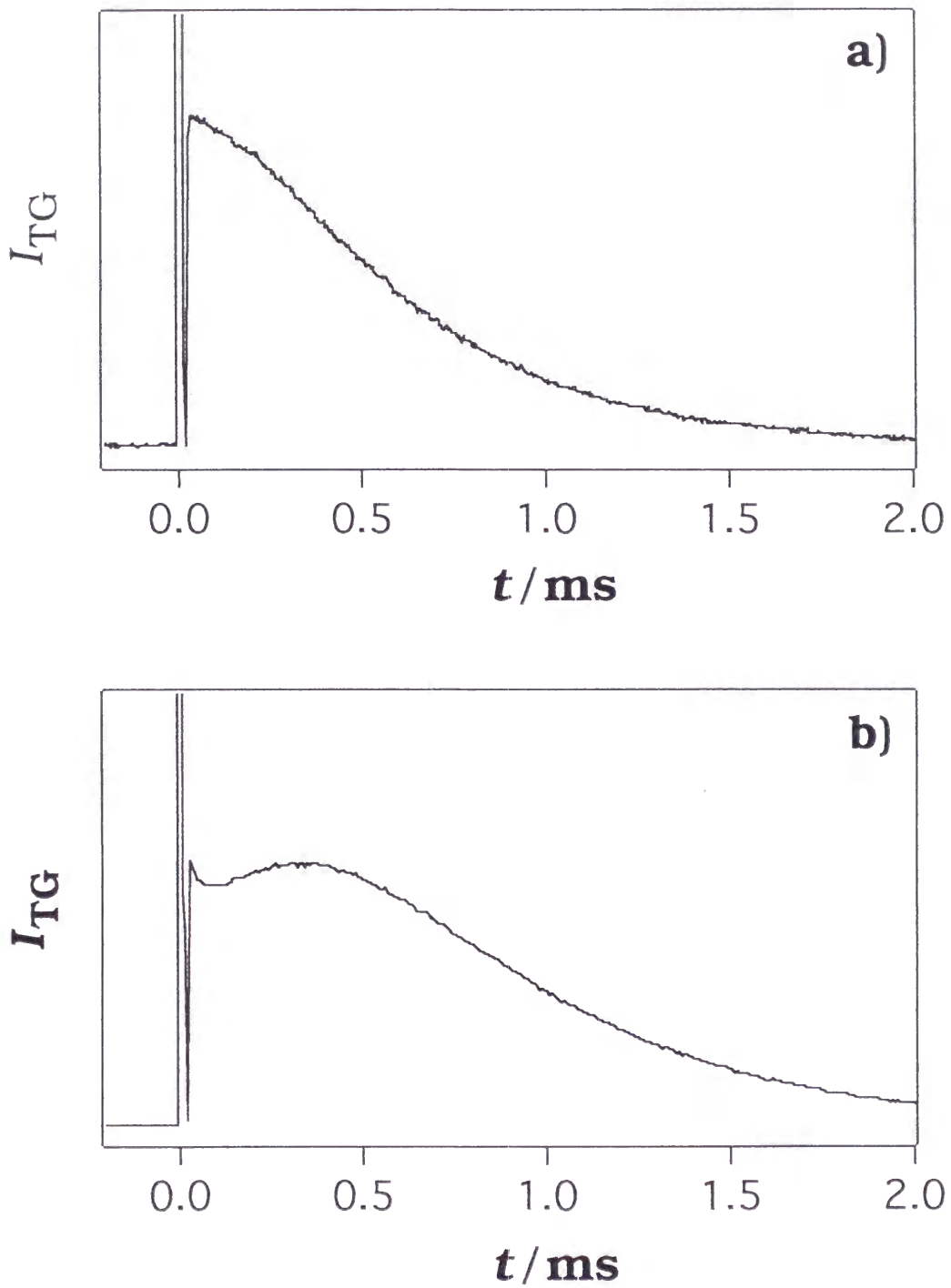

Fig. 3-2 Temporal profile of the TG signals after the photoexcitation of (a) pyrazine/2-propanol and (b) benzophenone/2-propanol at room temperature.

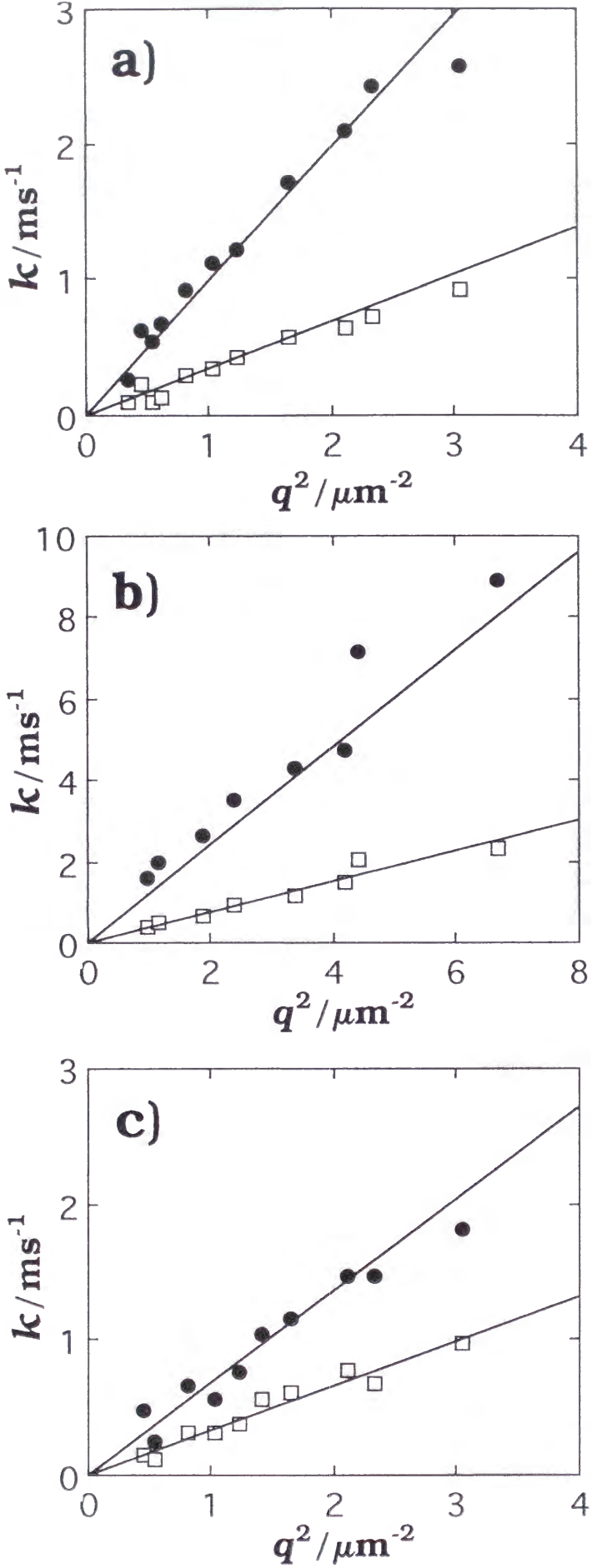

Fig. 3-3 Plot of the decay rate constants of TG signals due to the mass diffusion process of k_2 (circles) and k_3 (squares) against the square of the grating vector (q^2) of (a) benzoquinone, (b) pyrazine, and (c) benzophenone in 2-propanol.

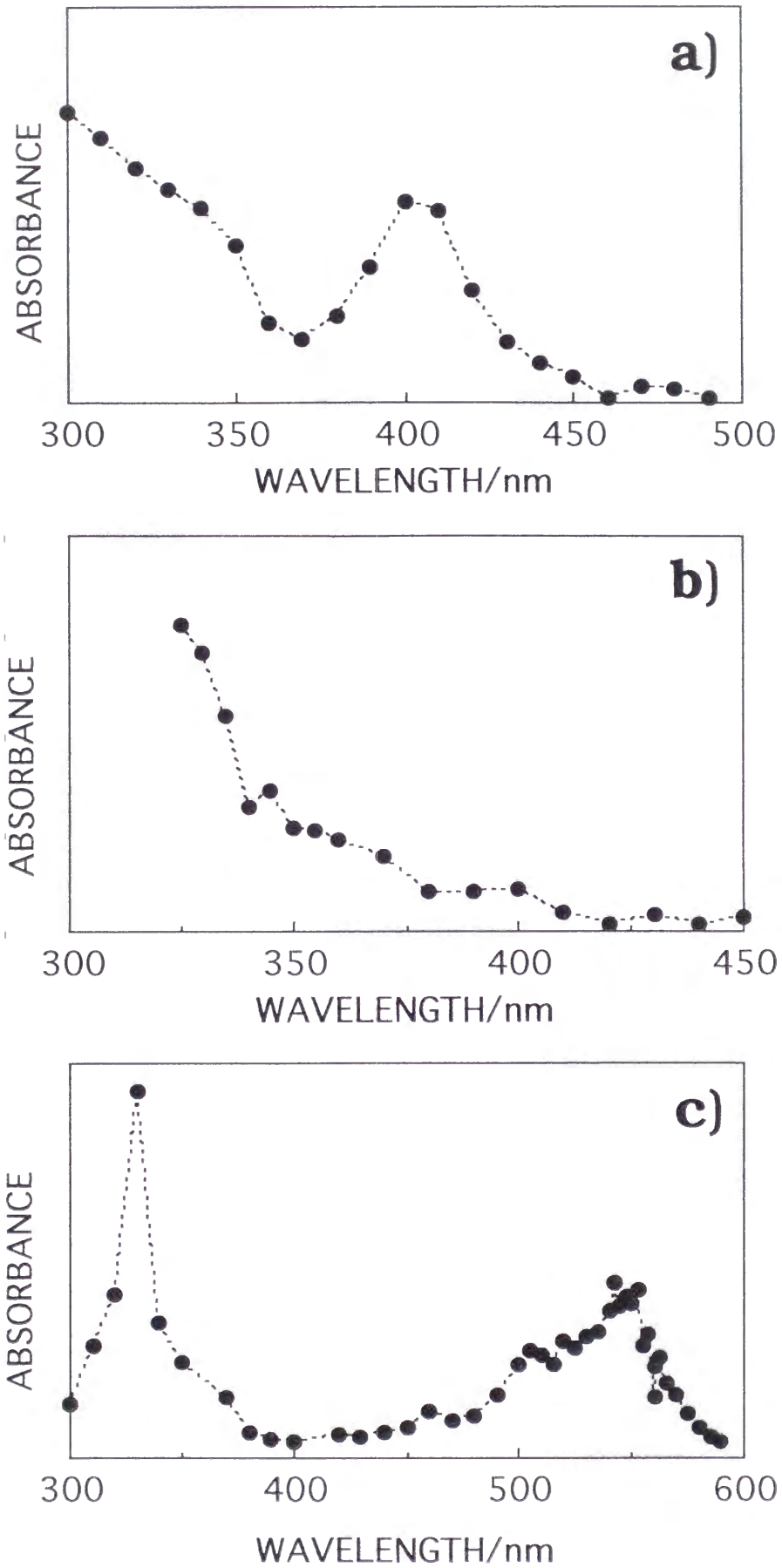

Fig. 3-4 Transient absorption spectra at a 100μs time delay after the excitation of (a) BQ in 2-PrOH, (b) Py in 2-PrOH, and (c) BP in 2-PrOH.

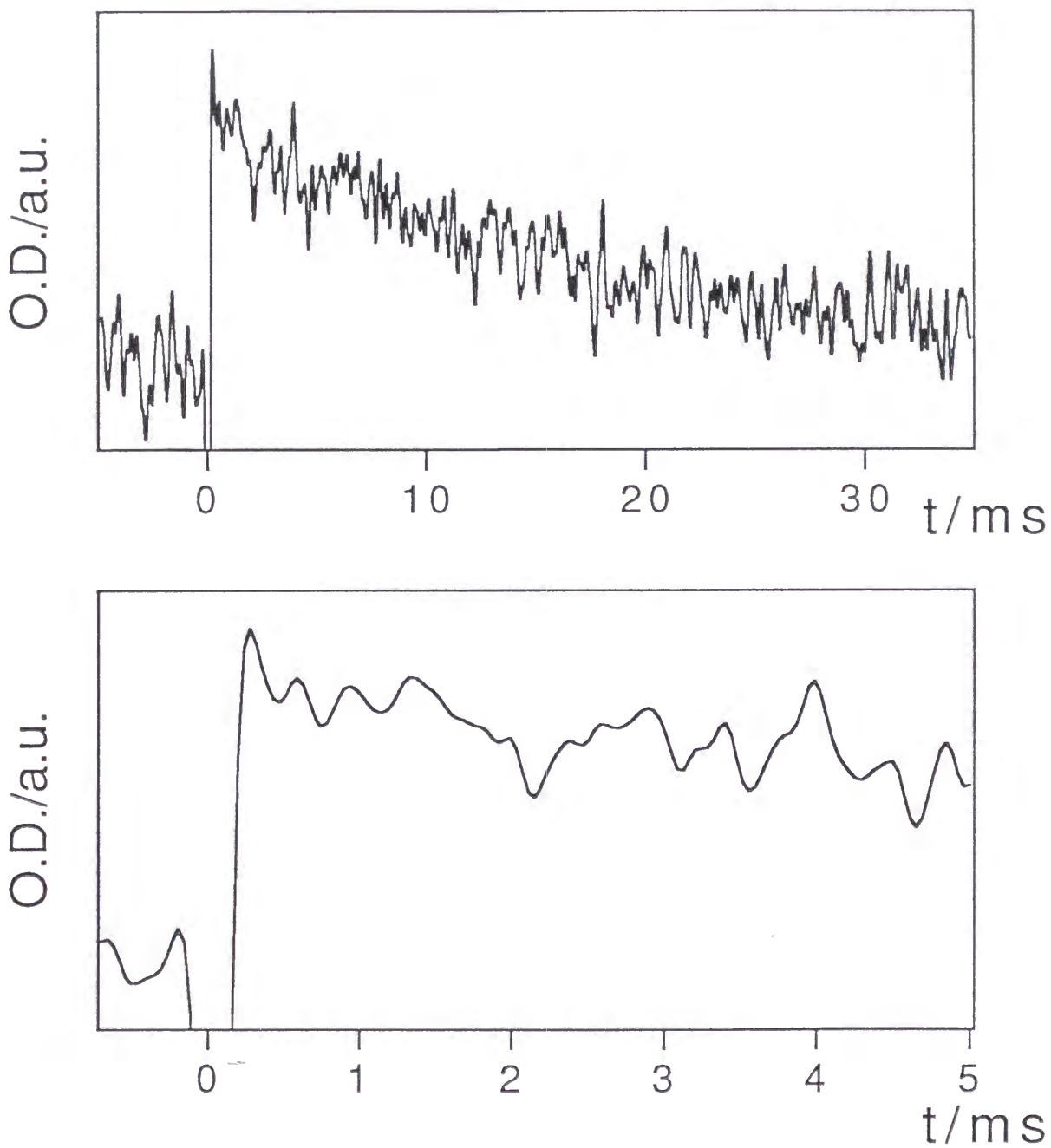

Fig. 3-5 Time profile of the transient absorption signal after the photoexcitation of benzoquinone in 2-propanol detected at 400 nm (upper). The negative spike around t ~ 0 is due to the scattering light of the excitation. Lower; the above profile is expanded in time to clearly show that the decay of the radical in the TG measurement is negligible.

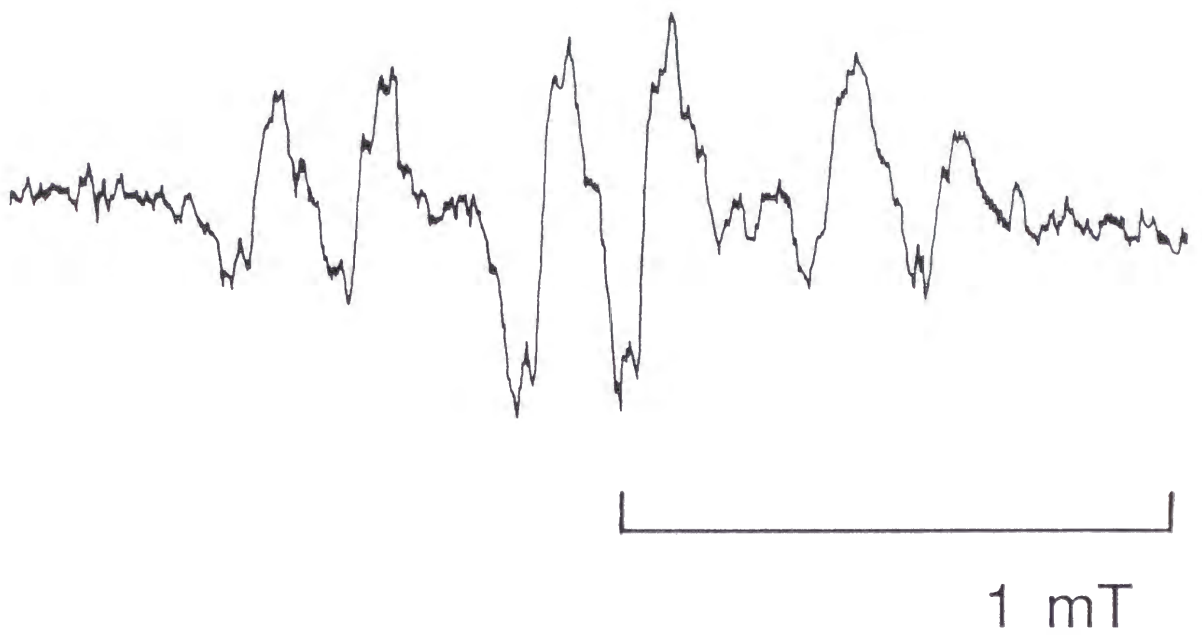

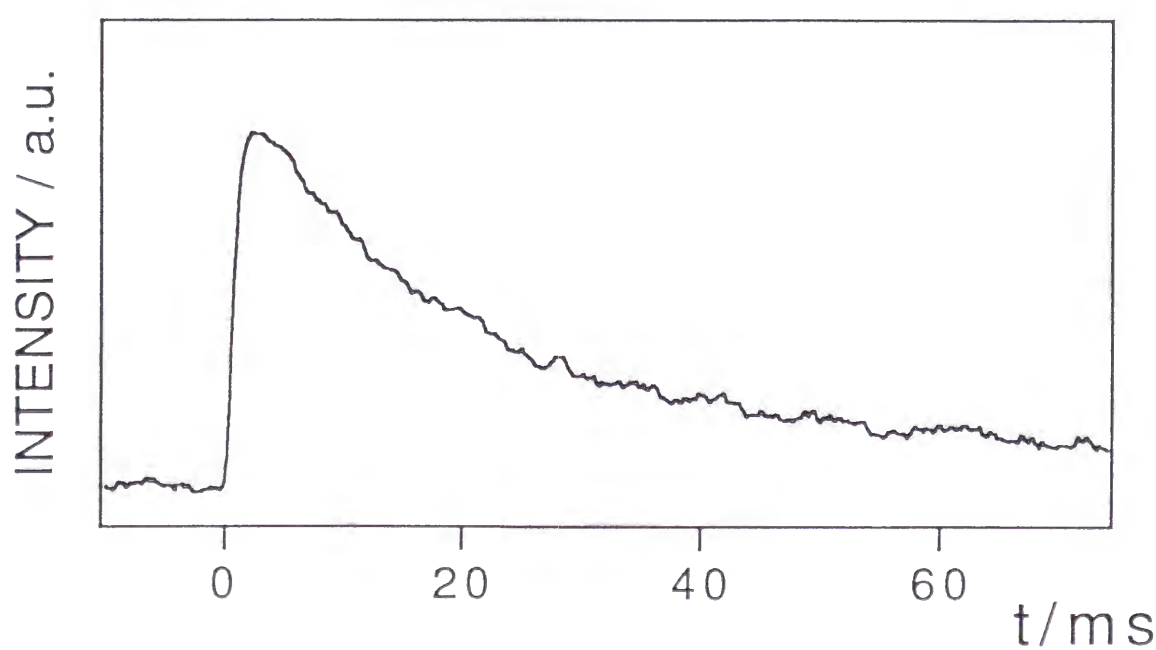

Fig. 3-6 A cw EPR spectrum measured during the pulsed laser photoexcitation of benzoquinone in 2-propanol with 20 Hz (upper) and a decay curve of the EPR signal (lower).

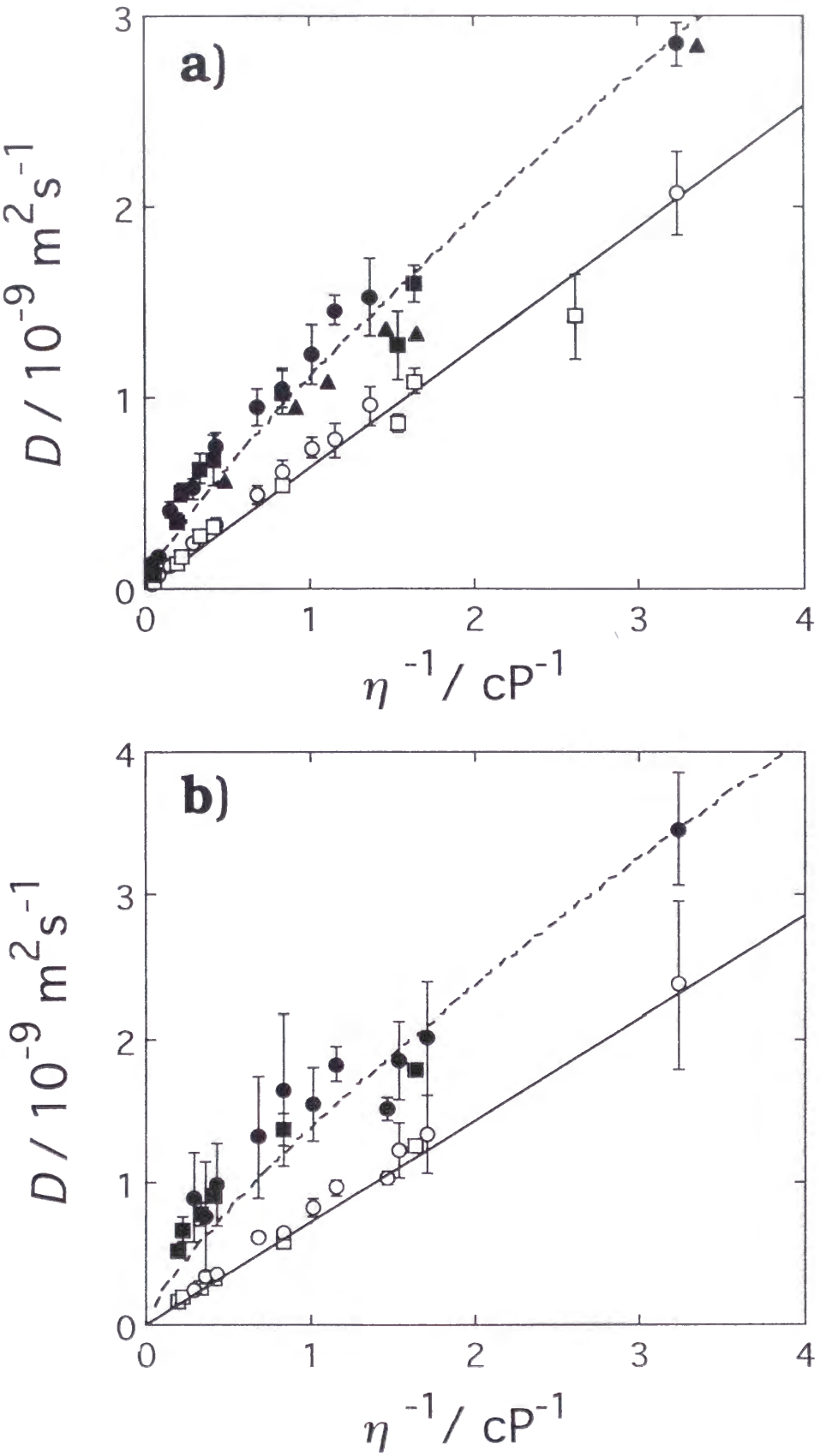

Fig. 3-7 Viscosity dependence of D_R (closed marks) and D_P (open marks) of (a) benzophenone and (b) acetophenone in polar (squares) and non-polar (circles) solutions. D_P determined from the TD method are presented by triangle (ref. 16). The broken line is D calculated from the equation proposed by Evans et al. [eq. (3-5)]. The solid line is D calculated from the Stokes-Einstein equation [eq. (3-4)].

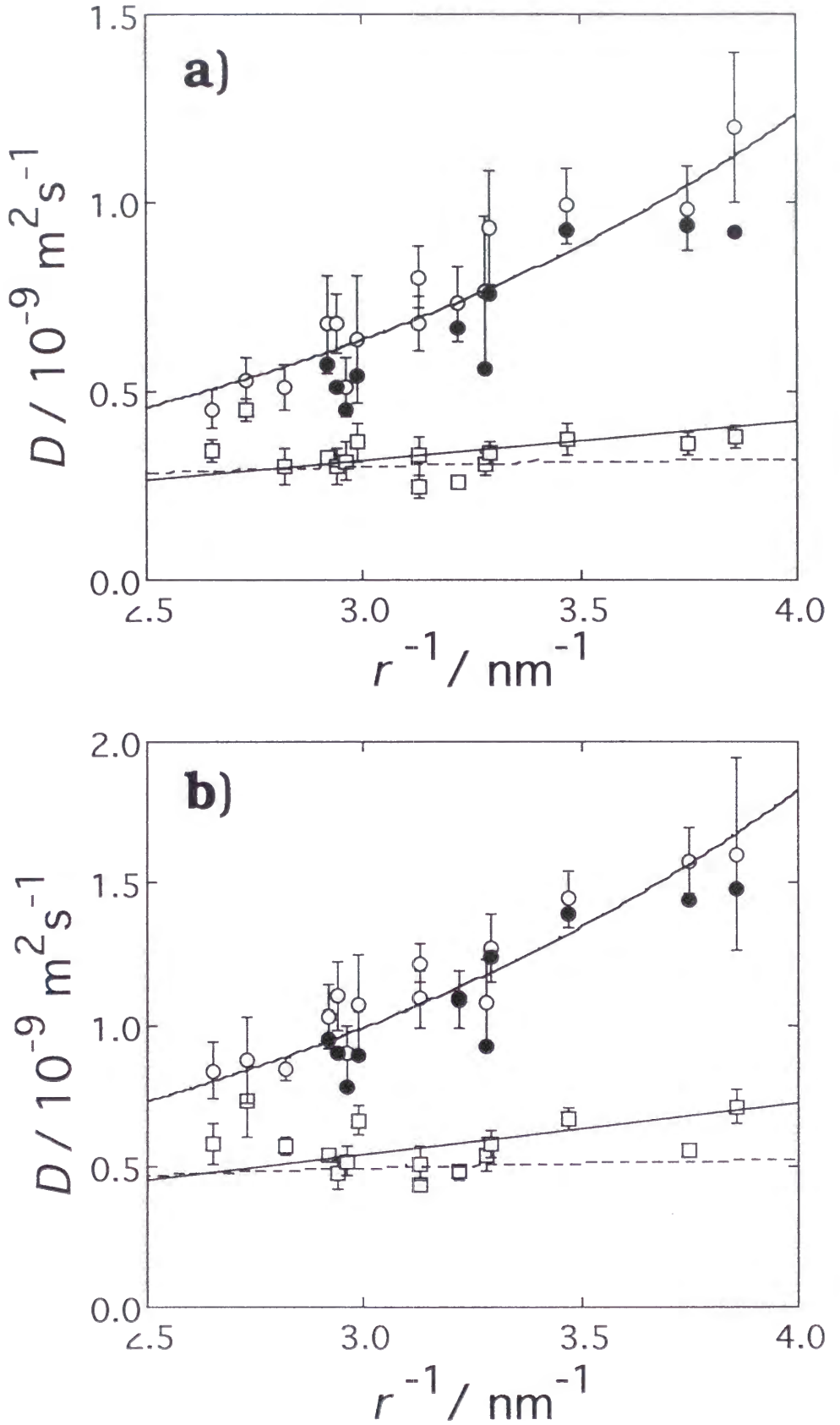

Fig. 3-8 Molecular size dependence of D_R (squares) and D_P (open circles) in (a) 2-propanol and (b) ethanol. D_P determined from the TD method are presented by closed circle (ref. 16). The curved solid line, straight solid line, and broken line are D calculated by the equation proposed by Evans et al. [eq. (3-5)], the SE equation [eq. (3-4)], and the excess volume model [eq. (3-15)] with $V_o = 5X10^2$ Å^3.

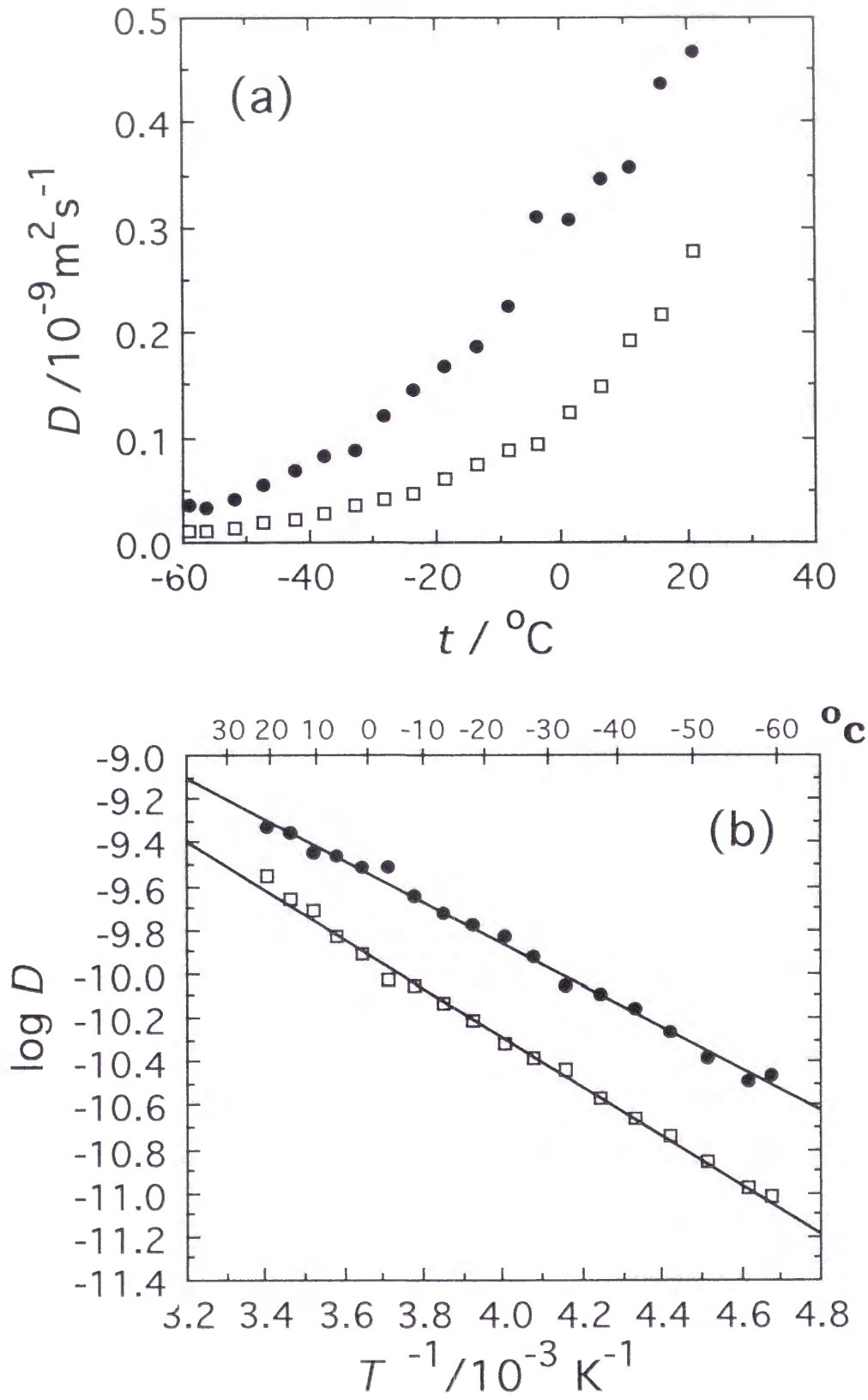

Fig. 3-9 (a) Temperature dependence of D obtained from the TG signals and (b) plot of log D vs. 1/T (Arrhenius plot) of BPK (□) and BP (●) in 2-PrOH.

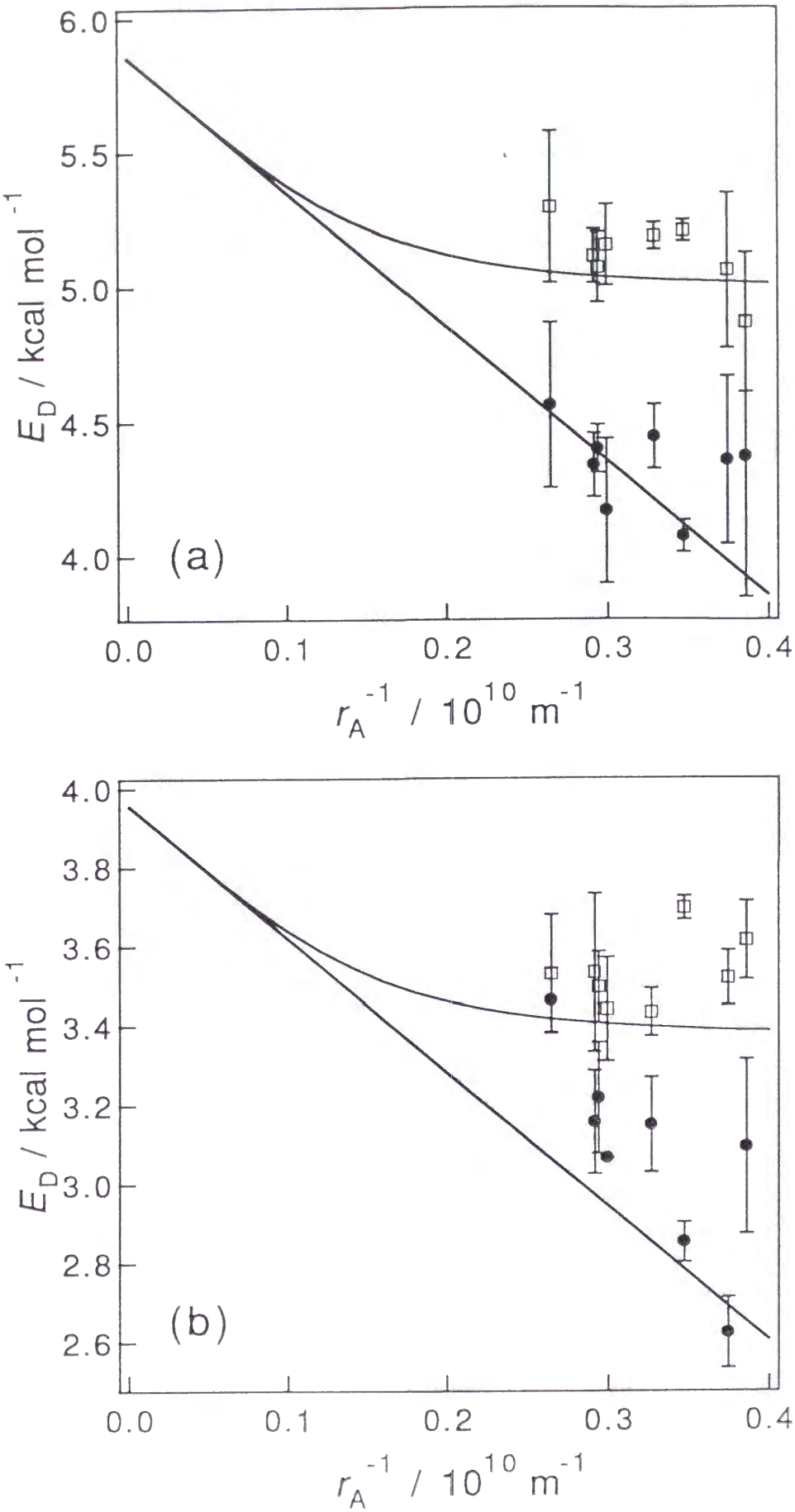

Fig. 3-10 Plot of the activation energies for diffusion of the radicals (□) and of the parent molecules (●) vs. radii of the solutes in (a) 2-PrOH and (b) EtOH. Straight line is the calculated one for the parent molecules from D_{EV} [eq. (3-11)]. Curved line is calculated one for the transient radicals from eq. (3-14) with $V_o = 8 \times 10^2$ Å^3.

Chapter 4

DIFFUSION OF THE BENZYL RADICALS CREATED BY PHOTODISSOCIATION

4.1 Photochemical Reaction of Photodissociation.

An anomalously slow diffusion of the hydrogen abstracted radicals should be due to a strong intermolecular interaction between the radicals and the surround molecules. The origin of such a strong molecular interaction of the radicals is still unclear. However, the difference between the radicals and the parent molecules is only the unpaired electron. That electron may lead to the anomalously slow diffusion process of the radicals. We must examine the role of the unpaired electron in affecting the diffusion process in solution. So far we have mostly studied the diffusion of the radicals created by photoinduced hydrogen abstraction reactions. [1-4] In this chapter, we measure D of the benzyl radical (BR), which is created by the photodissociation reaction from dibenzyl ketone (DBK). [5] We have two aims in this study. First, since BR frequently appears in chemical reactions as an intermediate radical, it would be interesting and important to know the diffusion constant of BR for the analysis of the chemical reaction. Second, D of BR is compared with those of other transient radicals created by the hydrogen abstraction reactions to see if there is a noticeable difference in D. If there is a difference, a detailed comparison of the molecular character could provide an insight into the mechanism of the slow diffusion of many transient radicals.

The photodissociation process of DBK has been studied extensively in various solvents.[6~16] The reaction scheme is shown in scheme 4-1. The lowest excited triplet (T_1) state of DBK is created by the intersystem crossing from the lowest excited singlet (S_1) state within a picosecond

time scale after the UV irradiation (process a~c). The α cleavage of the C-CO bond (Norish type 1) occurs from the excited triplet state of DBK and brings BR and the phenylacetyl radical within a few nanoseconds (process d).[6] Successively, carbon monoxide (CO) is separated from the phenylacetyl radical in a few hundred nanoseconds at room temperature in the solution phase and another BR is produced (process e).[7] The quantum yield of the photodissociation of DBK has been reported to be ~0.7.[8] BR is known as a relatively stable radical because the unpaired electron of BR is delocalized into the phenyl ring.[17] The recombination reaction of two BR to bibenzyl is a dominant subsequent reaction compared with a reaction between BR and the solvent molecules (process f). It has been reported that the reaction process of the self-termination of BR is a pseudo-diffusion-controlled reaction and the steric factor of this reaction is 0.8.[9] The rate constant ($2k_2$) of such a second ordered reaction has been measured in various solvents and it is reported to be ~$10^9 M^{-1}s^{-1}$ as discussed in a later section.[10~16]

We first examine the chemical stability of BR during the observation time range of the TG signal by the TA method. Fig. 4-1a shows the transient absorption spectrum monitored at 10μs after the photo excitation of DBK in 2-propanol (0.01M). This spectrum is in excellent agreement with the reported absorption spectrum of BR.[18] The time profile of the TA signal of BR is shown in Fig. 4-1b. The decay profile can be expressed well by the second-order self-termination reaction with $\tau_{1/2}=1/2k_2C(0)=150\mu s$ [C(0): initial concentration of BR] in 2-propanol at the excitation laser power ~1.3mJ/cm^2. The excitation laser power dependence of $2k_2C(0)$ is shown in Fig. 4-2a. Figure 2b shows the $\Delta OD = C(0) \cdot \varepsilon_{Max}$ at the peak of the extinction coefficient (ε_{Max}) of BR (314nm) plotted against the excitation laser power. ΔOD is proportional to the laser power, which indicates that the one photon excitation process is dominant within this range of the laser power.

4.2 Time Dependence of the TG Signals.

Figure 4-3 shows that the time dependence of the TG signal after the photoexcitation of DBK in 2-propanol. Similar signals were obtained in other solvents (n-hexane, cyclohexane, and ethanol). In a rather fast time scale (Fig. 4-3 a), three components are observable in the TG signal. The fast component decays in a few microseconds and an intermediate component decays in a few

tens of microseconds. Finally there is a background signal which does not decay to the baseline completely in this time scale. In a wider time range and an enlarged vertical scale (Fig. 4-3b), the slower component becomes apparent, and we found that the signal consists of a slow rise and a slow decay. The signal decays to the baseline completely in this time scale.

On the basis of a theoretical prediction as described later, we tried to reproduce the square root of the observed TG signal ($I_{TG}(t)^{1/2}$) with a four-exponential function [eq. (4-1)].

$$I_{TG}(t)^{1/2} = A_a \exp(-k_a t) + A_b \exp(-k_b t) - A_c \exp(-k_c t) + A_d \exp(-k_d t) \qquad (4\text{-}1)$$

where $k_a > k_b > k_c > k_d$, and $A_a \sim A_d > 0$ are the pre-exponential factors. By using the non-linear least-squares method, the TG signal can be fitted very well by eq. (4-1) as shown in Fig. 4-3c. Generally a rather large ambiguity is expected for the curve fitting with four exponential functions. However, in this case, since the time constants of the three components are very different [e.g., k_a=1.3 μs^{-1}, k_b=89 ms^{-1}, and (k_c=13 ms^{-1} and k_d=11 ms^{-1}) for the q^2=19 μm^{-2} case] and the signs of A_c and A_d are opposite, they can be easily separated. Even though k_c and k_d are rather close, the determined values are stable for varying the initial values for the least square method. The errors of the time constants obtained by this fitting are less than 10%. The TG signals observed in other solvents can be fitted by the same manner.

4.3 Origin of the TG Signals.

Any sinusoidally modulated refractive index or absorbance gives rise to the TG signal.[19] In this reaction system, no absorbance change was observed after the photoexcitation at the probe wavelength (633nm) as reported previously [18,20] and as confirmed in the previous section. Hence, we consider only the refractive index change as the cause of the TG signal. Apparently, the fastest decaying component (A_a) should be originated from the modulation of the temperature (thermal grating) caused by the non-radiative transitions of the photoexcited molecules (process a~c in scheme 4-1). The decay of the thermal grating signal is determined by the heat conduction process. By solving the thermal diffusion equation with an appropriate initial condition, the time

dependence of the temperature variation [$\Delta T(t, q)$] is expressed by eq. (2-14a). Comparing eq. (2-14a) with eq. (4-1), we obtain,

$$k_a = D_{th} q^2 \tag{4-2}$$

The thermal diffusion constant (D_{th}) determined from the TG signals in these solvents are in excellent agreement with the literature values in ref. 21. The other slower TG signal must represent the dynamics of chemical species.

As described in introduction, the photochemical reaction of DBK has been extensively studied (scheme 4-1). The photodissociation of DBK creates CO and BR. Therefore, three chemical species CO, BR and DBK could contribute to the TG signal. On the basis of these considerations, the TG signal obtained from this reaction system should be described as

$$I_{TG}(t)^{1/2} \propto \Delta n = \left(\frac{dn}{dT}\right)\Delta T(t) + \left(\frac{dn}{dC_{CO}}\right)C_{CO}(t) + \left(\frac{dn}{dC_{BR}}\right)C_{BR}(t) - \left(\frac{dn}{dC_{DBK}}\right)C_{DBK}(t) \tag{4-3}$$

where dn/dC_{CO}, dn/dC_{BR}, and dn/dC_{DBK} are the concentration dependence of the refractive index change by the presence of CO, BR, and DBK, respectively, and $C_{CO}(t)$, $C_{BR}(t)$, and $C_{DBK}(t)$ are the time response functions of the peak-null difference of the concentrations of these species. Since DBK is depleted in the bright region of the interference pattern, the sign of the DBK term is minus. As the refractive index decreases with the increase of the temperature, the refractive index change of the thermal grating is negative ($dn/dT < 0$). Since all of the absorption bands of both BR and DBK are located in a wavelength region shorter than the probe wavelength, the presence of both BR and DBK creates a positive refractive index change at the probe wavelength (dn/dC_{BR}, $dn/dC_{DBK} > 0$). According to the Kramers-Kronig relation and the absorption bands of CO, the refractive index change by the presence of CO is expected to be positive, too. However, the creation of CO increases the volume of the system so that a part of the space which is filled by the solvent molecule is placed by CO. Since the polarizability of CO is smaller than that of the solvent, the refractive index change by the creation of CO becomes negative ($dn/dC_{CO} < 0$) as previously shown by our

group.[22] On the basis of these considerations, it is concluded that only the dn/dC_{BR} term in eq. (4-3) gives a positive contribution, and the other contributions should be negative. Considering these signs in eq. (4-3) and the decay rate constants of the TG signal which are determined mainly by the diffusion constants of the chemical species as discussed in a later section, the fitted components, A_a, A_b, A_c and A_d in eq. (4-1) are attributed to dn/dT, dn/dC_{CO}, dn/dC_{BR}, and dn/dC_{DBK}, respectively.

$C_{CO}(t)$, $C_{BR}(t)$, and $C_{DBK}(t)$ are governed by the translational diffusion and subsequent chemical reactions of the transient species. The time dependence can be obtained from the following differential equations [See eq. (2-13)]

$$\frac{\partial C_i(x,t)}{\partial t} = D_i \frac{\partial^2 C_i(x,t)}{\partial x^2} - f_i(x,t) \qquad (4\text{-}4)$$

where i represents the chemical species (CO, BR, or DBK). $C_i(x, t)$ and $f_i(x, t)$ are time and space dependent concentrations and reaction velocities of these species, respectively.

In the case of the stable molecules, DBK and CO, the time profiles of the concentration modulation are determined by only the diffusion process ($f_i(x, t)=0$). The solution of this equation is given by

$$\hat{C}_i(q,t) = \hat{C}_i(q,0) \exp(-D_i q^2 t) \qquad (4\text{-}5)$$

where $\hat{C}_i(q, t)$ is the q-component of the Fourier transform of $C_i(x, t)$ [See eq. (2-14b)]. Therefore, by comparing eq. (4-5) with eq. (4-1), we obtain,

$$k_{CO} = D_{CO} q^2$$

and $$k_{DBK} = D_{DBK} q^2 \qquad (4\text{-}6)$$

The q^2 dependences of k_{CO} and k_{DBK} are shown in Fig. 4-4. The plots of CO and DBK show a good linear relationship with a negligibly small intercept with the ordinate axis, which agrees with

the prediction of eq. (4-6). D_{CO} and D_{DBK} in other solvents obtained from the slope of similar plots are listed in Table 4-1.

4.4 Analysis of the TG Signals from BR

The plot of k_{BR} vs. q^2 also shows a linear relationship in a certain q^2 range, but it deviates from the liner relation in a small q^2 range. The non linear behavior suggests that the modulation of the BR component decays by not only the diffusion process but also subsequent chemical reactions. If this reaction proceeds with the first-order reaction [$f(t)=k_1C(x, t)$], the solution of eq. (4-4) is given by

$$\hat{C}_{BR}(q, t) = \hat{C}_{BR}(q, 0) \exp [(- D_{BR} q^2 + k_1) t] \qquad (4\text{-}7)$$

The decay rate constants (k) of the TG signal in eq. (4-1) is given by

$$k = D_{BR} q^2 + k_1 \qquad (4\text{-}8)$$

Therefore, the intercept of the k vs. q^2 plot gives k_1 and the slope gives D_{BR}. However, previous researches on the BR reaction indicates that the main reaction of BR is the self-termination reaction and we also confirm it as described in section 4.1. In this case, eq. (4-4) should be described with $f(x, t)=2k_2C(x, t)^2$ and the differential equation can no longer be solved analytically, but numerical analysis is required. Here, we first consider an analytical treatment with a short time approximation and then the result is compared with the numerical result.

If we ignore the diffusion process in eq. (4-4), the time dependence of C(t) is described as

$$C(t) = \frac{C(0)}{1+2k_2C(0)\ t} \qquad (4\text{-}9)$$

During a short period after the excitation, in which a condition of

$$1+2k_2C(0)\ t >> \frac{(2k_2C(0)\ t)^2}{2!} + \cdots + \frac{(2k_2C(0)\ t)^n}{n!} + \cdots \qquad (4\text{-}10)$$

is satisfied, the second-order reaction can be approximated by the first-order reaction with a rate constant of $2k_2C(0)$. Under this approximation, the solution of eq. (4-4) is given by

$$\hat{C}_{BR}(q, t) = \hat{C}_{BR}(q, 0) \exp \{ [- D_{BR} q^2 t + 2k_2C(0)] t \} \qquad (4\text{-}11)$$

and the decay rate constant (k) of the square root of the TG signals is given by

$$k = D_{BR} q^2 + 2k_2C(0) \qquad (4\text{-}12)$$

Therefore as long as the short time approximation is correct, the TG signal can be analyzed with an exponential function and the intercept and the slope of the k vs. q^2 plot give $2k_2C(0)$ and D_{BR}, respectively.

To obtain a reliable fitting by eq. (4-11), we should make the fitting range for the least square method as wide as possible. Normally, the data up to a time when the square root of the TG signal intensity ($I_{TG}^{1/2}$) becomes 1/20 of the initial intensity of the species grating signal is used. For satisfying the short time approximation during this fitting range, we should limit the TG measurement in a rather large q^2 range. Neglecting the subsequent reaction, the TG signal decays to the ~1/20 intensity at around

$$D q^2 t \sim 3 \qquad (4\text{-}13)$$

by the diffusion process. Therefore, combining with eq. (4-12), we can conclude that the TG signal measured in a range of

$$\frac{Dq^2}{k_2C(0)} > 4 \qquad (4\text{-}14)$$

can be used for determining D from the k vs, q^2 plot. In other words, the TG signal measured in this range can be analyzed as if the subsequent reaction is the first order decay with a rate constant of $2k_2C(0)$. We solve the second ordered reaction-diffusion coupled equation [eq. (4-4) with $f(x,t)=2k_2C(x,t)^2$] numerically to examine this applicable range [eq. (4-14)]. Fig. 4-5 shows C(q, t)/C(q, 0) calculated numerically by eq. (4-4) (solid lines) and calculated by eq. (4-11) (doted lines) for $Dq^2/k_2C(0)$ = 1,2,4 and 6. Evidently from the figure, when eq. (4-14) is satisfied, the time profile from eq. (4-4) is sufficiently close to that from eq. (4-11) within the experimental error of this work (±10%).

In this way, we judged that the first and second points of the plot (Fig. 4-4) are out of the range of $q^2 > 4k_2C(0)/D_{BR}$. Therefore, we fit the other data by the least-squares method without these two points. The results of this fitting give $D_{BR}=0.64m^2s^{-1}$, $2k_2C(0)=1.31ms^{-1}$ in 2-propanol. The values of D_{BR} and $2k_2C(0)$ in various solvents determined by this method are listed in Table 4-1.

Next, a consistency of the results from the TG experiment and from the TA experiment is examined. The plot of $2k_2C(0)$ against the laser power from the transient absorption (Fig. 4-2b) shows $2k_2C(0)=1.6ms^{-1}$ at 0.3 mJ/cm^2 (a typical laser power for the TG measurement). The reaction rate obtained from the plot of the decay rate vs. q^2 ($1.3ms^{-1}$) is close to $2k_2C(0)$ from the transient absorption measurement. Therefore we believe that the above procedure for determining D_{BR} from the k vs. q^2 plot is adequate.

We further confirm the adequacy of our TG analysis by independent measurement of D_{DBK}. Though D of the transient species BR cannot be measured by other traditional methods, D of the stable parent molecule DBK can be measured besides the TG method. We use the PGSE method for D_{DBK}. The values of D_{DBK} determinedby the PGSE method at 30°C are shown in Table 4-2. This table also shows similar comparisons of D of benzophenone, pyrazine, and benzoquinone which have been reported in chapter 3 (table 3-1). All of D obtained by the PGSE method are very close to the values determined by the TG method. D_{CO} obtained by this work agrees with D reported in ref. 23 fairy well. This fact again supports the assignment of the signal.

At the laser power for the TG experiment ($0.3mJ/cm^2$), $\Delta OD=C(0) \cdot \varepsilon_{Max}$ is 0.006 and

k_2/ε_{Max}=1.19x10^{5}M^{-1}s^{-1}. This value is used to estimate the value of k_2 and C(0) in a later section. The initial concentration of BR (C(0)) at the condition of the TG measurement (~0.3mJ/cm^2) is estimated to be 5.0x10^{-7}~5.5x10^{-6} M from the reported ε_{Max} =1100~12000cm^{-1}M^{-1} as described in the next section. This value of C(0) is consistent with the estimated value (~10^{-6} M) from the excitation laser power (~0.3 mJ/cm^2), the extinction coefficient of DBK at 308nm (~200cm^{-1}M^{-1}) [20], and the quantum yield of photodissociation of DBK (~0.7). [8]

4.5 Estimation of Rate Constant $2k_2$ of Self-Termination Reaction

We plot the determined k_2/ε_{Max} in various solvents against the inverse of the viscosities ($1/\eta$) in Fig. 4-6. The linear relationship between k_2/ε_{Max} and $1/\eta$ supports the previously reported conclusion that the self-termination reaction of BR is the diffusion controlled process. Next, we compare these k_2/ε_{Max} from the TG measurement with those reported previously from the transient absorption measurements. The values of k_2 and ε_{Max} have been reported by many groups: ε_{Max} =1100 cm^{-1}M^{-1} and k_2=1.8x10^7 M^{-1}s^{-1} by McClarthy and MacLachlan reported in a mixed solvent of ethanol and glycol,[10] k_2=2.3x10^{9}M^{-1}s^{-1} and ε_{Max} =12000cm^{-1}M^{-1} by Hagemann and Schwartz in cyclohexane,[11] ε_{Max} =1500 cm^{-1}M^{-1}, k_2=6.8x10^9 M^{-1}s^{-1} by Meiggs et al. in methanol, [12] ε_{Max} =8800 cm^{-1}M^{-1}, k_2=1.8x10^9 M^{-1}s^{-1}, [13a] or k_2=2.3x10^9 M^{-1}s^{-1} [13b] by Fischer and co-workers in cyclohexane, ε_{Max} =5500cm^{-1}M^{-1} and k_2=1.55x10^{9}M^{-1}s^{-1} in water by Christensen et al., [14] k_2=3.5x10^{9}M^{-1}s^{-1} in benzene by Lauter and Dreeskamp,[15] and k_2=4x10^9 M^{-1}s^{-1} by Burkhart.[16] As shown above, the reported ε_{Max} and k_2 are so much scattered. Even if we plot these reported k_2 against $1/\eta$, we cannot see any correlation between k_2 and $1/\eta$. However, if we plot k_2/ε_{Max} against $1/\eta$ (Fig. 4-6), it is found that both quantities have a linear relationship (broken line in Fig. 4-6). Probable cause of the scattered k_2 in various literatures comes from the uncertainty of ε_{Max} estimated by these groups. The k_2/ε_{Max} values obtained in this work are plotted together in Fig. 4-6. We find that our determined k_2/ε_{Max} from the TG experiment are consistent with these literatural values.

4.6 D of the Chemical Species

In Fig. 4-7, D is plotted against $1/\eta$. D of the each species (DBK, CO, and BR) decrease with decreasing $1/\eta$ regardless of the solvent properties (polarity, dipole moment, protic character etc.). The calculated D from the SE equation (D_{SE}) are shown in Fig. 7 (full lines). It is known that D_{SE} underestimates D in many cases and actually, the experimental values of D in Fig. 7a,c are larger than D_{SE}. In section 3.6, we found that D of stable molecules can be reproduced by an empirical equation derived by Evans. et al (D_{EV}) [See eq. (3-5)]. [24]

$$D_{EV} = \frac{T \exp (a/r + b)}{\eta^{(c/r + d)}} \qquad (17)$$

The broken lines in Fig. 4-7 indicate the viscosity dependence of D_{EV}. We found that D_{EV} is closer to D for all species.

In chapter 3, we have reported that the D of various transient radicals created by the photoinduced hydrogen abstraction of ketones, quinones, and N-hetero aromatic molecules show anomalously slow diffusions. D of such radicals are close to D_{SE} rather than D_{EV} (section 3.6). However, Fig. 4-7c shows that D_{BR} is larger than D_{SE} and close to D_{EV} similar to D_{BR} and D_{DBK}. This fact suggests that the diffusion process of BR is analogous to those of stable molecules. Indeed, D of BR are close to the literature values of D of toluene (closed square of Fig. 7c), [23] which is a stable molecule with nearly the same size and shape as BR.

Furthermore, we compare D_{DBK} with D_{BR}. According to the SE relationship, D should be inversely proportional to the radii of the solute molecules. As the molecular volume of BR is close to the half of that of DBK, the ratio D_{BR}/D_{DBK} should be near equal to $2^{1/3}$=1.25. Actually, these ratios obtained by experimental D are very close to 1.25 in all of the solvents (table 4-1). Therefore, the diffusion process of BR created by the photodissociation of DBK is not like those of the transient radical we have previously investigated, but it is similar to that of a stable molecule. Moreover, we showed the molecular size dependence of D of BR, toluene, other hydrogen abstracted radicals and their parent molecules in ethanol in Fig. 4-8. D_{BR} is not close to D of the hydrogen abstructed radicals bet close to D of the parent molecules. A possible origin of the

difference between the previous radicals and BR is discussed in the next section.

D of short-lived radicals have been scarcely reported because of the experimental difficulties. Exceptionally, Burkhat et al. measured D of some alkyl radicals and BR created by photodissociation of alkanes and toluene, respectively, in cyclohexane by using the photochemical space intermittency (PCSI) method.[25] For the PCSI measurement, the sample solutions are illuminated by a "leopard" light-dark pattern of circular spot and the steady-state concentrations of radicals are detected as a function of the light intensity as well as of the total area illuminated. To estimate D from the experimental data, one must know independently the quantum yield for the production of the radicals, the rate of absorption of the light, and the rate constant of the recombination of the radicals. Moreover, this method is based on some assumptions such as, the reaction process of the radical is diffusion controlled and follow the Smoluchowski equation, etc.. Considering the many assumptions and many ambiguous parameters used in the method, it is rather surprising that their value of D_{BR} in cyclohexane ($D=1.1x10^{-9}m^2s^{-1}$) is close to our value ($D=0.95x10^{-9}m^2s^{-1}$).

4.7 Properities of Benzyl Radical.

In chapter 3, we have described anomalously slow diffusion of many transient radicals created by the hydrogen abstraction reaction compared with the stable parent molecules with similar sizes and shapes in various solvents. While, D of BR, which is also a transient radical, is similar to that of the stable molecule with a similar size and a shape such as toluene. The cause of the different diffusion behaviors between BR and the other radicals produced by hydrogen abstraction ($RH^{\cdot}$) is important to study because it will provide a clue to understand the diffusion process of the radicals in solution. There are three factors which might cause the difference.

(a) distribution of the unpaired electron in the molecule

(b) hydrogen bonding effect

(c) electrostatic effect

(a) Burkhart et al. have also found that some alkyl radicals diffuse slower than the parent molecules, while BR diffuses with a similar velocity as toluene. They attributed the species

dependent diffusion to the degree of the delocalization of the unpaired electron in the molecule. Since the unpaired electron of BR is delocalized to the phenyl ring by the π-electron resonance, the spin density on each atom of BR is reduced and the intermolecular interaction between the unpaired electron and other molecules could be weak. On the other hand, the unpaired electron of an alkyl radical is localized on several carbon atoms and the intermolecular interaction which comes from the unpaired electron could be enhanced. In order to examine this idea, we tried to see a correlation between the spin density distribution and D of the transient radicals we have studied so far by the TG method. α-hydroxy benzyl radical (BR-OH) and benzophenone ketyl radical (BPK) are taken as example for the comparison with BR. D of these species are listed in table 3. D of BR-OH in ethanol and 2-propanol are about 2 times smaller than D of BR. Furthermore, D of BR-OH is smaller than the parent molecule (benzaldehyde), while D of BR is similar to toluene. The spin density on each atom of BR was determined from an EPR measurement [26] and also from an MO calculation. [27] About 50% of the unpaired electron is localized on the α-carbon and the other is delocalized on the ortho and meta carbons in the phenyl ring. The hyperfine splitting of BR-OH [28] was also reported. More directly Ficher and co-workers compared the spin density distribution of BR with that of BR-OH.[29] They found that the spin density on the O atom of BR-OH is less than a few % and the spin density distribution of BR-OH is nearly the same as that of BR. Therefore, contrary to the very different diffusion constant, the spin density distribution of BR and BR-OH is very similar. We should conclude that the slow diffusion of BR-OH than BR cannot be attributed to the property of the unpaired electron distribution of the molecule.

(b) Next, we consider the effect of the hydrogen bonding. Recently, Tominaga et al. reported that the molecules which have -OH or $-NH_2$ substituent diffuse anomalously slowly in protic solvents due to the strong intermolecular interactions between the substituent and the solvents.[30] All of $RH^{\cdot}$ we investigated have -OH or -NH substituent while BR does not. The hydrogen bonding could be the main origin of the slow diffusion of $RH^{\cdot}$. However, there are some evidence to exclude the participation of the hydrogen bonding in the radical diffusion as follows

(1) If the hydrogen bonding is the main cause of the slow diffusion of the radicals, the effect should be pronounced in a solvent which can make the hydrogen bond easily. In section 3.6,

however, we found that the radicals diffuse slower than the parent molecules not only in protic solvents but also in nonpolar solvents such as benzene or cyclohexane (Fig. 3-7).

(2) D of BPK is close to that of diphenyl methyl radical, which does not have an -OH group to form a hydrogen bond. [31]

(3) Temperature dependence of D of the radicals can be expressed by the Arrhenius relation with a single activation energy and it is close to that of the viscosity of the solvent (section 3.7). The similarity indicates that the activation energy of the hydrogen bond is not involved in the diffusion process.

(4) Our recent investigation on the substituent effect of several radicals indicates that $>\dot{C}-OH$ and $>\dot{N}H$ groups can make only a weak hydrogen bonding with solvents. [32]

We conclude that the interaction of the hydrogen bonding cannot be the origin of the slow diffusion of the radicals.

(c) Finally, we consider the interaction of the electrostatic force. It is well established that the molecules with a large dipole, or a large polarizability, diffuse slowly by the electrostatic interaction with solvent molecules. This phenomenon has been explained by dielectric friction. This dielectric friction depends on the electrostatic property of the solvent and has been believed to be effective only in a polar solvent. [33~35] However, Maroncelli et al. proposed that even in a non-polar solvent (no dipole moment), the dielectric friction can occur by the interaction with the quadrupole moment of the solvent from the dynamic Stokes shift measurement. [36] Recently, Okazaki et al. reported that D of the merocyanine form of benzospiropyran, which has a large dipole moment (about 12 Debye) are ~2 times smaller than that of the spiro form in cyclohexane and ethanol, [37] although cyclohexane has no dipole and no quadrupole. We considered that the origin of a solute-nonpolar solvent electrostatic interaction could be due to the interaction between the solute and the intramolecular partial dipole of solvent (for example, C-H). As both BR and $RH^{\cdot}$ radicals have no charge, possible electrostatic forces of the radicals are due to dipole interaction and/or dispersion force. If the charge distributions of the radicals are quite different from these of the parent molecules and the radicals have large dipole moments and/or polarizabilities, the diffusion could be slower by the enhanced dielectric friction in polar and non-polar solvents. We calculated the dipole

moments and polarizabilities of BR, $RH^{\cdot}$, and parent molecules by using a semiempirical molecular orbital (MO) calculation with modified neglect of diatomic overlap (MNDO) method.[38] The results are listed in table 4-3 (toluene is used as the parent molecule of BR). Actually, the dipole moments of benzoquinone and pyrazine are increased from 0 D to 2.5~3 D by converting to the radicals. On the other hand, both BR and toluene have no dipole moment. The dipole moments of ketones decrease from 2.5~3 D (for parent molecules) to 0 D (for the radicals). Apparently the slow diffusion of such radicals cannot be explained by the dipole interaction. The polarizability of the radicals and their parent molecules are similar. The charge distribution of both radicals and the parent molecules are similar, too.

We could not find any significant differences which can affect the molecular diffusion by the simple MO calculations. However, recently, Morita and Kato revealed a very prominent difference in the electric character between a transient radical (pyrazinyl radical) and the closed shell molecules (pyrazine and benzene) by the ab initio MO method.[39] They calculated the charge sensitivity for each atom of the molecule by an external electric field, and found that the intramolecular local polarizability of the pyrazinyl radical is much larger than that of pyrazine or benzene despite the fact that the usual polarizability under a uniform electronic field is very similar for these molecules. The normal mode analysis of the local polarizability indicates that the charge sensitivity of the pyrazinyl radical is due to the σ–π mixing that is caused by the deformation of the π electron orbital. A similar enhanced local polarizability was observed for BPK but not for BR.[40] This weak local polarizability of BR comes from the stable π electron resonance structure. Although the dynamic property such as the translational diffusion should be calculated by another method e.g. MD simulation with taking into account this character, it is plausible that such an enhanced polarizability increases the friction during the molecular movement and slows down the diffusion process.

In a series of our studies, we have reported slow diffusion for many transient radicals in many solvents even in supercritical fluids.[41] Among the radicals so far studied BR is only one radical that has D similar to that of the closed shell molecule (toluene).

4.8 Conclusion.

Diffusion processes of the benzyl radical (BR) created by the photodissociation from dibenzyl ketone (DBK) were studied by the transient grating (TG) method in several organic solvents (hexane, cyclohexane, ethanol, and 2-propanol). The observed TG signals can be well fitted by a sum of four exponential functions and they are attributed to the thermal grating signal and the species gratings due to CO, BR, and DBK. From the slope of the decay rate constants against q^2 plots, the thermal diffusion constants, the diffusion constants (D) of CO and DBK are determined. The plot of the BR component has a finite intercept with the ordinate, which indicates that the subsequent chemical reaction cannot be neglected. By applying a short period approximation, we found that the slope and the intercept represent D of BR and the self-termination reaction rate constants ($2k_2$), respectively. D of CO, DBK, and BR are larger than those calculated by using the SE equation (D_{SE}) and closer to those calculated by an equation proposed by Evans et al. (D_{EV}). In all solvents we examined, the ratios of D of BR to those of DBK are close to 1.25, which is expected from the difference of the molecular volumes of BR and DBK. Furthermore D of BR is close to that of toluene. This result is very different from what is expected from the previous studies of the transient radicals created by the hydrogen abstraction reaction. We compare the property of BR with those of the radicals produced by hydrogen abstraction ($RH^{\cdot}$) to find a possible origin of the different diffusion process of BR and others. The spin densities, dipole moments, and the polarizabilities cannot explain the difference satisfactorily. Recently, Morita and Kato showed an enhancement of the intramolecular charge sensitivity to local electric field for $RH^{\cdot}$ based on the ab initio molecular orbital theory. This effect is not observed for BR because the $\sigma-\pi$ mixing, which is the origin of the particular sensitivity enhancement is less effective due to the stability of π-electron orbital of BR. The intermolecular interaction between the radicals and solvents could be the origin of the anomalously slow diffusion process.

References to Chapter 4

1. (a) Terazima, M.; Hirota, N. *J. Chem. Phys.* **1993**, 98, 6257.; (b) Terazima, M.; Okamoto, K.; Hirota, N. *Laser Chem.***1994**, 13, 169.

2. Terazima, M.; Okamoto, K.; Hirota, N. *J. Phys. Chem.* **1993**, 97, 13387.

3. Terazima, M.; Okamoto, K.; Hirota, N. *J. Chem. Phys.* **1995**, 102, 2506.

4. Okamoto, K.; Terazima, M.; Hirota, N. *J. Chem. Phys.* **1995**, 103, 10445.

5. K.Okamoto, N. Hirota, and M. Terazima, J. Phys. Chem. A, 1997, **101**, 5269.

6. (a) Turro, N. J.; Gould, I. R.; Baretz, B. H. *J. Phys. Chem.* **1983**, 87, 351. (b) Arbour, C.; Atkinson, G. H. *Chem. Phys. Lett.* 1989, 159, 520. (c) Meiggs, T. O.; Grossweiner, L. I.; Miller, S. I. *J. Am. Chem. Soc.* **1972**, 94, 7981. (d) Porter, G.; Strochan, E. *Trans Faraday Soc.* **1988**, 34, 1595. (e) Hinze, J.; Jaffe, H. H. *J. Am. Chem. Soc.* **1962**, 84, 540.

7. (a) Lunazzi, L.; Ingold, K. U.; Scaiano, J. C. *J. Phys. Chem.* **1983**, 87, 529. (b) Kajii, Y.; Obi, K.; Tanaka, I. *J. Chem. Phys.* **1987**, 86, 6115.

8. (a) Engel, P. S. *J. Am. Chem. Soc.* **1970**, 92, 6074. (d) Robbins, W. K.; Eastman, R. H. *ibid.* **1970**, 92, 6076.

9. (a) Khudyakov, I. V.; Koroli, L. L. *Chem. Phys. Lett.* **1984**, 103, 383. (b) Lehni, M.; Suehuh, H.; Fischer, H. *Intern. J. Chem. Kinet.* **1979**, 11, 705.

10. McCarthy, R. L.; MacLachlan, A. *Trans. Faraday. Soc.* **1960**, 56, 1187.

11. Hagemann, B. J.; Schwartz, H. A. *J. Phys. Chem.* **1967**, 71, 2694.

12. Meiggs, T. O.; Grossweiner, L. I.; Miller, S. I. *J. Am. Chem. Soc.* **1972**, 94, 7986.

13. (a) Huggenberger, C.; Fischer, H. *Helv. Chem. Acta.* **1981**, 64, 338. (b) Claridge, R. F. C.; Fischer, H. *J. Phys. Chem.* **1983**, 87, 1960.

14. Christensen, H. C.; Sehested, K.; Hart, E. J. *J. Phys. Chem.* **1973**, 77, 983.

15. Laufer, M.; Dreeskamp, H. *J. Magn. Reson.* **1984**, 60, 357.

16. Burkhart, R. D. *J. Am. Chem. Soc.* **1968**, 90, 273.

17. (a) Schuh, H-H.; Fischer, H. *Helv. Chim. Acta* **1978**, 61, 2130. *Int. J. Chem. Kint.* **1976**, 8, 341. (b) Lehni, M.; Schuh, H.; Fischer, H. *ibid.* **1979**, 11, 705. (c) Sitarski, M. *ibid.* **1981**, 13, 125. (d) Lehni, M.; Fischer, H. *ibid.* **1983**. 15, 733.

18. (a) Meisel, D.; Ous, P. K.; Hug, G. L.; Bhattacharyya, K.; Fessenden, R. W. *J. Am. Chem. Soc.* **1986**, 108, 4706. (b) Tokumura, K.; Udagawa, M.; Ozaki, T.; Itho, M. *Chem. Phys. Lett.* **1987**, 141, 558. (c) Robert, C. B.; Zhang, J.; Brenmecke, J. F.; Chateauneul, J. E. *J. Phys. Chem.* **1993**, 97, 5618.

19. (a) Kogelmik, H. *Bell. Syst. Tech.* **1969**, J 48, 2909. (b) Gaylord, T. K.; Moharam, M. G. *Appl. Phys.* **1982**, B28, 1.

20. Schmitz, F. J.; Pattabhiraman, T. *J. Am. Chem. Soc.* **1970**, 92, 6074.

21. (a) Touloukian, Y. S. *Thermophysical Properties of Matter* (Plenum, New York, **1970**), vol III. (b) *International Critical Tables* (McGraw-Hill, New York, **1928**), vol. III. (c) *Landolt-Bornstein Tabellen* (Springer, Berlin, **1972**), 6 Aufl., Bd. IV.

22. Hara, T.; Hirota, N.; Terazima, M. *J. Phys. Chem.* **1996**, 100, 10194.

23. (a) Shroff, G. H.; Shemilt, L. W. *J. Chem. Eng. Data.* **1966**, 11, 183. (b) Lewis, J. W. *J. Appl. Chem.* **1955**, 5, 228. (c) Lemonde, H. *Annal. Physique* **1938**, 9, 560. (d) Wiener, O. *Annal. Physique* **1843**, 49, 313. (e) Grushka, E.; Kikta, E. J. *J. Phys. Chem.* **1974**, 78, 2297. 183.

24. (a) Davis, H. T.; Tominaga, T.; Evans, D. F. *AIChE J.* **1980**, 26, 313. (b) Evans, D. F.; Davis, H. T.; Tominaga, T. *J. Chem. Phys.* **1981**, 74, 1298. (c) Chen, S. H.; Davis, H. T.; Evans, D.F. *J. Chem. Phys.* **1982**, 77, 2540.

25. (a) Burkhart, R. D. *J. Phys. Chem.* **1969**, 73, 2703. (b) Burkhart, R. D.; Boynton, R. F.; Merrill, J. C. *J. Am. Chem. Soc.* **1971**, 93, 5013. (c) Burkhart, R. D.; Wong, R. J. *ibid.* **1973**, 95, 7203.

26. (a) Carrington, A.; Smith, I. C. P. *Mol. Phys.* **1965**, 9, 138. (b) Lloyd, R. W.; Wood, D. E.; Mukai, M. *Mol. Phys.* **1971**, 20, 735. (c) Roothaan, C. C. J. *Rev. Mol. Phys.* **1960**, 32, 179. (d) Dixon, W. T.; Norman, R. O. C. *J. Chem. Soc.* **B1964**, 4857. (e) Hudson, A.; Hussain, H. A.; Mukai, M. *J. Chem. Soc.* **B1969**, 793.

27. (a) Harriman, J. E.; Sando, K. M. *J. Chem. Phys.* **1968**, 48, 5138. (b) Amos, A. T.; Burrows, B. L. *J. Chem. Phys.* **1970**, 52, 3072. (c) Snyder, L. C.; Amos, T. A. *J. Chem. Phys.* **1965**, 42, 3670. (d) Benson, H. G.; Hudson, A. *Mol. Phys.* **1971**, 20, 185. (e)

McLachlan, A. D. *Mol. Phys.* **1960**, 3, 233.

28. (a) Kawai, A.; Kobori, Y. K.; Obi, K. *Chem. Phys. Lett.* **1993**, 215, 203. (b) Koyanagi, M.; Futami, H.; Mukai, M.; Yamauchi, S. *Chem. Phys. Lett.* **1989**, 154, 577.

29. Fischer, H. Z. *Naturforsch.* **1965**, 20a, 488.

30. Tominaga, T.; Tenma, S.; Watanabe, H. *J. Chem. Soc. FaradayTrans.* **1996**, 92, 1863.

31. Terazima, M.; Tomioka, H.; Hirai, K.; Tanimoto Y.; Fujiwara, Y.; Akimoto, Y. *J. Chem. Soc. FaradayTrans.* **1996**, 92, 2361.

32. Okamoto, K.; Hirota, N.; Terazima, M. *To be published.*

33. Zwanzig, R. *J. Chem. Phys.* **1963**, 38. *ibid.* **1970**, 52, 3625.

34. (a) Hubbard, J. B.; Onsager, L. *J. Chem. Phys.* **1977**, 67, 4850. (b) Hubbard, J. B. *J. Chem. Phys.* **1978**, 68, 1649.

35. Biswas, R.; Roy, S.; Bagchi, B. *Phys. Rev. Lett.* **1995**, 75, 1098.

36. Reynolds, L.; Gradecki, J. A.; Frankland, J. V.; Horng, M. L.; Maroncelli, M.; *J. Phys. Chem.* **1996**, 100, 10337 (b) Maroncelli, M.; Fleming, G. R. *J. Chem. Phys.* **1997**, 106, 1545.

37. Okazaki, T.; Hirota, N.; Terazima, M. *J. Photochem. Photobiol.* **1996**, 99, 155.

38. Dewar, M. J. S.; Thiel, W. *J. Am. Chem. Soc.* **1977**, 99, 4899.

39. Morita, A.; Kato, S. *J. Am. Chem. Soc. in press*

40. Morita, A.; Kato, S. *personal communication.*

41. Kimura, Y; Kanda, D; Terazima, M; Hirota, N. *J. Phys. Chem. in press*

42. Okamoto, K.; Hirota, N.; Terazima, M. *J. Phys. Chem.* A, 1997, **101**, 5380.

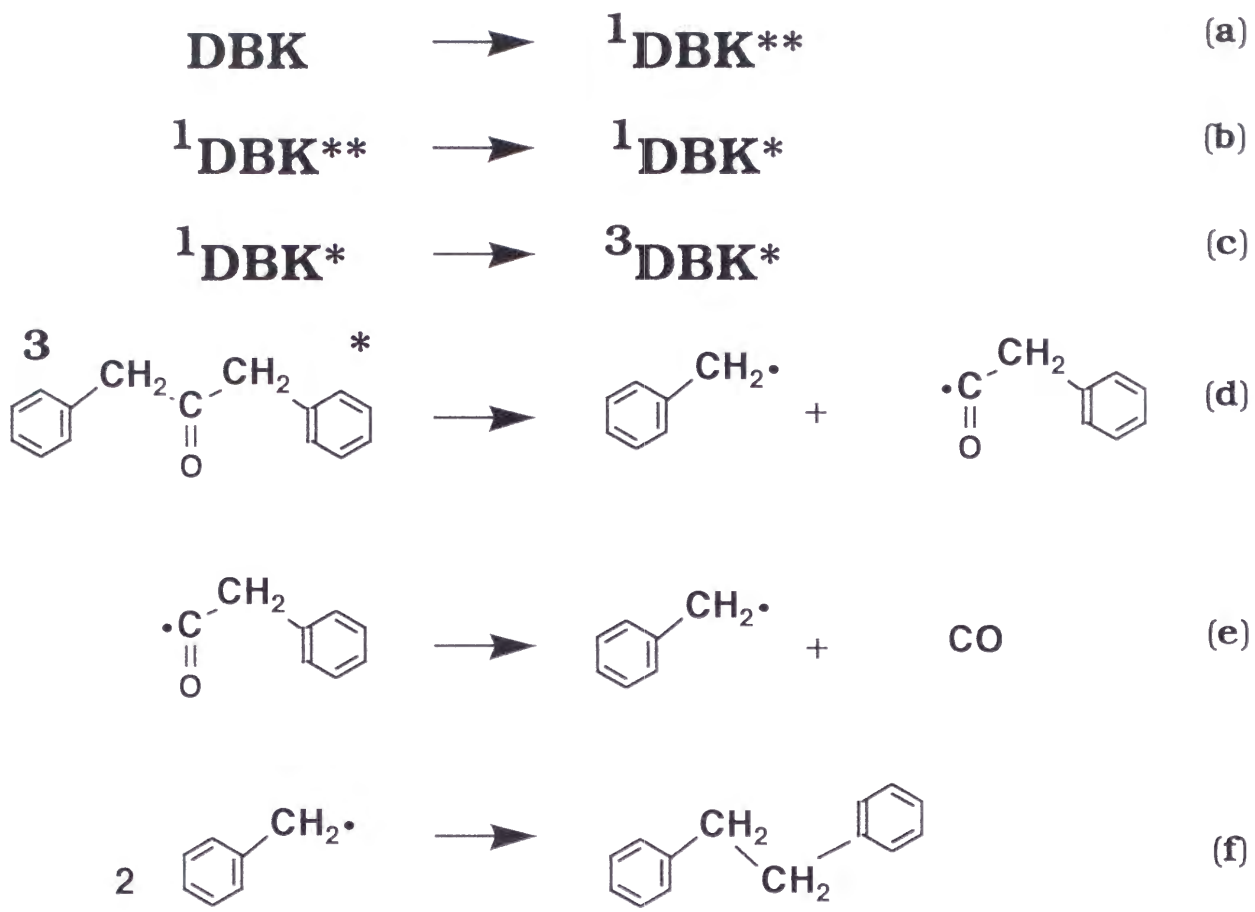
DBK
1DBK**
(a)
1DBK**
1DBK*
(b)
1DBK*
3DBK*
(c)
3
CH2
C
CH2
O
*
CH2•
+
•C
CH2
O
(d)
•C
CH2
O
CH2•
+
CO
(e)
2
CH2•
CH2
CH2
(f)

Scheme 4-1

Table 4-1 Diffusion constants (D) of CO, DBK, and BR and rate constans ($2k_2$) of the self-termination reaction of BR measured by the TG method in several solutions at the room temperature.

solvent	D / 10^{-9} m^2s^{-1}				$2k_2C_o$ / ms^{-1}
	CO	**DBK**	**BR**	**BR/DBK**	
hexane	8.8±1.2	3.3±0.3	4.1±0.2	1.24±0.17	6.7±2.2
cyclohexane	5.5±0.8	0.78±0.1	0.95±0.1	1.22±0.15	2.5±0.6
ethanol	5.7±0.6	0.92±0.08	1.1±0.06	1.20±0.08	1.9±0.4
2-propanol	4.9±0.4	0.57±0.04	0.64±0.06	1.12±0.09	1.3±0.4

Table 4-2 Diffusion constants (D) of the radicals and parent molecules measured by the TG method at ~20C° and D of the parent molecules measured by the PGSE method at ~ 30C°.

		D/$10^{-9}m^2s^{-1}$		
		TG (~20C°)		**PGSE** (~30C°)
solute	**solvent**	**radical**	**parent**	**parent**
dibenzyl ketone	2-propanol	0.64	0.57	0.57
	cyclohexane	0.95	0.78	0.73
pyrazine	2-propanol	0.38	1.2	1.5
	ethanol	0.74	1.6	1.6
benzoquinone	2-propanol	0.36	0.98	1.1
benzophenone	2-propanol	0.33	0.68	0.65

Table 4-3 Diffusion constants by the TG method and dipole moments and polarizabirities calculated by the semiempirical MO method (MNDO) of BR, the radicals produced by hydrogen abstraction, and each parent molecules.

		diffusion constants/ $10^{-9}m^2s^{-1}$		dipole moment / D		polarizabirity / $Å^3$	
		parent	radical	parent	radical	parent	radical
benzyl	in ethanol		1.1	0.02[a)]	0.02	8.62	7.99
	in 2-propanol		0.64				
αOH-benzyl	in ethanol	1.5	0.66	2.85	1.06	9.13	8.78
	in 2-propanol	0.99	0.37				
benzoquinone	in ethanol	1.6	0.57	0.00	3.10	8.24	8.01
pyrazine	in ethanol	1.6	0.74	0.01	2.97	6.30	6.21
benzophenone	in ethanol	1.0	0.55	2.52	1.36	17.13	16.39
acetophenone	in ethanol	1.3	0.58	2.72	1.55	10.31	9.99

a) toluene is used as the parent molecule of BR

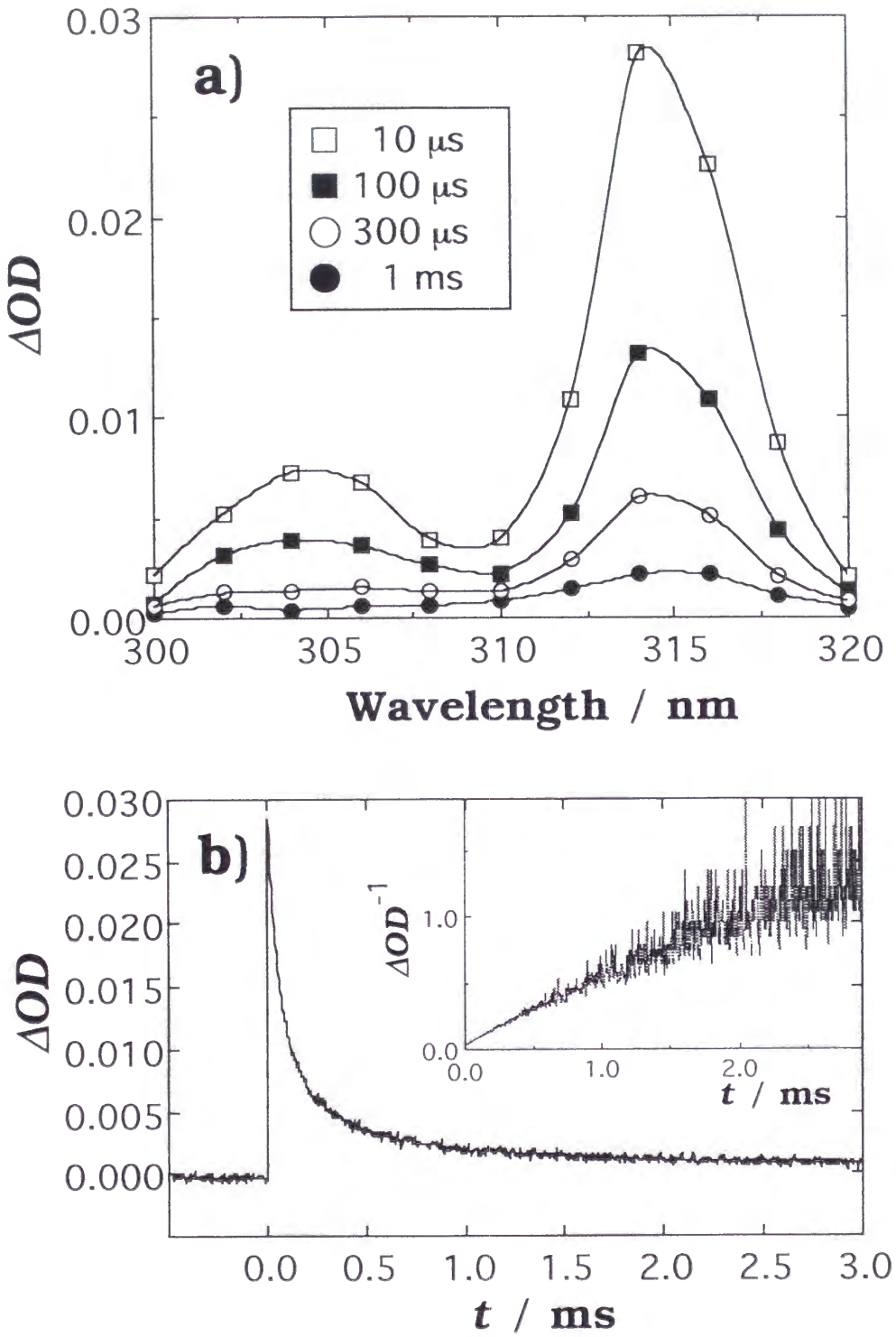

Fig. 4-1 (a) Transient absorption spectrum after photoexcitation of DBK in 2-propanol during 10μs~ 1ms. (b) Time profile of the TA signal at 314nm.

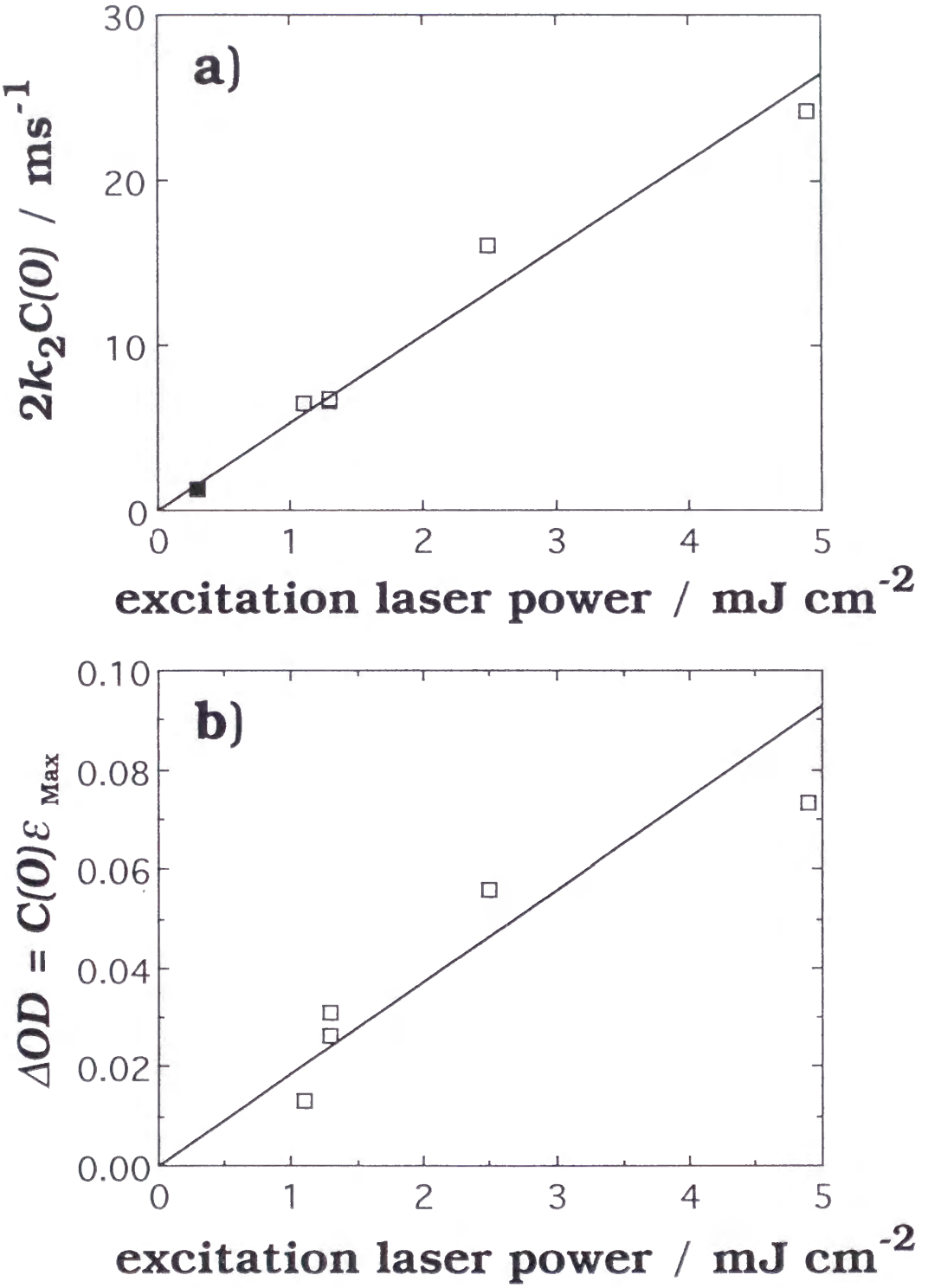

Fig. 4-2 (a) Relationship between $2k_2C(0)$ and excitation laser power. $2k_2C(0)$ are obtained from the time profile of the TA signal (open square) and from the intercept of q^2 plot of k of the TG signal (Fig. 4-4) (closed square). (b) Relationship between C(0) ε_{Max} and excitation laser power.

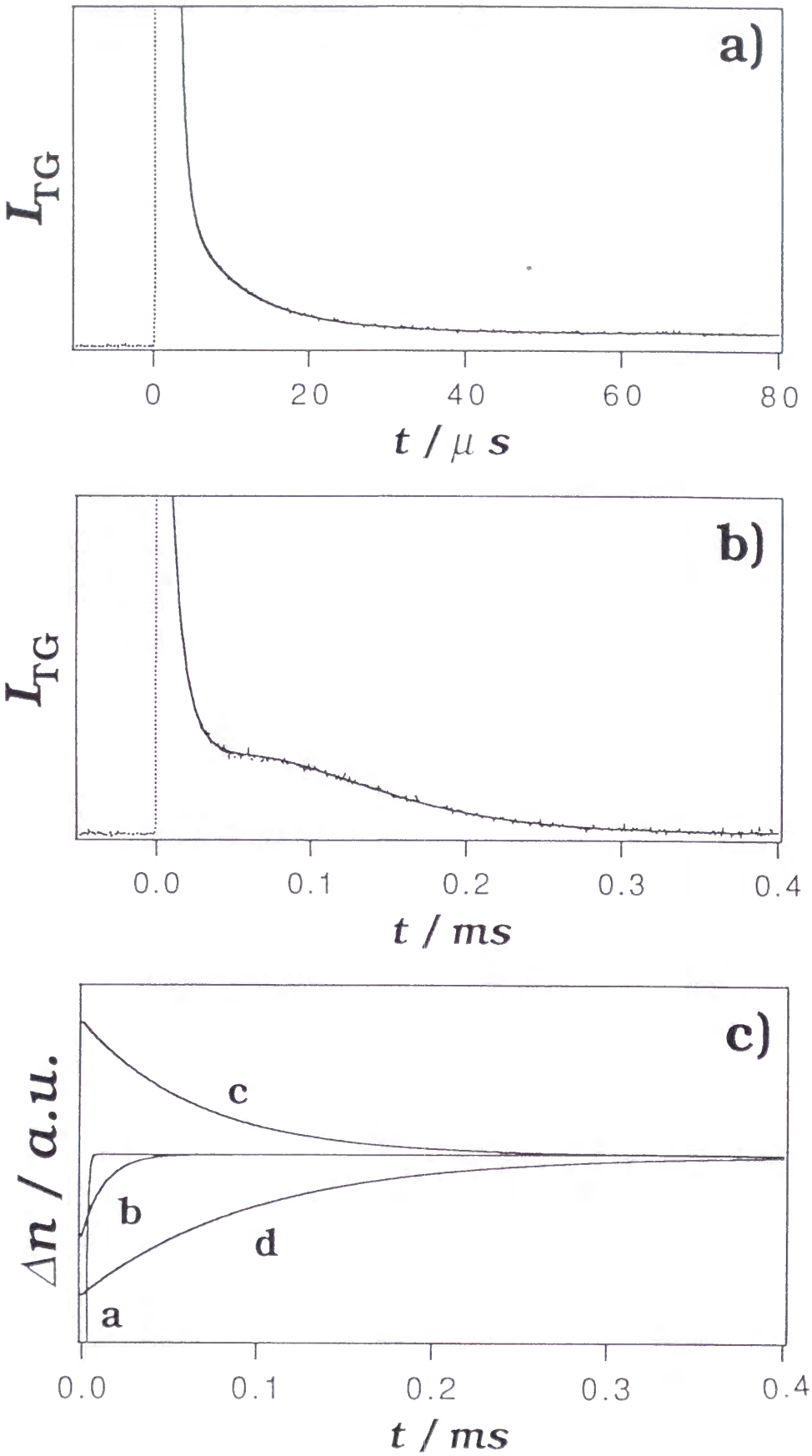

Fig. 4-3 (a) Time profiles of the TG signal after the photoexcitation of DBK in 2-propanol at room temperature with q^2=19 μm^{-2} (broken line) and the fitting line by eq. (2) (full line) in μs time scale and (b) in ms time scale. (c) The assignment of these components are a; heat conductivity, b,c,d; translational diffusion process of CO, BR, and DBK, respectively.

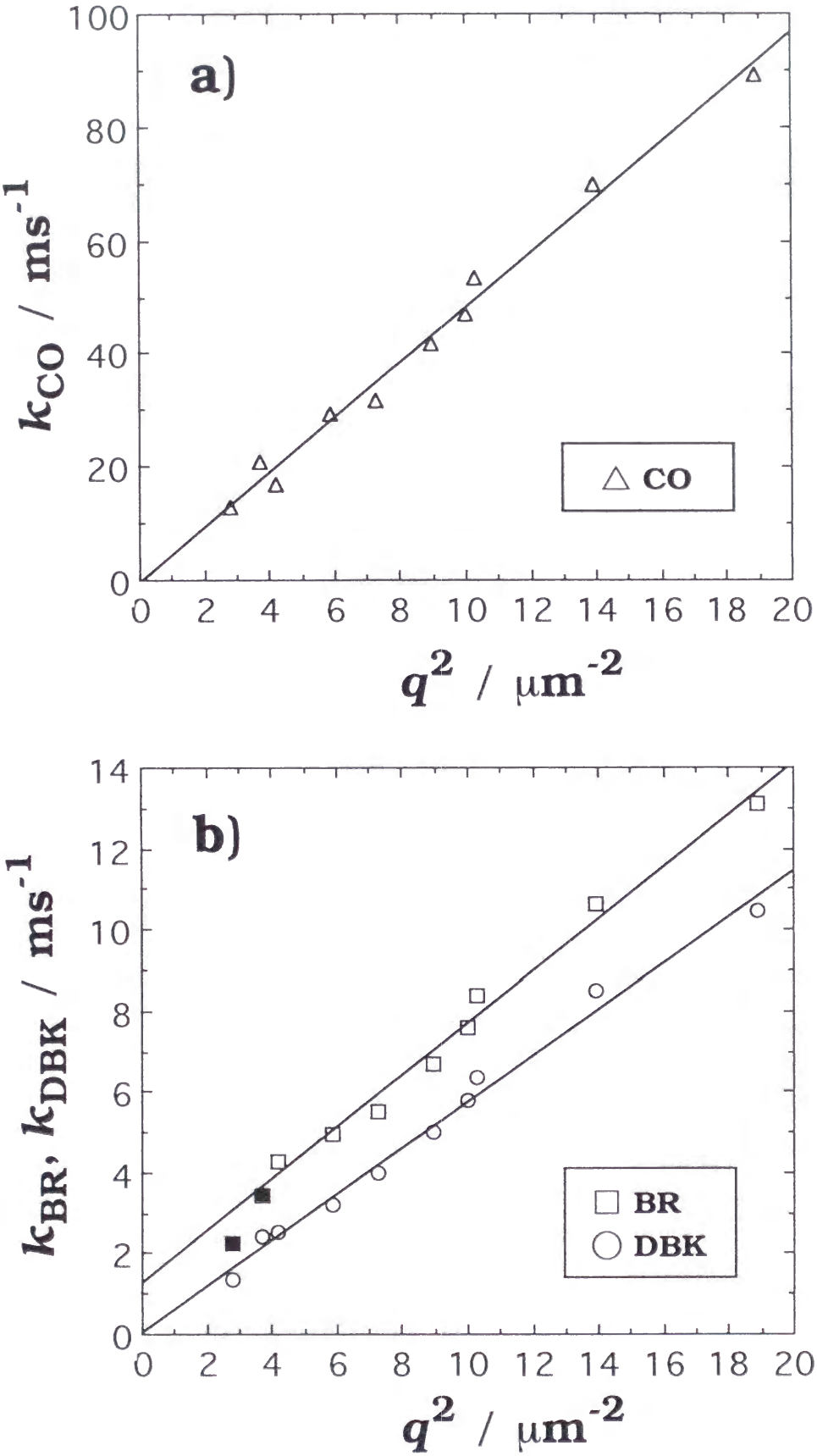

Fig. 4-4 Plots of the decay rate constants (k) of (a) CO and (b) BR (squares), and DBK (circles) components of the TG signal against q^2.

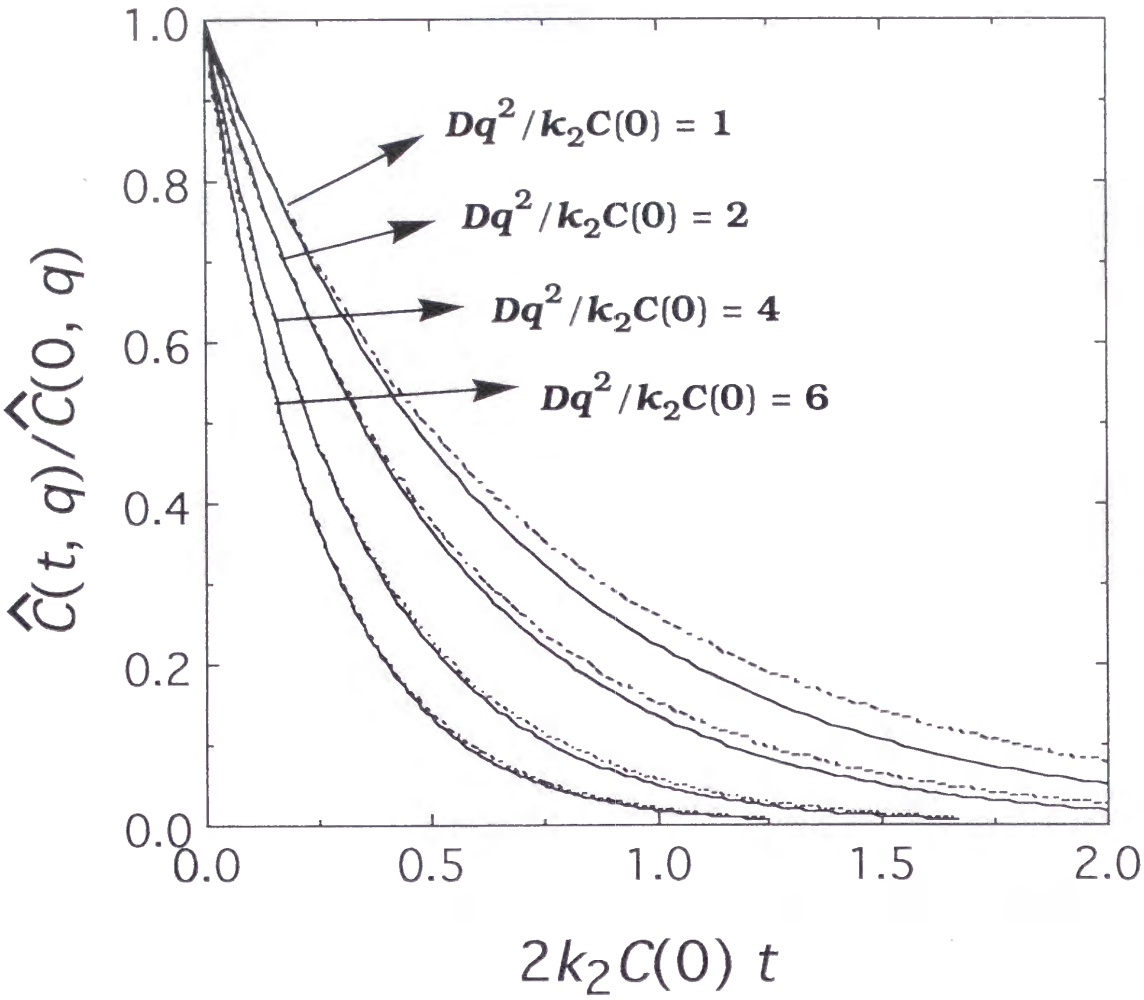

Fig. 4-5 Comparison of the time profiles of the concentrations which decay by the second order reaction-diffusion coupled equation calculated from eq. (4-4) with $f(x, t)=2k_2C(x, t)^2$ (solid lines) and from eq. (4-11) (doted lines) with $Dq^2/k_2C(0) = 1$, 2, 4, and 6.

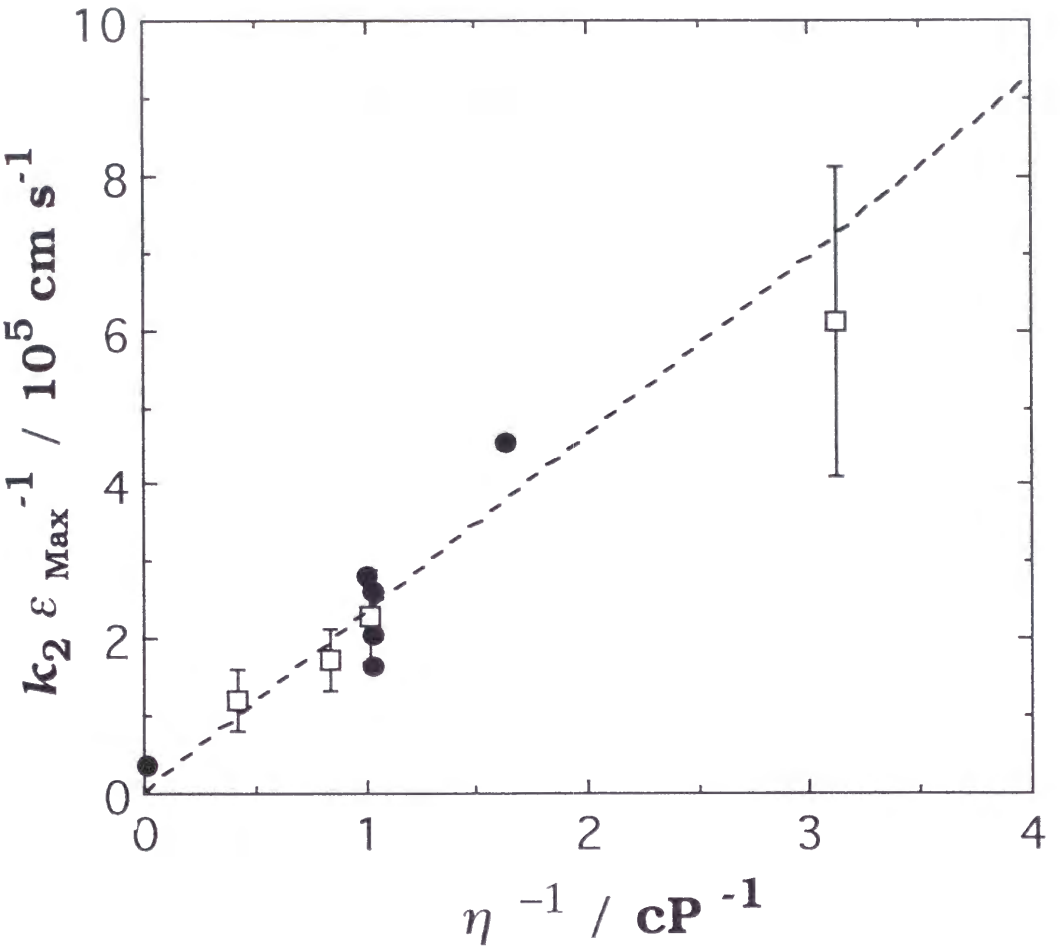

Fig. 4-6 Plot of k_2/ε_{Max} vs. $1/\eta$. The dotted line is guide for eyes. Data from previous studies are shown by the closed circles and those determined from the TG method are shown by the open squares.

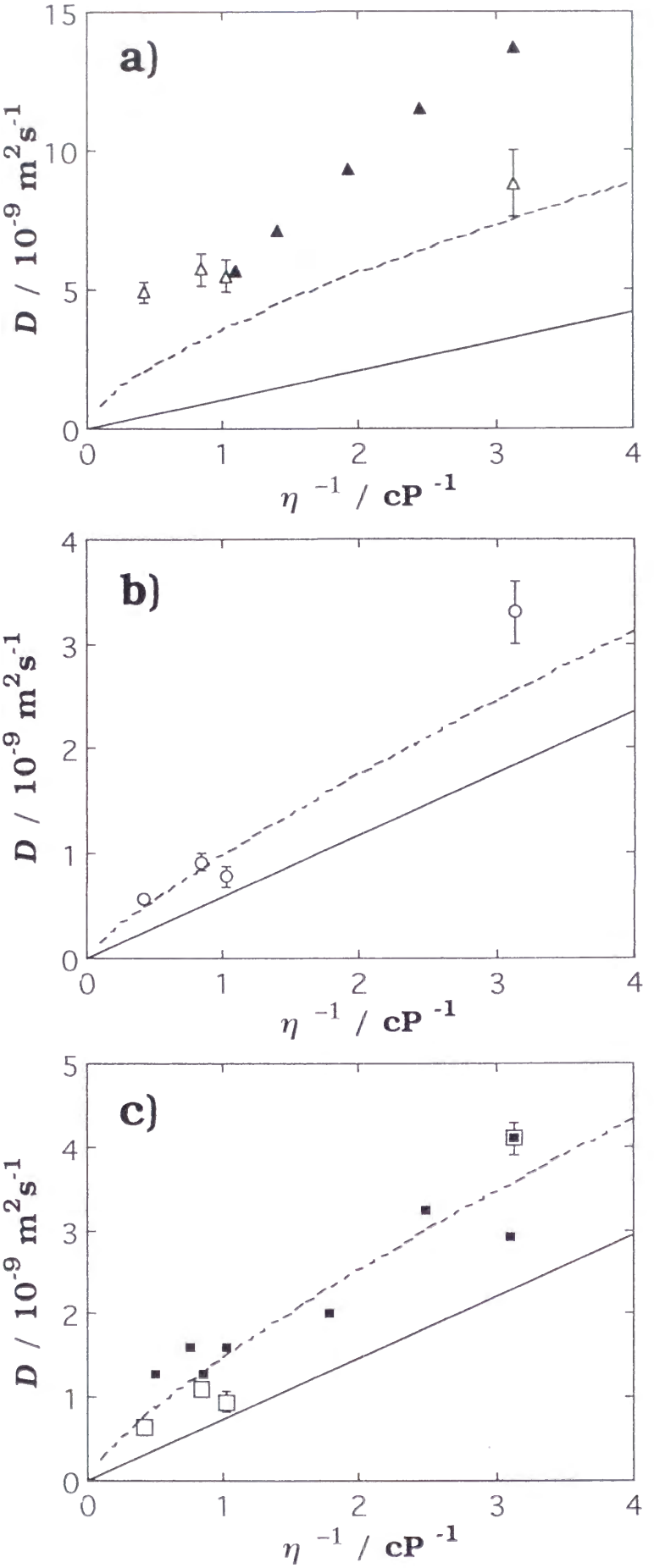

Fig. 4-7 The viscosity dependence of diffusion coefficients of (a) CO, (b) DBK, and (c) BR from the TG measurement (this work)(open marks) and from previous work (closed marks). Solid lines of these figures are calculated from the Stokes-Einstein equation [eq. (4-2)] and broken lines are calculated from eq. (4-15).

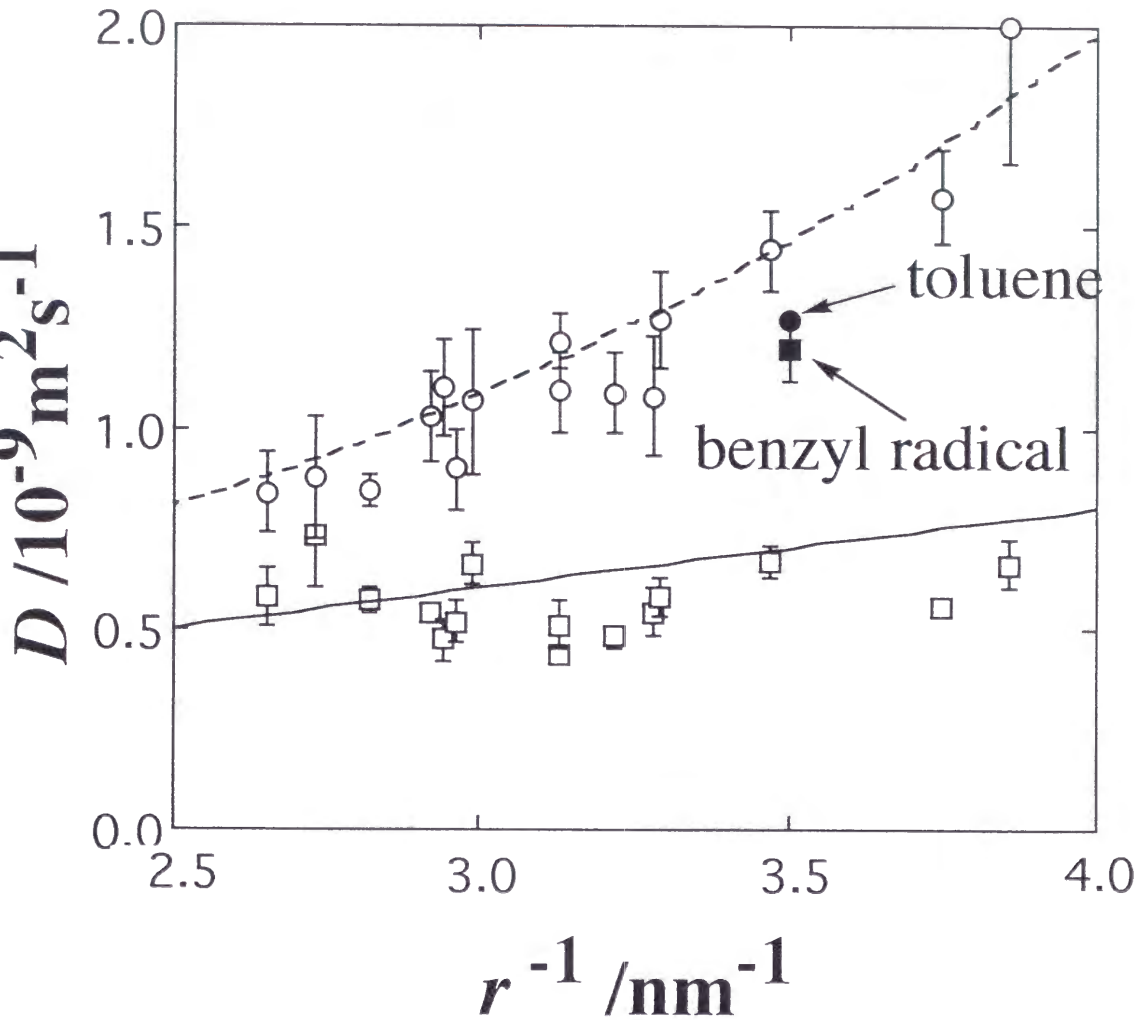

Fig. 4-8 The solute radii dependence of diffusion coefficients of BR(■), toluene(●), the hydrogen abstracted radicals (□) and thire parent molecules (○) in ethanol. Solid line is calculated from the Stokes-Einstein equation [eq. (4-2)] and broken line is calculated from eq. (4-15).

Chapter 5

DIFFUSION OF ELECTRICALLY NEUTRAL RADICALS AND ANION RADICALS

5.1 Charge Effect of Diffusion.

In the previous chapter, we showed that the hydrogen abstracted radicals diffuse slower than that of the parent molecules by the dielectric interaction, though, benzyl radical diffuse normally. On the other hand, ions and ion radical have been known to behave the slow diffusion processes. Mobilities (μ) or conductivities (λ) of ions have been measured by several methods to elucidate solvation structures and charge effects on mobilities.[1,3] The mobilities of ions can be transformed to the diffusion constants by the Nernst relationship. [1,3] Generally, D of ions are smaller than those of neutral molecules of similar sizes in the same solvent and at the same temperature.[3] This is due to the strong intermolecular interaction between the charge of ions and solvent molecules by Coulomb force. With decreasing the molecular size, this effect becomes stronger and the difference between the ion's D and stable molecule's D will increase. Two models are well known to interpret this size dependence of ionic mobilities. One is the excess size model,[4] which is based on an increase of the molecular radius by the solvation structure of ions. The other is the dielectric friction model, [5] which is based on a friction which arises when the polarization of solvents follows the movement of the charges of ions. Both of two models can explain the size dependence of ion's D qualitatively. Boyd, [6] Zwanzig, [7] and Hubbard-Onsager [8] proposed equations to estimate the contribution of the dielectric friction by the continuous fluid theory. These equations can reproduce the experimental D qualitatively, but not quantitatively. Recently, Bagchi et al. succeeded in reproducing the experimental D quantitatively by a theory based on the dielectric

friction. [9]

A natural extension of these researches is the studies of the diffusion of ion radicals, which have an unpaired electron and a charge. In this case, since the motion of the radicals can be detected as electronic current, experimental measurement is easier. Indeed, the mobilities of the photochemically produced intermediate radical cations and anions probed by the time of flight (TOF) technique have been reported by Houser and Jarnagin, [10] Freeman and co-workers, [11] and Albrecht and co-workers. [12] They found that D of the ion radicals are smaller than those of neutral molecules of similar shapes and sizes. Freeman and co-workers attributed the origin of the slow diffusion to the electrostrictive drag by the charged species and dimerization for some compounds. [11] Albrecht and co-workers found that D of the charged radicals can be well reproduced by the SE equation. [12] This result, good agreement with the SE relation, is similar to that found for the neutral radicals we have studied. However, even if one wants to extract the effect of the charge or the unpaired electron by comparison of D of the charged radicals determined by this method with those of closed shell molecules, one has to use D of closed shell molecules measured by other methods under different conditions. Because D is very sensitive to environment and experimental conditions, accurate comparison should be very difficult. However, if we use the TG method, D of the stable molecules can be measured simultaneously with those of the transient species. For example, Terazima et al. have determined D of a cation radical and its parent molecule, N,N,N',N'-tetramethyl-p-phenylendiamine (TMPD), by the TG method under exactly the same condition. [13] The result showed that the TMPD cation radical diffuses only half as quickly as the TMPD parent molecule in ethanol. However, the contribution of the charge and the unpaired electron could not be separated from this measurement. It would be very useful, if D of closed shell molecules, neutral radicals, and ion radicals of similar shapes and sizes can be measured under the same condition.

In this chapter, we performed TG experiments along this line. D of parent molecules, neutral radicals, and anion radicals of ketones are determined by the TG method under the same condition and compared with each other. [14]

5.2 Photochemical Reaction.

To create the neutral radicals, we used the hydrogen abstraction reaction (See scheme 3-1). Charged radicals can be created from the neutral radicals by subsequent reactions. For example, the photochemical process of acetophenone (AP) is described in scheme 5-1. [15]

The lowest excited triplet (T_1) state of AP is created by the intersystem crossing from the lowest excited singlet (S_1) state by the UV irradiation within a excitation laser pulse width (~10ns). The neutral radical is created from the T_1 state of AP by the hydrogen abstraction (process b). The neutral radical and the anion radical are in equilibrium (process c). Therefore, one can create the anion radical or the neutral radical selectively by controlling the pH (pOH) of the solution. In an aqueous solution, such a selective creation of the AP anion radical was reported and pKa was determined to be 9.9. [16] Here we create the anion radicals or the neutral radicals of acetophenone, benzaldehyde, xanthone, benzophenone, and benzil in alcoholic solvents by controlling the concentration of sodium hydroxide (NaOH). D of the anion radicals, the neutral ketyl radicals, and the parent stable molecules are measured under the same condition and compared with each other. The role of the charge and unpaired electron in the diffusion is discussed on the basis of the obtained results.

We examine the created intermediates in pure ethanol and ethanol+NaOH by the transient absorption (TA) method. Figure 5-1a shows the TA spectra with a 100μs time delay after the excitation in pure water and in NaOH+water. The observed TA spectrum in pure water (closed circle in Fig. 5-1a) is assigned to the AP neutral radical (reported TA spectrum [16] is shown by the solid line in Fig. 5-1a). Upon adding NaOH to that solution, the TA spectrum changes and it becomes similar to the reported spectrum of the AP anion radical (dotted line in Fig. 5-1a). [16] Hayon et al. have reported pKa of AP, benzophenone, and benzil as 9.9, 9.25, and 5.5, respectively. [16]

The TA spectra observed in pure ethanol and NaOH+ethanol are shown in Fig. 5-1b. The TA spectrum in pure ethanol (closed circle in Fig. 5-1b) is close to the reported spectrum of the AP neutral radical in ethanol (solid line). [17] The TA spectrum in AP/NaOH+ethanol (open square in Fig. 5-1b) is similar to the spectrum of the AP anion radical in water [16] (dotted line in Fig. 5-1a,

b). Therefore, we assigned this spectrum to the AP anion radical.

Based on these observations, we conclude that the electrically neutral radicals and the anion radicals can be created selectively by controlling the concentration of NaOH in alcoholic solvents. The created radicals are relatively stable and their TA signals are observable for tens milliseconds after the excitation (1~5 mJ/cm^2). The TA signals show the second-order decay which should be due to the self-termination reaction of the radicals. [16,18] Under a week excitation laser power for the TG measurement (~0.3 mJ/cm^2), the intensities of the TA signals are almost constant and the shapes of the TA spectra do not change within the time range for the TG measurement (a few milliseconds). Therefore, it is evident that the created radicals do not react with the solvent or the parent molecules, and the time profile of the TG signal can be analyzed by only the diffusion process of each species similar to chapter 3 [eq. (3-2)].

5.3 Assignment of the TG signal.

The time profile of the TG signal after the photoexcitation of AP in ethanol is shown in Figure 5-2a. The time profile of the root square of the TG signal [$I_{TG}(t)^{1/2}$] can be fitted well with a sum of three exponential functions.

$$I_{TG}(t)^{1/2} = a_1 \exp(-k_1 t) + a_2 \exp(-k_2 t) - a_3 \exp(-k_3 t) \qquad (5\text{-}1)$$

where, $k_1 > k_2 > k_3$ are the decay constants and $a_1 > a_3 > a_2 > 0$ are the pre-exponential factors. The solid line in Fig. 5-2a is the line fitted by using the non-linear least-squares method with eq. (5-1) and the profiles of the three components are shown in Fig. 5-2b. The method for assignment of each exponential component of the TG signal to its origin has been described in chapter 3 in detail. Therefore, we assign component 1 in the obtained TG signal to the thermal grating. We also assign component 2 to the species grating of AP and component 3 to that of the AP ketyl radical.

Next, we performed a similar measurement for AP in ethanol which contains sodium hydroxide. Figure 5-3a shows the time profile of the TG signal of AP / ethanol+(0.01M) NaOH.

The shape of this signal is slightly different from that given in Fig. 5-2a. This time profile can be fitted by eq. (5-1) very well, too (solid line in Fig. 5-3a). The three exponential components are shown in Fig. 5-3b. Comparing Fig. 5-3b with Fig. 5-2b, we find that the intensity of component 3 is enhanced relative to the other components. The enhancement suggests that the transient in pure ethanol is different from that in ethanol+NaOH.

Figure 5-4 shows the intensities of the TA signals at 450nm and the intensities of the TG signals at various concentrations of NaOH in ethanol. Both of the intensities steeply change at pOH $\equiv$ -log[NaOH] = 3~4. Under the dilute condition of NaOH below ~10^{-4} M, the neutral radical is created. If the concentration of NaOH is larger than ~10^{-3} M, the anion radical is dominant in ethanol. Since the spectra do not depend on the monitoring time (10μs ~ a few ms), the neutral radical and the anion radical of AP are in equilibrium within 10μs after the creation (scheme 5-1) in water and in ethanol. The pK_b value of this equilibrium is pK_b=3~4 in ethanol (pK_b= 14 - 9.9 = 4.1 in water [16]). According to this result, component 3 in the TG signal in pure ethanol (Fig. 5-2b) is assigned to the AP neutral radical and that in ethanol + NaOH(0.01) (Fig. 5-3b) is to the AP anion radical.

5.4 Comparison of D of the Neutral Radicals with the Anion Radicals.

We plotted the decay rate constants k_2, k_3 against the square of the grating vector q in Fig. 5-5. The linear relationship between the decay rate constants and q^2 with small intercepts with the ordinate (Fig. 5-5) and also the slow radical decays measured by the TA method ensure that D can be determined from the slope of the plot [See eq. (3-3)]. The obtained D of the parent molecule, the neutral radical, and the anion radical in ethanol are listed in table 5-1. D of AP in ethanol is the same as that in ethanol + NaOH within experimental error. This suggests that the effect of addition of NaOH (0.01M) on diffusion is negligibly small. A main source of the experimental error comes from the fitting error of the double-exponential function and D of parent molecules have large errors. [19] Recently, Donkers and Leaist have reported D of AP by using the Tayler dispersion (TD) method as 1.24×10^{-9} and 0.76×10^{-9} m^2s^{-1} in ethanol and 2-propanol, respectively. [20] Our values from the TG method are close to their values from the TD method with relative errors of

10% and 17% in ethanol and 2-propanol, respectively.

The solvent viscosity depends on the concentration of electrolytes. In diluted solution (< 1M), the Jones-Dole equation describes the concentration dependence of the viscosity well. [21]

$$\eta / \eta^{o} = 1 + AC^{1/2} + BC \qquad (5\text{-}2)$$

where η and η^0 are the viscosities of the electrolytes solution and the pure solvent, respectively. The parameter A expresses the ion-ion interaction and A=0 when the solvent is neutral. C is the concentration (M) of the solute, while B is well known as the B coefficient of the solvent viscosity, which indicates the ion-solvent interaction. B of Na^+, and OH^- have been reported; 0.086, and 0.112 dm^3mol^{-1}, respectively in water. [22] Generally, B depends on the ion volume mainly and does not change much with variation of solvent. [23] We estimated the viscosity change of the solution by the addition of NaOH from eq. (5-2). Using B data in water, we obtained η/η^{o}=1.002 at 0.01M of NaOH. Because, roughly, D is inversely proportional to the viscosity, this small change of the viscosity is within the experimental error of this work. Therefore, the viscosity change upon the addition of NaOH (0.01M) is negligible and D of the neutral radical and the anion radical can be compared directly.

Both D of the neutral radical and anion radical of AP are smaller than that of the parent molecule. Previously, the reductions of D of neutral radicals from D of the parent molecules were explained in terms of intermolecular interactions between the radicals and the solvent molecules. In this case, we suspect that the intermolecular interactions between both the neutral and anion radical and the solvent molecules are similarly strong. Before this study, we expected that D of the anion radicala to be smaller than those of the neutral radicals because the anion radical has both charge and an unpaired electron, both of which can affect the diffusion process. However, this is not the case, although a slight difference between D of the neutral radical and the anion radical is just detectable beyond experimental error (table 5-1). This slight difference may be due to the contribution of the charge to the diffusion process or a possible ion pair formation between the anion and sodium cation. However, previous EPR studies showed that the ion pairs of ketyls tend

to dissociate in alcohol. [24] Another possibility is that the anion radicals are associative active and from the dimer. [25] In this case, D of the anion radical dimer is expected to be ~1.25(=$2^{1/3}$) times larger than that of monomer, [12a] because D is inversely proportional to radius of solute.

It is interesting to note that this charge effect on D of the anion radical is much smaller compared with the reported charge effect on D of the ions of similar sizes. [1,3] The charge effect on diffusion in the anion radical may be reduced by some factors. This phenomenon could be related with the origin of the anomalously slow diffusion of the radicals. In later sections, we discuss the solvent viscosity dependence, the solute size dependence, and the temperature dependence of D of the neutral and anion radicals to clarify this behavior.

5.5 Solvent Viscosity, Solute Size, and Temperature Dependence of D

Contrary to our initial expectation, the diffusion of the AP anion radical is similar to that of the neutral radical. In order to further examine the cause of the effects of the charge and unpaired electron on the diffusion process, we investigate D under various conditions. According to the Stokes-Einstein (SE) equation, D is proportional to temperature (T) and inversely proportional to viscosity of solvent (η) and radius of solute (r). Below, dependencies of D of these species on solvent viscosity, solute size, and temperature are reported below.

In order to monitor the effect of viscosity, we measured the TG signal of AP in methanol, 2-propanol, 1-butanol, and 1-pentanol. The time profiles of the TG signals in various solvents are similar to that in ethanol and D can be determined by the same method as before. D of the parent molecules, the neutral radicals, and the anion radicals in these solvents are listed in table 1 and plotted against η^{-1} in Fig. 5-6.

To monitor the effect of molecular sizes, benzaldehyde, xanthone, benzophenone, and benzil were studied with their neutral radicals and the anion radicals being created by the same method for AP. The time profiles of the TG signals of such solutes are quite similar to that of AP in both pure ethanol and ethanol + NaOH(0.01M). The obtained D of these species are listed in table 5-2 and plotted against 1/r in Fig. 5-7. D of the parent molecules are close to the literature values (1.39, 0.90, and $0.95 \times 10^{-9} m^2 s^{-1}$ of benzaldehyde, xanthone, and benzophenone, respectively) within ±

15%. [20] From Fig. 5-6 and 5-7, it is evident that the anion radical's D of all solutes in all solvents in this work are close to those of the neutral radicals. Therefore the reduction of the charge effect on D seems to be general for the intermediate ketyl radicals created by the hydrogen abstraction reaction.

We compare the experimental D of these species with theoretical calculations where D is described by the Stokes low. [1]

$$D = \frac{k_B T}{\xi} \tag{5-3}$$

where ξ is the friction of the solute molecules in the solvent. Einstein estimated ξ by assuming the solvent to be a continuous fluid. [1]

$$\xi_{SE} = f\pi\eta r \tag{5-4}$$

Equations (5-3) and (5-4) are well known as the Stokes-Einstein (SE) formula, which gives one of the most fundamental equation for D [eq. (3-4)]. Constant f in eq. (5-4) indicates the boundary condition of the friction between the solute and solvent. For the stick boundary condition, f=6, and for the slip boundary condition, f=4. The calculated D of the SE equation (D_{SE}) generally reproduce experimental D well when the sizes of solute molecules are sufficiency large. However, if the volume of a solute molecule is small or close to the solvent volume, D_{SE} underestimates the experimentally observed D because the continuous fluid approximation for the solvent is no longer valid.

Some modifications of the SE equation have been proposed. [2] Evans et al. proposed an empirical equation, which is given by [26]

$$\xi_{EV} = \frac{\eta^{(c/r + d)}}{k_B \exp(a/r + b)} \tag{5-5}$$

where a=5.9734 Å, b= -7.3401, c=-0.86365 Å and d=1.0741 [eq. (3-5)]. [27] In previous chapter,

we have shown that the calculated D from this equation (D_{EV}) agree very well with D of the parent molecules. On the other hand, D of the radicals are close to D_{SE} under the stick condition. Figs. 5-6 and 5-7 show plots of D_{EV} and D_{SE} (stick boundary). As can be seen, D of the parent molecules are close to D_{EV} and D of both the neutral and anion radicals are close to D_{SE}. It is interesting to note that the experimental data indicate that the difference in D between the parent molecules and the anion radicals increases with increasing η and/or decreasing r. This tendency is what we observed before in the neutral radicals.

The temperature dependence of D in pure ethanol and ethanol+NaOH between $50^{\circ}C \sim -50^{\circ}C$ is shown in Fig. 5-8. The temperature dependence of D in various solutions can generally be expressed by the Arrhenius-type equation with the diffusion activation energy (E_D) and the pre-exponential factor (D_o) [eq. (3-6)]. [1] The logD vs. 1/T plots of Fig. 5-7 indicate that the Arrhenius type relation holds for this system. Determined E_D and D_o are listed in table 5-3. It is worth while to note that, although D of the parent molecules and neutral (or anion) radicals are very different, D_o of these species are very similar. On the other hand, E_D of the both radicals are larger than those of the parent molecules. This behavior can be again reproduced by the calculation from eqs. (5-4) and (5-5), both qualitatively and quantitatively (Fig. 5-8). Again this is similar to the case of the neutral radicals reported in section 3.8. In chapter 3, we explained the temperature dependence by the excess size model. The activation energy of the anion radical is almost the same as that of the neutral radical. The charge in the radical does not change the activation energy of diffusion. We consider a possible origin of this fact below.

5.6 Comparison of D between the Ionic Radicals and Stable Ions.

In the previous section, we compared D of the charged radicals with those of the neutral radicals. This comparison will provide information of the charge effect on the radicals. In order to discuss the charge effect on the radicals and also that on the closed shell molecules, D of stable ions are compared with those of the closed shell molecules. A large number of studies have been made on the diffusion process of metal ions. [1] As the metal ions become small, the effect of the Coulomb force becomes remarkably large and D of the metal ions become much smaller than D_{SE}.

This effect has been explained by the formation of the complex with a large number of solvent molecules. [4] Since the sizes of the metal ions are too small for the hydrodynamic theory based on the continuous fluid model, it would not be appropriate to use such data for comparison with our samples. D of larger non-metallic ions have been measured by the ionic conductance method for some tetraalkylammonium ions and the values are compared with D of some tetraalkyltins by the Trylor dispersion technique. [3] The results show that the ionic mobility is slower than that of non -ionic molecules and such difference was analyzed by the dielectric friction model.

The effect of the dielectric friction is given by

$$\xi = \xi_o + R/r^3 \tag{5-6}$$

where ξ_o is the hydrodynamic friction and the R/r^3 term is the dielectric friction. Generally, ξ_o is calculated from the Einstein's formula [eq. (5-4)]. According to the theory by Zwanzig, R is given by [7]

$$R_Z = \frac{A\, e^2(\varepsilon_o - \varepsilon_\infty)\tau_D}{\varepsilon_o(2\varepsilon_o + \varepsilon_\infty)} \tag{5-7}$$

Based on the Hubbard-Onsager (HO) theory, R is written as [8]

$$R_{HO} = \frac{A\, e^2(\varepsilon_o - \varepsilon_\infty)\tau_D}{\varepsilon_o^2} \tag{5-8}$$

where, ε_o and ε_∞ are the static and optical dielectric constants, respectively, and τ_D is Debye's relaxation time. Constant A have a value of A=3/8 for the stick boundary condition and A=3/4 for the slip boundary condition of eq. (5-7), A=17/280 for the stick boundary condition and A=1/15 for the slip boundary condition of eq. (5-8).

Evans et al. experimentally determined R of some tetraalkylammonium ions in several solvents by comparison of D of non ionic molecules. The experimentally obtained D of the ionic molecules by Evans et al. are plotted against 1/r and 1/η in Fig. 5-9 along with our data. Both D_{SE} and D_{EV}

calculated from eqs. (5-4) and (5-5) are plotted. It is evident from the figures that D of the ions are close to D_{SE} of stick condition, which is similar to the radical's case. This agreement indicates that the diffusion of the stable ions is expressed by the stick boundary condition of the hydrodynamic model rather than the dielectric model. (The agreement of non-ionic molecule's D with D_{EV} is expected since equation (5-5) was empirically determined from these data.)

5.7 Models of the Slow Diffusion.

For a detailed comparison of D of the neutral radicals, the anion radicals, and the stable ions, the size dependence of diffusion of three species are plotted in Fig. 5-9b. Although D_{SE} (straight solid line in Fig. 5-9b) reproduce D of three species, some difference is notable. D decreases in order of stable ions, neutral radicals, and anion radicals.

We have explained the diffusion process of the neutral radicals based on the excess volume model in section 3.9. In this model, the equation derived by Evans et al. was modified as if the molecular volume of the radical was expanded. An equation from this model is given by

$$\xi_V = k_B^{-1} \exp\left[\frac{-a}{(r^3+3V_o/4\pi)^{1/3}} - b \right] \eta^{\left[\frac{c}{(r^3+3V_o/4\pi)^{1/3}} + d \right]} \qquad (5\text{-}9)$$

where V_o is the apparent excess volume of the radical [See eq. (3-15)]. In a series of our investigations on the radical diffusion, we succeed in reproducing the size dependences of the radical's D by this model with $V_o = 5 \times 10^2$ Å^3 (Fig. 3-8). Although D calculated from this model (D_V) are close to D_{SE}, the size dependence of the diffusion activation energies of radicals agrees better with the calculation based on this model than on the SE equation. D_{SE} are proportional to 1/r (straight line in Fig. 5-9b), while the dependence of D_V on 1/r is more moderate (dotted line in Fig. 5-9b). D_V are close to D of the neutral and anion radicals but those of the stable ions are slightly larger than D_V.

Felderhof showed that the HO theory for ionic mobility need to be corrected and performed more careful numerical studies based on the dielectric friction theory.[28] In a similar manner, Ibuki and Nakahara tested the dielectric friction theory for ion mobility in polar solvents. They found that

the HO theory is better than the Zwanzig theory to describe D of an ionic species and proposed an approximate HO equation. [29]

$$\xi = \xi_o + \eta R_{HO}' \sum_n a_n (R_{HO}' / r)^n \qquad (5\text{-}10a)$$

$$R_{HO}' = \left[\frac{e^2(\varepsilon_o - \varepsilon_\infty)\tau_D}{16 \pi \eta \varepsilon_o^2} \right]^{1/4} \qquad (5\text{-}10b)$$

where, a_n are constants and Ibuki and Nakahara recommended a_1=-2.78664, a_2=8.62163, a_3=-3.34252, and a_4=0.395501 for the stick condition and a_1=-2.21448, a_2=6.95787, a_3=-2.72959, and a_4=0.337796 for the slip condition. We calculated D from their approximated equation and compared them with the experimental D. However, the calculated D are very different from the experimental values. For example, D of Et_4N^+ in ethanol is $0.72 \times 10^{-9} m^2 s^{-1}$, while the calculated D is $0.47 \times 10^{-9} m^2 s^{-1}$. A similar result has been reported by Terazima et al. for the TMPD cation radical. [13] The disagreement is expected because Ibuki and Nakahara used the Einstein equation [eq. (5-3)] for ξ_o in eq (5-6), yet D_{SE} cannot reproduce the experimental D. In order to improve ξ_o, we used ξ_{EV} [eq. (5-5)] instead of ξ_{SE}. The calculated values by the corrected HO equations with the slip boundary constants (D_{HO}) are plotted in Fig. 5-9 (broken line) and compared with the experimental D of these species. We find that D_{HO} reproduce well D of the stable ions rather than those of the radicals in region of $r^{-1} < 0.3 \text{ Å}^{-1}$. From Fig. 5-9, it is evident that D_{HO} increase exponentially with increasing 1/r. This deviation becomes larger with increasing 1/r of ions. In this region, the corrected HO equations can no longer reproduce the experimental D,therefore, in a wide range of 1/r, the experimental D can be better reproduced by D_{SE} rather than D_{HO}.

5.8 Intermolecular Interreaction of the Neutral and Anion Radicals.

One of main interesting findings in this research is that D of the neutral radicals are quite close to those of the anion radicals and ions. This fact indicates that the friction of the neutral radicals, (whatever the origin is), and the dielectric friction of ions are not additive. It is interesting to note

that D of the ions, the neutral radicals, and ionic radicals are close to D_{SE} under the stick boundary condition under a variety of conditions of solvent, temperature, and molecular size (although there is a slight difference). This fact may suggest that D_{SE} of stick boundary condition could be the lowest limit of D. If the boundary condition is already completely stick-like for the neutral radicals and ions, the condition cannot be 'more stick-like' even if a charge is attached to the neutral radical or an unpaired electron is attached to the ion. Another possible explanation for the similar D of the neutral and ionic radicals may be related to the origin of the slow diffusion of the neutral radicals.

D of the neutral radicals and that of the stable ions are very similar over wide ranges of viscosities and molecular sizes (Fig. 5-9). It suggests that the solute-solvent intermolecular interaction of the ions and the neutral radicals could be similar, in more specifically, similar to the electrostatic interaction. Of course the neutral radicals have no charge in total, but if the charge densities of the radicals are polarized significantly, they can interact with the solvent molecules by the electrostatic interaction.

Nee and Zwanzig proposed a theory of the dielectric friction for a dipolar molecule, [30] and subsequently, many theories have been proposed to account for the dielectric friction to the rotation of polar solutes in polar solvents [31] or reorientation of polar solute molecules interacting with polar solvents. [32] No theory to explain the dielectric friction effect of a polar solute to the translational diffusion have not been reported. However, by analogy with the rotation process, it is natural to consider that the diffusion process of the polar solute should be influenced by the dielectric friction.

Such the remarkable polar character of the radicals has been certified very recently by Morita and Kato, which have been described in section 4.7. [33] They proposed that the origin of the anomalous slow diffusion of radicals should be due to the enhanced sensitivities of the intramolecular charge polarization of radicals by an ab initio MO calculation. According to their analysis, such an enhancement is due to the σ–π mixing that facilitates the deformation of the π-electron orbital of aromatic radicals. They suggested that this particular sensitivity of aromatic radicals could be the origin of the anomalous slow diffusion of the radicals. Their theoretical suggestion seems to be consistent with our finding that the friction of the neutral radicals is similar to that of the ions.

Their calculation show that the charge sensitivity depends on the molecular structure. When a charge is attached to the neutral radical, the structure should be changed and the $\sigma-\pi$ mixing which is the origin of the enhanced charge sensitivity could diminish. In that case, only the intermolecular interaction by the electric charge (not the charge sensitivity) causes the slow diffusion of the ionic radicals like that of stable ions. This exclusive mechanism of the slow diffusions of the neutral and ionic radicals may answer to the question as to why the effect of the charge and the unpaired electron is not additive.

5.9 Conclusion.

The translational diffusion constants (D) of the electrically neutral ketyl radicals, the anion radicals, and the parent molecules were measured by the transient grating (TG) method in alcoholic solutions. The neutral radicals and the anion radicals could be created selectively by controlling the concentration of sodium hydroxide not only in aqueous solution but also in alcoholic solutions. The presence and the decay kinetics are examined by the transient absorption and the time profile of the TG signal is interpreted in terms of the mass diffusion of these species. It was found that both the neutral and anion radicals diffuse slower than the parent molecules. D of the anion radicals are compared to those of the neutral radicals for studying the effect of the charge and the unpaired electron on the diffusion process. We measured the solvent viscosity dependence, the solute size dependence, and the temperature dependence of D. These D are compared with the values calculated based on the Stokes-Einstein equation (D_{SE}) and the equation proposed by Evans et al. (D_{EV}). D of the parent molecules are close to D_{EV}, while D of the both radicals are close to D_{SE}. D of the anion radicals are close to that of the neutral radicals in wide ranges of solvent viscosities, solute size, and temperatures. Comparing this result with reported D of stable ions, we found that the diffusion of the neutral radicals, the ionic radicals, and the ions are similar. For a more careful comparison, we calculated D using the excess volume model based on D_{EV} (D_V) and the dielectric friction model, which is corrected by the Hubbard-Onsager equation (D_{HO}). The radicals D are close to D_V. On the other hand, D of ions agree with D_{HO} rather than D_V. At present, we think that the slow diffusion of the radicals and ions may be due to a similar origin, which could be solute-

solvent electrostatic interaction. Recently, Morita and Kato reported that the sensitivities of the intramolecular charge polarization of the radicals are enhanced remarkably by the external electrostatic field. They proposed that such an enhancement is the origin of the anomalous slow diffusion of the radicals. Their proposal is consistent with our explanation.

References to Chapter 5

1. (a) E. L. Cussler, *Diffusion* (Cambridge University, Cambridge, 1984).; (b) H. J. V Tyrrell, and K. R. Harris, *Diffusion in Liquid* (Butterworths, London, 1984).; (c) *Landolt-Bornstein Tabellen* (Springer, Berlin, 1961), 6 Aufl., Bd. II.

2. (a) F. Perrin, J. Phys. Radium., 1931, **7**, 1.; (b) A. Spernol and K. Z. Wirtz, Naturforsch., 1953, **8a**, 352.; 1953, **8a**, 522.; (c) E. G. Scheibel, Indu. Eng. Chem., 1954, **46**, 2007.; (d) C. R Wilke and P. C. Chang, Am. Inst. Chem. Eng. J.,1955, **1**, 264.; (e) C. J. King, L. Hsueh, and K. W. Mao, J. Chem. Eng, Data., 1965, **10**, 348.

3. (a) F. D. Evans, C. Chan, and B. C. Lamartine, J. Am. Chem. Soc., 1977, **28**, 6492.; (b) D. F. Evans, T. Tominaga, and C. Chan, J. Solu. Chem., 1979, **8**, 461.

4. (a) H. S. Frank and W. Y. Wen, Disc. Faraday Soc., 1957, **24**, 133.; (b) O. Ya. Samoilov, ibid, 1957, **24**, 141.; (c) E. Waisman and J. L. Lebowitz, J. Phys. Chem., 1970, **52**, 4307.

5. (a) H. Sadek and R. M. Fuoss, J. Am. Chem. Phys., 1959, **81**, 4507.; (b) D. S. Berns and R. M. Fuoss, ibid., 1960, **82**, 5585.

6. R. H. Boyd, J. Chem. Phys., 1961, **35**, 1281.; 1963, **39**, 2376.

7. R. Zwanzig, J. Chem. Phys., 1963, **38**, 1603.; 1970, **52**, 3625.

8. (a) J. B. Hubbard and L. Onsager, J. Chem. Phys., 1977, **67**, 4850.; (b) J. B. Hubbard, ibid., 1978, **68**, 1649.

9. R. Biswas, S. Roy, and B. Bagchi, Phys. Rev. Lett., 1995, **75**, 1098.

10. N. Houser and R. C. Jarnagin, J. Chem. Phys., 1970, **52**, 1069.

11. (a) S. S. Sam and G. R. Freeman, J. Chem. Phys., 1979, **70**, 1538. ibid., 1980, **72**, 1989.; (b) J. P. Dodelet and G. R. Freeman, Can. J. Chem., 1975, **53**, 1263.

12. (a) S. K. Lim, M. E. Burba, and A. C. Albrecht, J. Phys. Chem., 1994, **98**, 9665.; (b) K. S. Haber and A. C. Albrecht, J. Phys. Chem., 19984, **88**, 6025. (c) D. Roy and A. C. Albrecht, J. Phys. Chem., 1989, **93**, 2475. (d) S. K. Lim, M. E. Burba, and A. C. Albrecht, Chem. Phys. Lett., 1993, **216**, 405.

13. M. Terazima, T. Okazaki, and N. Hirota, J. Photochem. Photobiol., 1995, **92**, 7.

14. K. Okamoto, N. Hirota, M. Terazima, J. Chem. Soc. Faraday Trans, in press.

15. J. I. G. Cadogan, *Principles of Free Radical Chemistry* (The Chemical Society Monographs For Teachers No. 24, 1973).

16. (a) E. Hayon, T. Ibata, N.N. Lichtin and M. Simic, J. Phys. Chem., 1972, **76**, 2072.; (b) A. Beckett, A. D. Osborne, and G. Porter, Trans. Faraday. Soc., 1964, **60**, 873.

17. H. Lutz, E. Breheret and L. Lindquist, J. Phys. Chem., 1973, **77**, 1753.

18. I. V. Khudyakov and L. L.Koroli, Chem. Phys. Lett., 1984, **103**, 383.

19. K.Okamoto, N. Hirota, and M. Terazima, J. Phys. Chem. A, 1997, **101**, 5380.

20. L. R. Donkers and G. Leaist, J. Phys. Chem. B, 1997, **101**, 304.

21. G. Jones, M. Dole, J. Am. Chem. Soc., 1932, **51**, 2950.

22. R. Shimha, J. Phys. Chem., 1940, **44**, 25.

23. A. Einstein, Ann. Phys., 1966, **19**, 289., ibid., 1967, **34**, 591.

24. K. Nakamura, B. F. Wong, and N. Hirota, J. Am. Chem. Soc., 1973, **95**, 6919.

25. M. Chanon, M. Rajzmann, and F. Chanon, Tetrahedron, 1990, **46**, 6193.

26. (a) H. T. Davis, T. Tominaga, and D. F. Evans, AIChE J, 1980, **26**, 313.; (b) D. F. Evans, H. T. Davis, and T. Tominaga, J. Chem. Phys., 1981, **74**, 1298.

27. S. H. Chen, H. T. Davis, and D.F. Evans, J. Chem. Phys., 1982, **77**, 2540.

28. B. U. Felderhof, Mol. Phys., 1983, **49**, 449.

29. K. Ibuki and M. Nakahara, J. Chem. Phys., 1986, **84**, 2776.

30. T. W. Nee and R. Zwanzig, J. Chem. Phys., 1970, **52**, 6353.

31. (a) J. B. Hubbard and P. G. Wolynes, J. Chem. Phys., 1978, **69**, 998.; (b) J. B. Hubbard, J. Chem. Phys., 1978, **69**, 1007.; (c) P. Madden and D. Klveison, J. Chem. Phys., 1978, **86**, 4244.; (d) B. U. Felderhof, Mol. Phys., 1983, **48**, 1269.; (e) E. Nowak, J. Chem. Phys., 1983, **79**, 976.

32. (a) G. Zwan and J. H. Hynes, J. Phys. Chem., 1985, **89**, 4181.; (b) M. Maroncelli, G. R. Fleming, J. Chem. Phys., 1987, **86**, 6221.

33. A. Morita and S. Kato, J. Am. Chem. Soc., 1997, **119**, 4021.

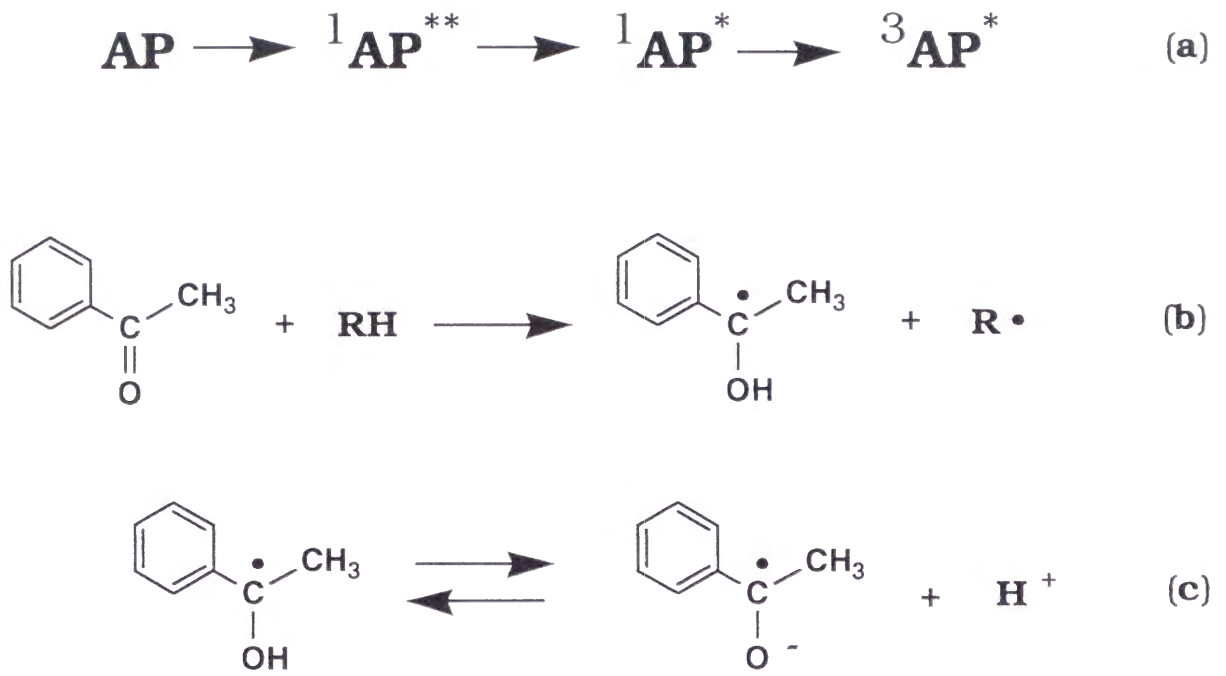

Scheme 5-1

Table 5-1 Diffusion constants (D / 10^{-9} m^2s^{-1}) of acetophenone (AP), the neutral radical of AP in alcoholic solvents, and the anion radical of AP in alcohols + NaOH (0.01M) obtained by the TG method.

solvent	D in pure solvent		D in solvent + NaOH (0.01M)	
	AP	neutral radical	AP	anion radical
ethanol	1.36±0.11	0.58±0.01	1.37±0.10	0.52±0.03
methanol	1.78±0.05	1.25±0.04	1.91±0.12	1.15±0.02
2-propanol	0.89±0.03	0.33±0.01	0.89±0.05	0.28±0.02
1-butanol	0.77±0.08	0.26±0.01	0.80±0.20	0.19±0.03
1-pentanol	0.66±0.09	0.19±0.01	0.63±0.06	0.14±0.05

Table 5-2 Size dependence of the diffusion constants (D / 10^{-9} m^2s^{-1}) of the parent molecules, the neutral radicals, and the anion radicals in ethanol and ethanol + NaOH (0.01M).

solute	D in ethanol		D in ethanol + NaOH (0.01M)	
	parent molecule	neutral radical	parent molecule	anion radical
benzaldehyde	1.60±0.05	0.58±0.01	1.52±0.02	0.48±0.02
xanthone	0.90±0.05	0.50±0.01	0.87±0.04	0.46±0.01
benzophenone	0.80±0.05	0.49±0.03	0.80±0.10	0.43±0.02
benzil	0.77±0.05	0.50±0.03	0.70±0.10	0.45±0.01

Table 5-3 Activation energy for diffusion (E_D) and the pre-exponential factor (D_o) [$D=D_o \exp(-E_D/k_BT)$] of AP, the neutral radical, and the anion radical obtained by the Arrhenius plot of D (Fig. 5-8) in ethanol and ethanol + NaOH(0.01M).

	D_o / 10^{-7} m^2s^{-1}	E_D / kcal mol^{-1}
parent molecule (in ethanol)	2.0±0.1	2.97±0.04
(in ethanol+NaOH 0.01M)	1.7±0.2	2.88±0.05
neutral radical (in ethanol)	2.3±0.2	3.52±0.06
anion radical (in ethanol+NaOH 0.01M)	1.9±0.1	3.56±0.03

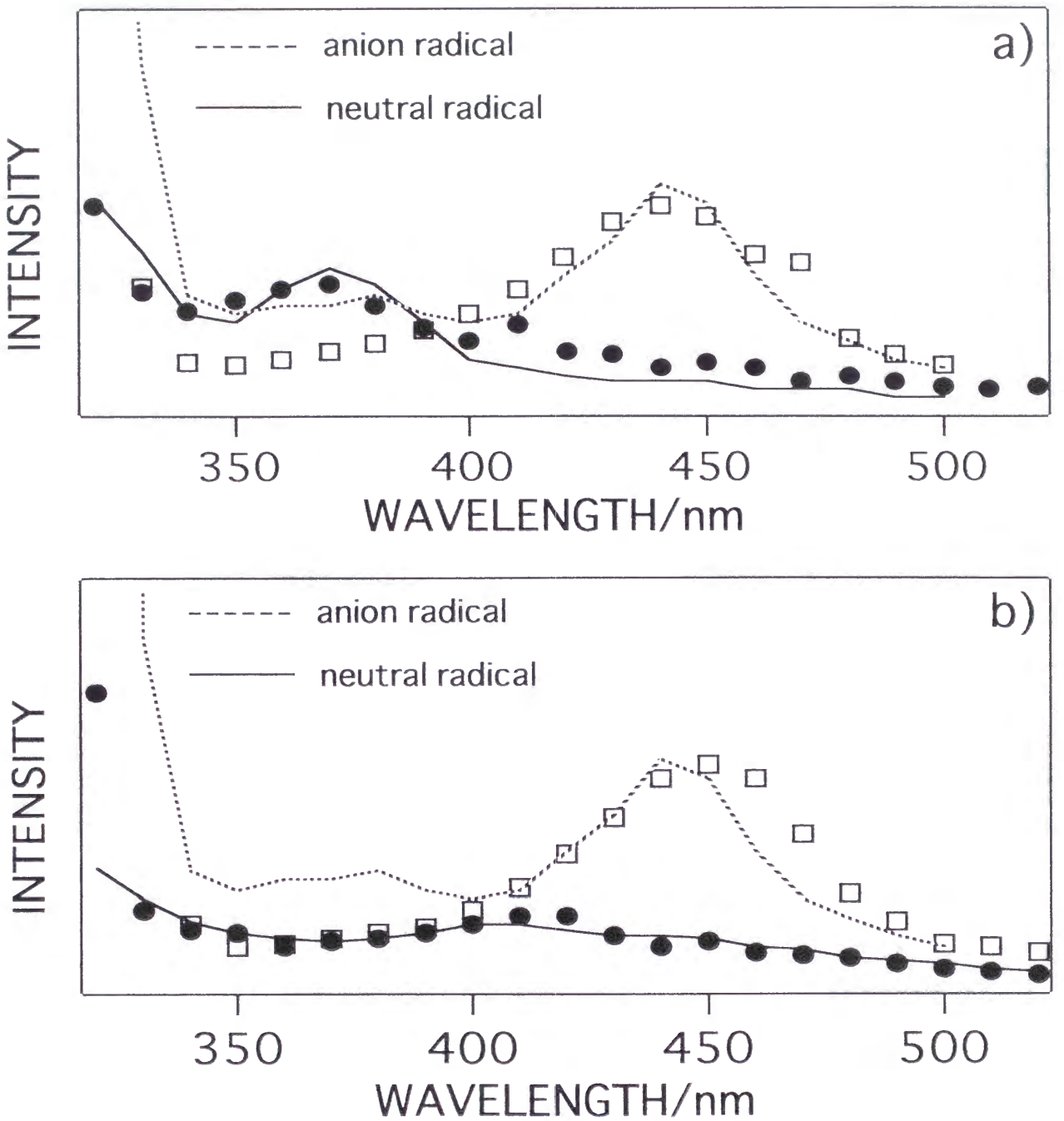

Fig. 5-1 (a) Transient absorption spectra at a 100μs time delay after the excitation of AP in water (●) and AP in water + NaOH (0.01M)(□). (b) Transient absorption spectra of AP in pure ethanol (●) and AP in ethanol + NaOH (0.01M)(□). Spectra of the neutral radical of AP (solid line) and the anion radical of AP (dotted line) from ref. 16 (in water), 17 (in ethanol) are shown in both figures for comparison.

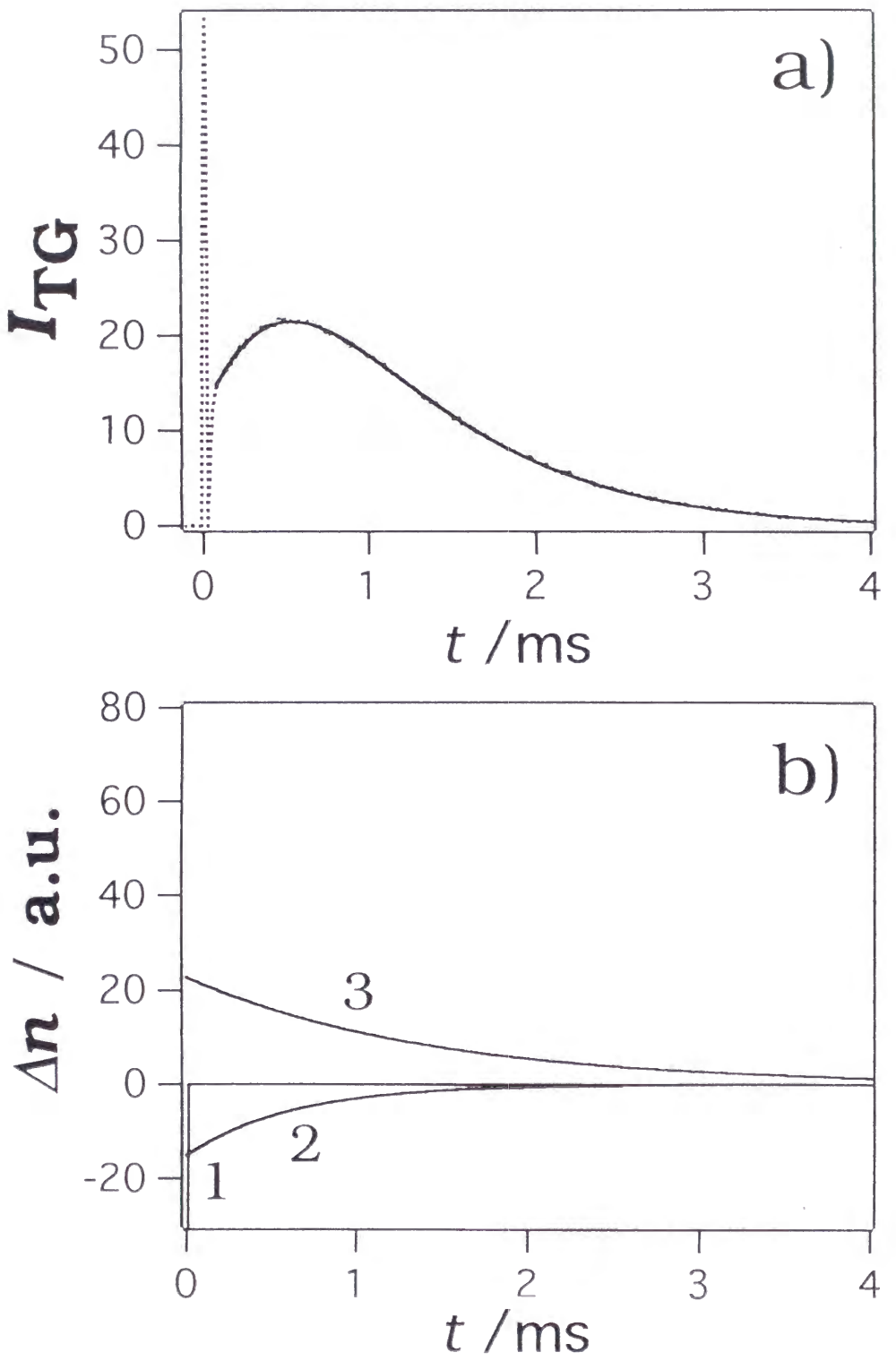

Fig. 5-2 (a) Time profile of the TG signal after the photoexcitation of AP in ethanol at 20°C (dotted line) and best fitted curve (solid line) by eq (6-1). (b) Three components for the fitting in (a) are shown separately. The assignments of these components are 1; thermal grating, 2 and 3; species grating of AP and that of the neutral ketyl radical of AP, respectively.

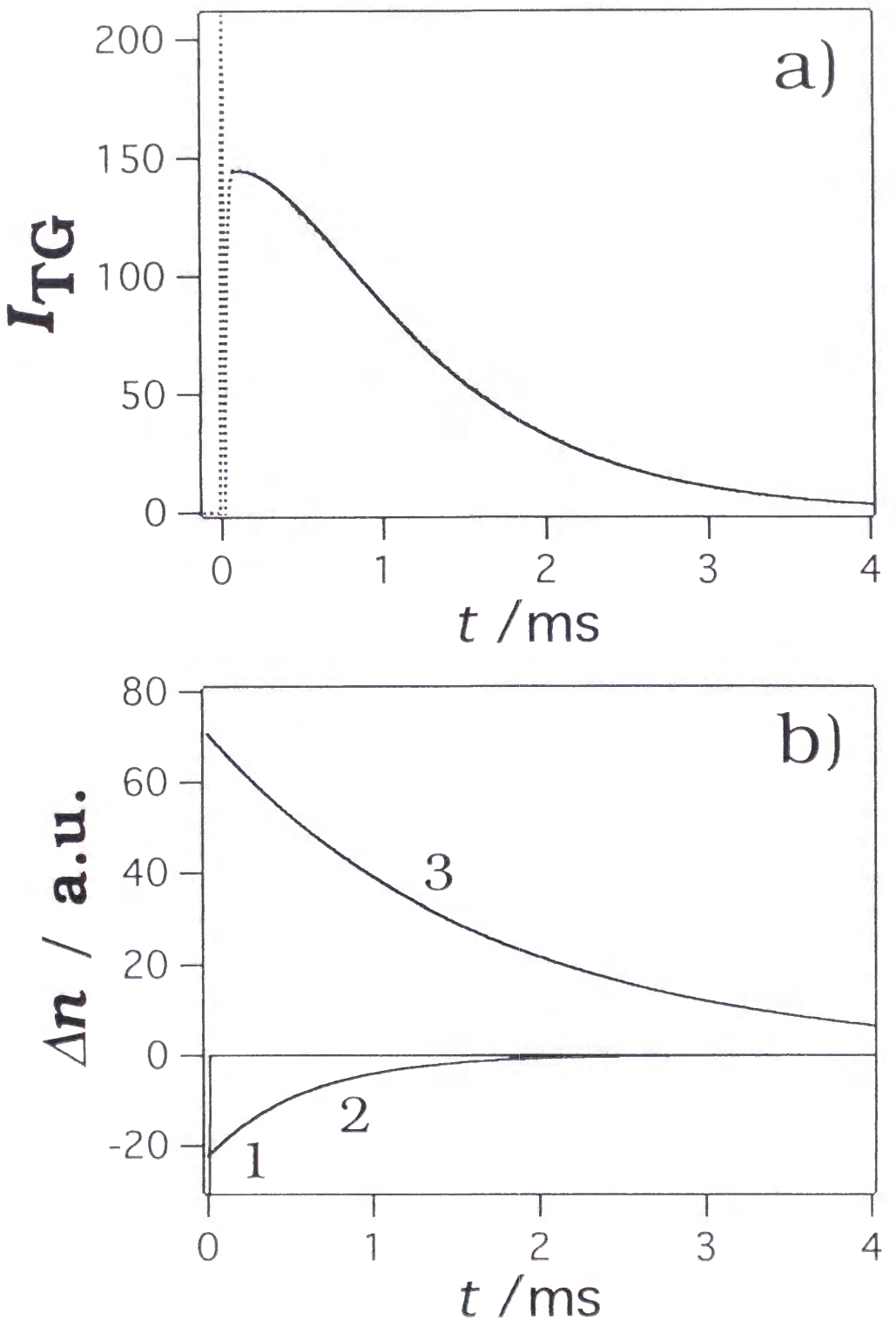

Fig. 5-3 (a) Time profile of the TG signal after the photoexcitation of AP in ethanol + NaOH (0.01M) (dotted line) and best fitted curve (solid line) by eq (6-1). (b) Three components for the fitting in (a) are shown separately. The assignments of these components are 1; thermal grating, 2 and 3; species grating of AP and that of the anion ketyl radical of AP, respectively.

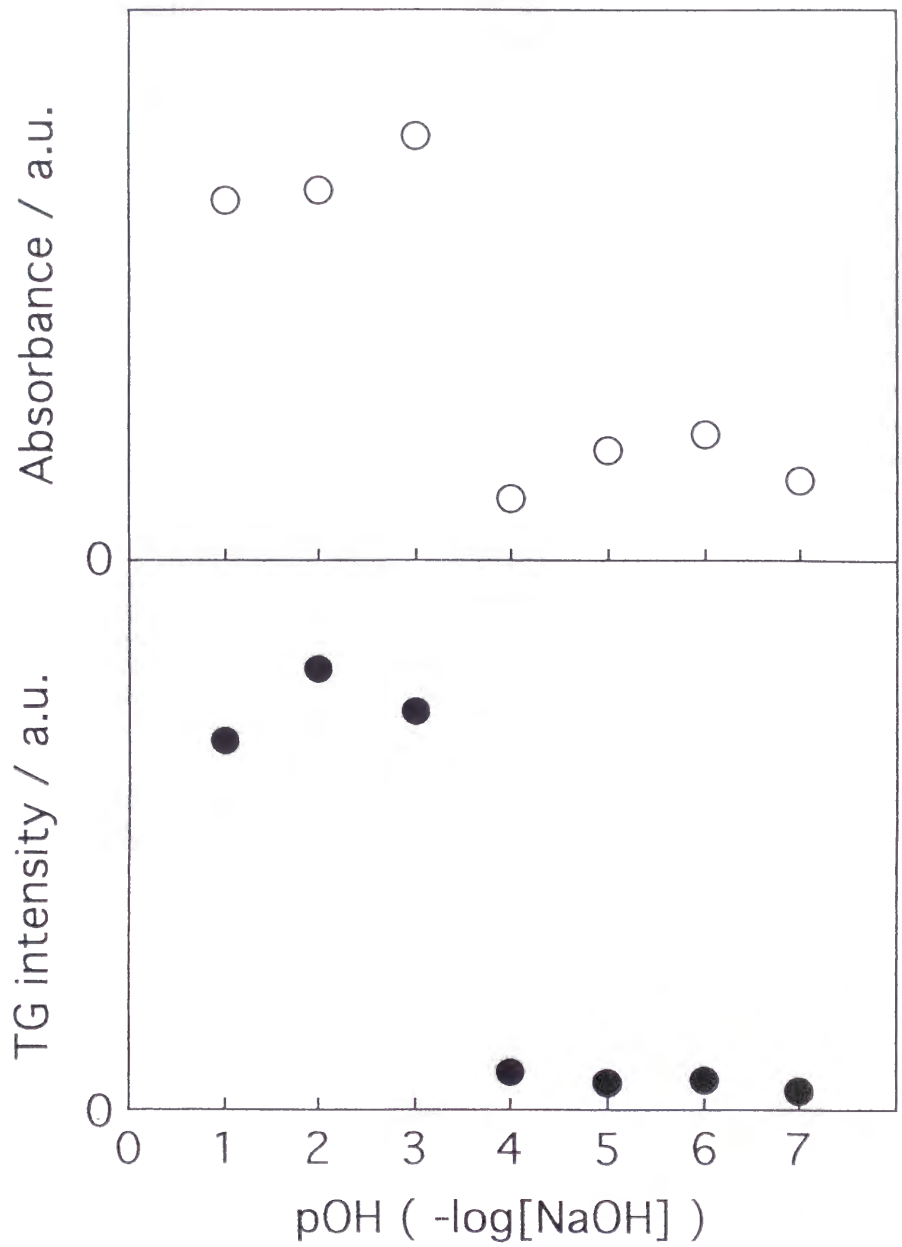

Fig. 5-4 Plot of the signal intensity of the transient absorption at 450 nm (top) and that of the transient grating (bottom) at a 100μs delay after the excitation against the concentration of NaOH in AP / ethanol + NaOH.

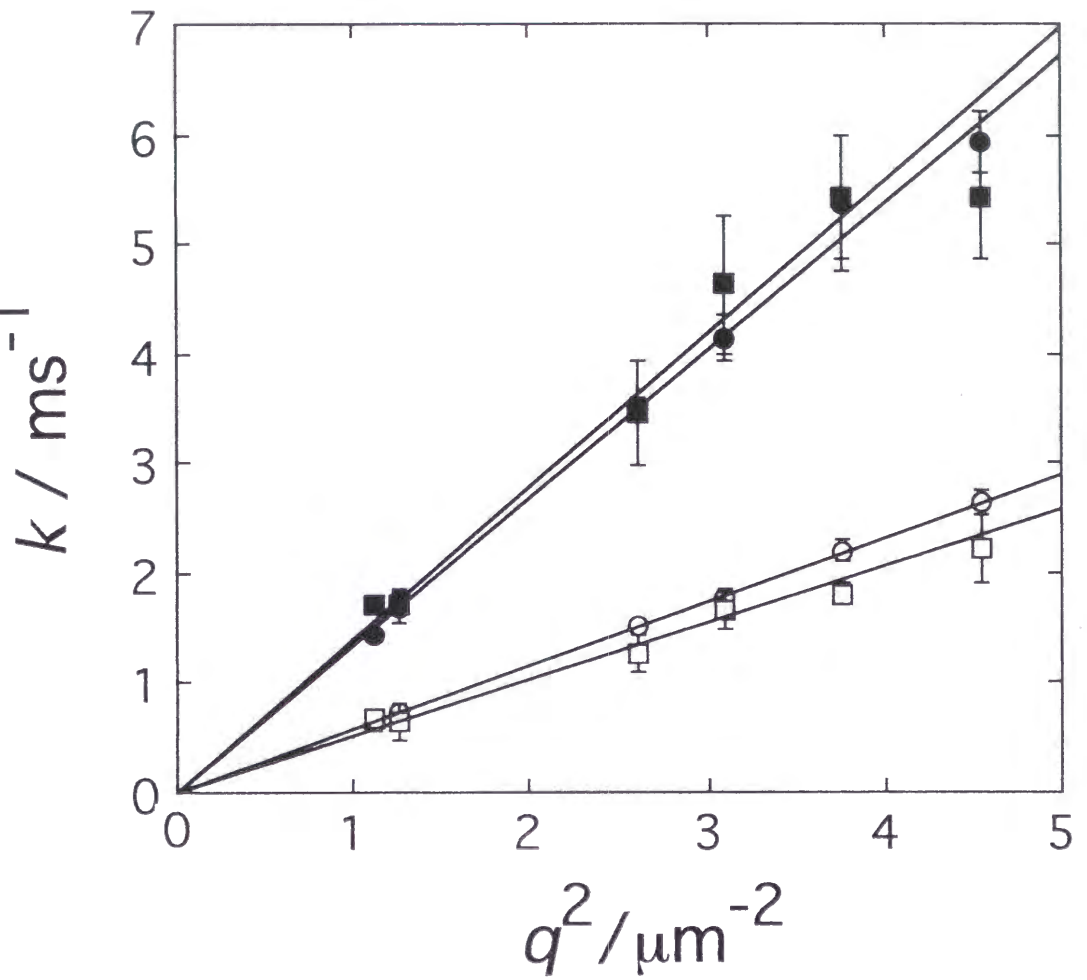

Fig. 5-5 Relationship between the decay rate constants (k) of each component of the TG signal and q^2. ●, ○ denote the parent molecule (AP), the neutral radical of AP in ethanol, respectively. ■, □ denote the parent molecule (AP), and the anion radical of AP in ethanol + NaOH (0.01M), respectively.

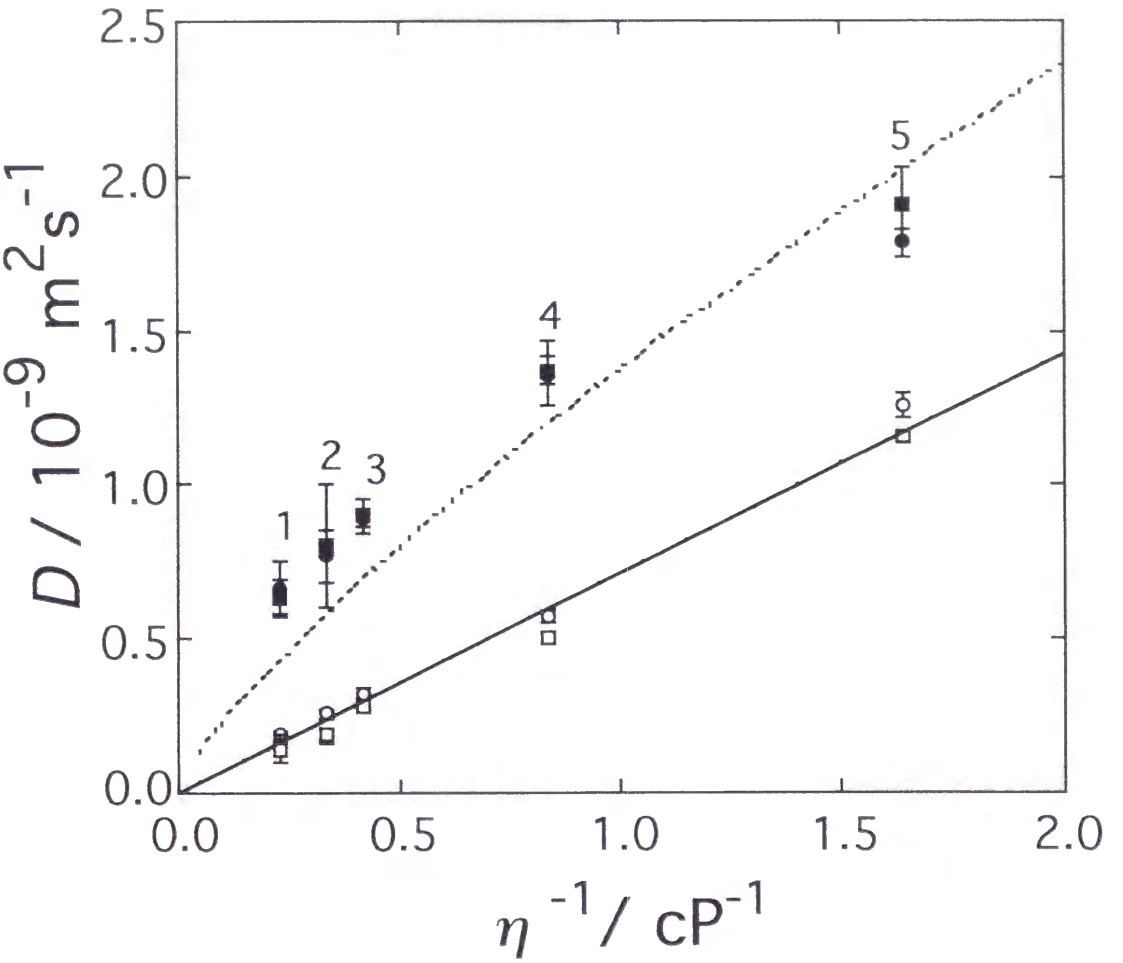

Fig. 5-6 Viscosity dependence of D of AP in alcohols (●), the neutral radical of AP in alcohols (○), AP in alcohol + NaOH (0.01M) (■), the anion radical of AP in alcohol + NaOH (0.01M) (□). Solvents are 1; 1-pentanol, 2; 1-butanol, 3; 2-propanol, 4; ethanol,and 5; methanol. Solid line and dotted line are D calculated from qes. (5-4) and (5-5), respectively.

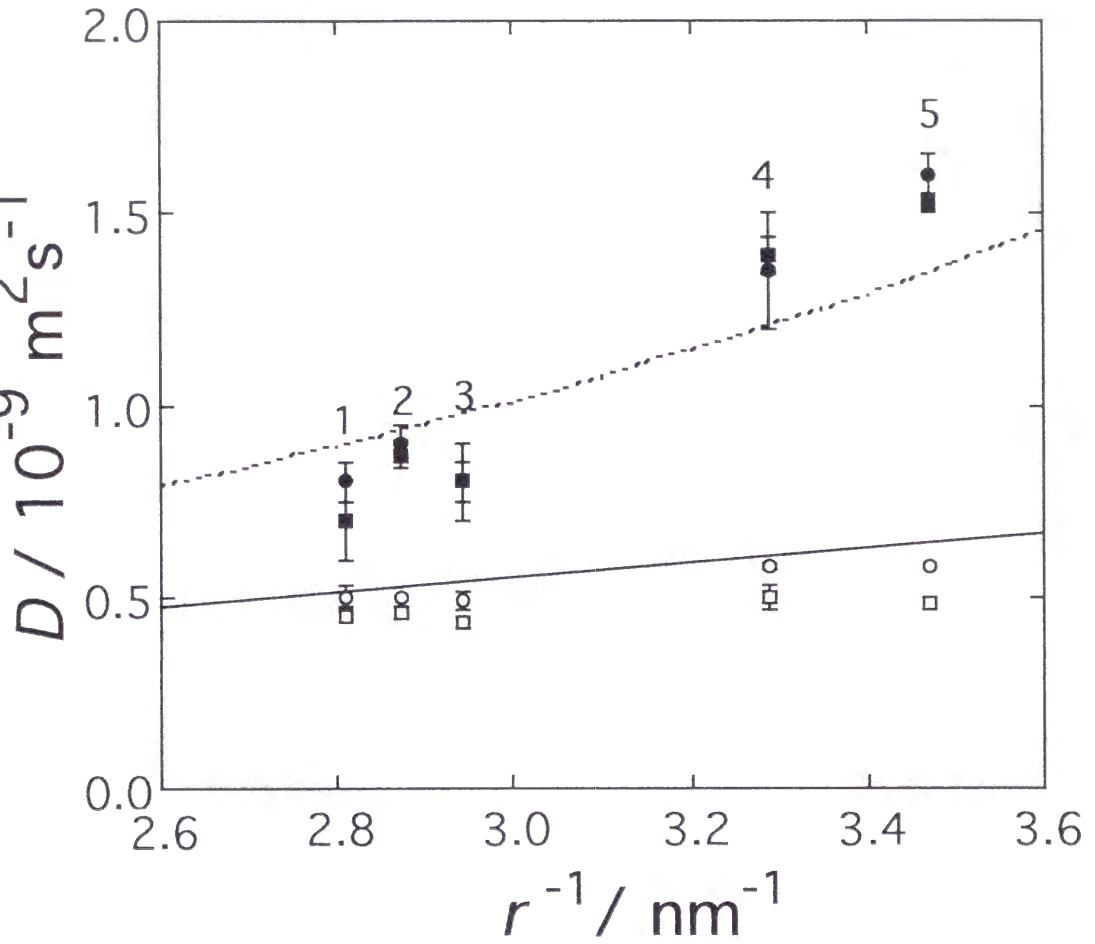

Fig. 5-7 The solute size dependence of D of parent melecules in ethanol (●), neutral radicals in ethanol (○), AP in alcohol + NaOH (0.01M) (■), the anion radical of AP in alcohol + NaOH (0.01M) (□). Solute ketones are 1; benzil, 2; benzophenone, 3; xanthone, 4; acetophenone, and 5;benzaldehyde. Solid line and dotted line are D calculated from eqs. (5-4) and (5-5), respectively.

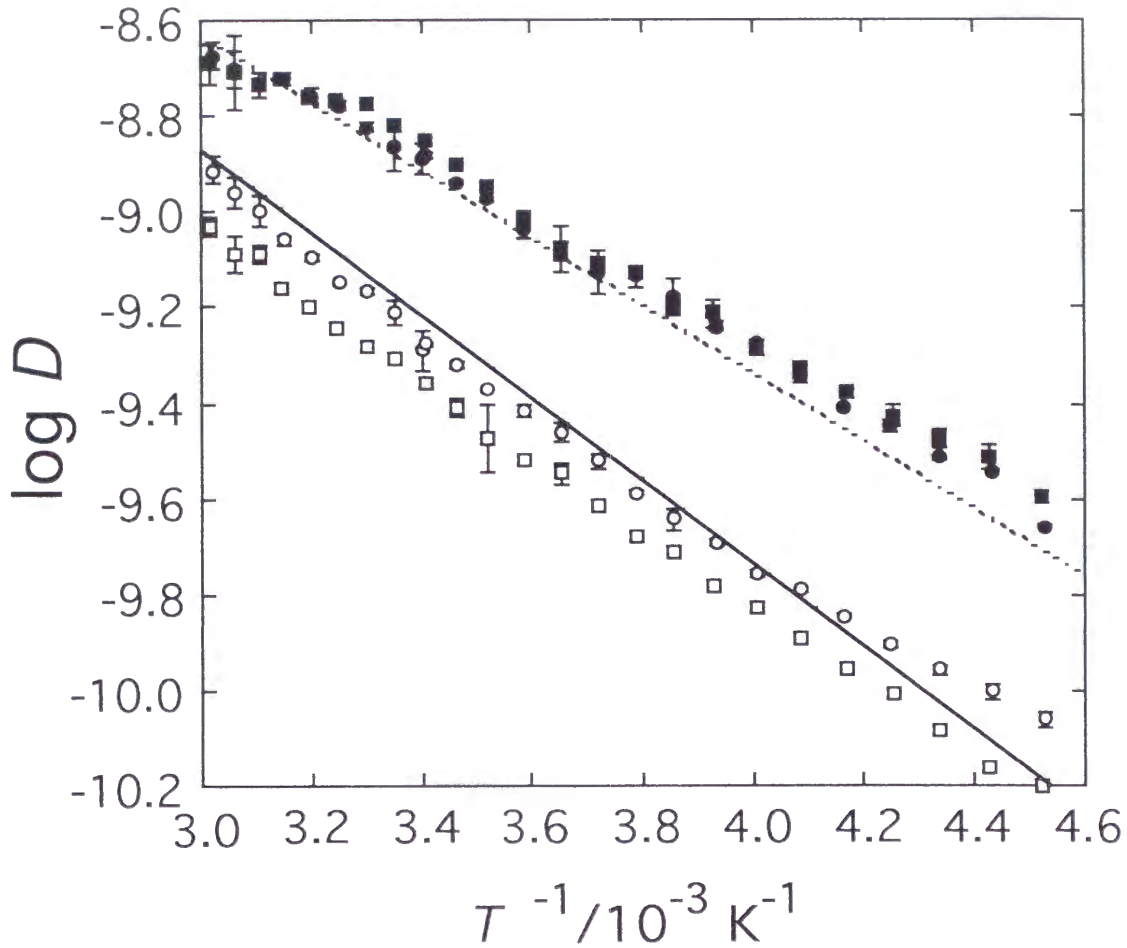

Fig. 5-8 The temperature dependence of D of AP in ethanol (●), the neutral radical in ethanol (○), AP in ethanol + NaOH (0.01M) (■), the anion radical in ethanol + NaOH (0.01M) (□). Solid line and dotted line are D calculated from qes. (5-4) and (5-5), respectively.

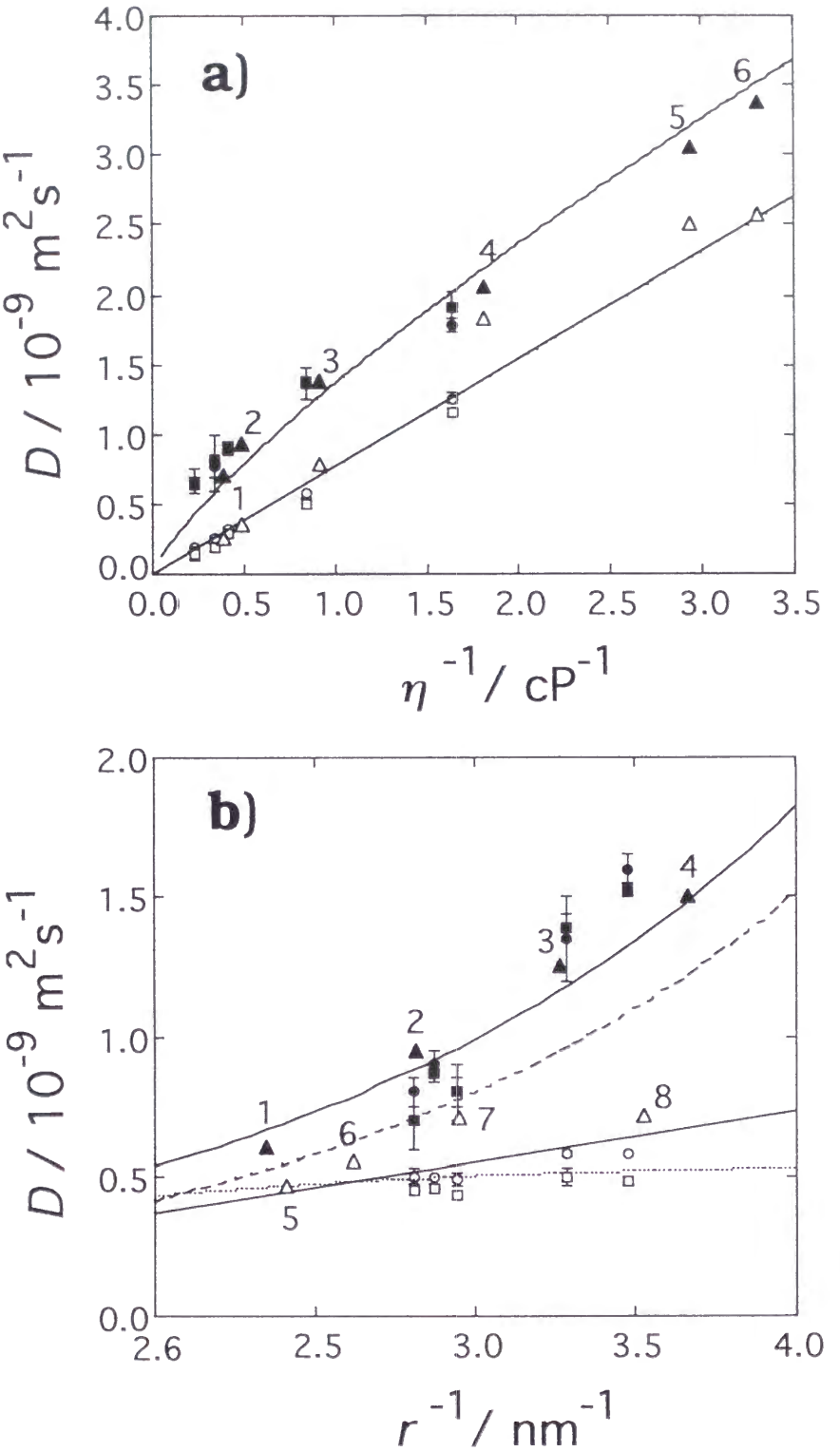

Fig. 5-9 The reported D of the tetraalkyltins (▲) and D calculated from the reported λ of the tetraalkylammonium ions (△) from ref. 3 with our data. (a) The solvent viscosity dependence of D of Me_4Sn, Me_4N^+ (radii are 3.06 Å and 2.84 Å, respectively) in 1; 1-butanol, 2; 2-propanol, 3; ethanol, 4; methanol, 5; acetonitrile, and 6; acetone. (b) The solute size dependence of D of the stable molecules 1; Bu_4Sn, 2; Et_4Sn, 3; Me_4Sn, 4; CCl_4, and the ions 5; Bu_4N^+, 6; Pr_4N^+, 7; Et_4N^+, 8; Mt_4N^+ in ethanol. The curved solid line, straight solid line, dotted line, and broken line are D calculated by eq. (5-5), the SE equation [eq. (5-4)], the excess volume model [eq (5-9)], and the dielectric model corrected by the Hubbard-Onsager equation (ref. 28), respectively.

Chapter 6

RADICAL DIFFUSION IN AQUEOUS SOLUTONS

6.1 Properties of the Water.

In this chapter, the effect of water to the translational diffusion of the transient radicals was studied. [1] Water is a unique solvent in many senses. One of the most remarkable character of water is the strong and steric solvent structure fromed by the hydrogen bonding network. In particular, the solvent structures play a very important roll in the hydrophobic case. If the solute molecule is strongly hydrophobic, water network around the hydrophobic solute tends to be stronger than that of the bulk phase. It is called the hydrophobic hydration. In 1938, Butler et al. found that the dissolution entropy change of non-polar solutes are negative and heat capacity change are very large. [2] In 1945, Frank and Evans interpreted this observation by the iceberg hydration model, which is the basic model of the hydrophobic hydration. [3] In 1959, Kauzmann proposed the concept of the hydrophobic interaction, [4] and since ~1970, Ben-Naim has developed the concept of the hydrophobic hydration. [5] After that, many observations [6~8] and calculations [9] of the hydrophobic hydration have been reported. The solvent structure of water has been elucidated by the X-ray diffraction, [10] the neutron diffraction, [11] and several calculations. [12] The hydrogen bond of the water molecule can extend to four directions and the solvent structure is tetrahedral like diamond. [13~14]

Because of this structure, the diffusion in water is different from that in organic solvents. [13] The diffusion processes of stable molecules in aqueous solution have been reported in many literatures so far. [14] Generally, D in the aqueous solutions are smaller than that in the organic

solutions. These observation have been interpreted based on several theories from the hydrodynamic model. Simply, D is calculated by the Stokes-Einstein (SE) equation (D_{SE}) with parameters r, η, T, and f [eq. (3-4)]. [14] f is a constant which depends on the boundary condition between the solute-solvent molecules; f=4 (slip) ~ 6 (stick). However, in many organic solutions, f should be much smaller than 4 (slip) to reproduce experimental D by D_{SE}.

While f in an organic solvent becomes smaller with increasing η (decreasing T), Tominaga et al. found that f in water is nearly 6 and rather insensitive to the temperature. [15] This fact suggests that the hydrodynamic description with the stick boundary condition is more appropriate in water than in organic solvents. Tominaga et al. explained this observation by two factors; (1) the molecular size of water is smaller than that of many other organic solvents, so the continuous fluid approximation of the hydrodynamic theory becomes reasonable, (2) even if f in water becomes smaller with decreasing T like in an organic solvent, hydrogen bonding of water becomes stronger so that friction between solute and solvent increases (f increases) with decreasing T, and this effect may compensate the decrease of f. [15] Moreover, although the solute and solvent hydrogen bonding generally decreases the diffusion constant in protic solvents, D in water, which is one of protic solvents, does not decrease. [16]

In other to examine the diffusion behavior in the hydrogen bond network, the diffusion constant of neutral radicals, anion radicals, and parent molecules are measured in mixed solutions of ethanol and water. Ethanol is miscible with water in any proportion and water-ethanol mixed solution is one of the typical mixed solution. The properties of this mixed solutions such as thermodynamic character, [17] structure, [18] and viscosity [19] have been already reported.

We found that the difference in D between the radicals and the parent molecules becomes smaller with increasing the water concentration in the solution. This feature is discusses in terms of the solution structure of the mixture. We think that the difference in D between the radicals and the parent molecules decreases because of the hydrophobic hydration around the solutes.

6.2 Photochemical Reactions in Aqueous Solutions.

Before going into the TG experiment, we first examine the photochemistry of the solutes we

used (benzoquinone (BQ) and acetophenone (AP)). The photochemical scheme of BQ and AP are similar to scheme 3-1. The lowest excited triplet (T_1) state is created by the intersystem crossing from the lowest excited singlet (S_1) state by the UV excitation. The benzosemiquinone radical ($BQH^{\cdot}$) or the AP ketyl radical ($APH^{\cdot}$) is created by the hydrogen abstraction from the lowest excited triplet (T_1) state created by the intersystem crossing from the lowest excited singlet (S_1) state by the UV irradiation. [20]

We investigate this reaction scheme and also the chemical stability of the radicals in ethanol+water mixed solution by the transient absorption (TA) and time-resolved EPR (TREPR) methods. The TA spectrum at a 10μs time delay after the excitation of BQ and AP in ethanol and in a ethanol (10 % (v/v)) + water (90 % (v/v)) mixed solution (E/W (1/9)) is shown in figure 6-1. In pure ethanol (Fig. 1a,b), the observed spectra are similar to the reported spectra of $BQH^{\cdot}$ and $APH^{\cdot}$, [21~23] and it is reasonable to assign these species to $BQH^{\cdot}$ and $APH^{\cdot}$. The TA spectrum of AP in E/W (1/9) is also similar to the reported spectrum of $APH^{\cdot}$ in an aqueous solution (Fig. 1d). [24] Therefore, $APH^{\cdot}$ should be created dominantly in ethanol and E/W (1/9). Although, the neutral radical ($MH^{\cdot}$) and the anion radical ($M^{\cdot -}$) are in equilibrium, [23~25]

$$MH^{\cdot} \rightleftarrows M^{\cdot -} + H^{+} \qquad \text{(a)}$$

$$\text{or} \quad MH^{\cdot} + OH^{-} \rightleftarrows M^{\cdot -} \qquad \text{(b)}$$

pKa of $APH^{\cdot}$ was reported to be 9.9 [24] and the relatively large pKa makes $APH^{\cdot}$ dominant even in aqueous solution [See section 2 in chapter 5]. On the other hand, the TA spectrum of BQ in E/W (1/9) is similar to the reported spectrum of BQ anion radical ($BQ^{\cdot -}$) in an aqueous solution (Fig. 1c). [23] Therefore, we assign the chemical species in water rich solution to $BQ^{\cdot -}$. Since pKa of $BQH^{\cdot}$ is 4.0, [23] $BQ^{\cdot -}$ is created dominantly in an aqueous solution (pH=7). On the other hand, as the autoprotolysis constant of ethanol is much smaller than that of water, $BQH^{\cdot}$ is created dominantly in pure ethanol.

Considering the chemical equilibrium (a) and (b), one can create the anion radical or the neutral radical selectively by controlling pH of the solution. The TA spectra of BQ in E/W (1/9)

with H_2SO_4 (0.1M) and AP in E/W (1/9) with NaOH (0.1M) are shown in Fig. 1e,f and each spectrum is similar to the reported spectra of $BQH^{\cdot}$ [23] and $AP^{\cdot -}$ [24] well, respectively. The time profiles of all the TA signals can be expressed well by the second ordered kinetics and the half life period is ~10ms at a power of ~1 mJ/cm^2 for photoexcitation.

Since the TA spectra of $BQH^{\cdot}$ and $BQ^{\cdot -}$ are rather similar, it is difficult to distinguish which species are dominantly created in mixed solvents. To identify the chemical species more clearly, we use the TREPR technique. The EPR spectra of $BQH^{\cdot}$ and $BQ^{\cdot -}$ have been reported and the spectra shape of both species are quite different. [26] Figure 6-2 shows the observed EPR spectra of BQ at a 1μs time delay after the excitation (a) in ethanol, (b) in E/W (1/9), and (c) in E/W (5/5). The shapes of the obtained EPR spectra of three systems are quite different and it was found that $BQH^{\cdot}$ and $BQ^{\cdot -}$ are created in ethanol and E/W (1/9), respectively. [26] This fact is consistent with the conclusion from the TA measurement. The equilibrium process (f) and (g) should be very fast (the equilibrium should complete within 1 μs). The EPR spectrum of BQ in E/W (5/5) can be analyzed by the superposition of the spectra (a) and (b). It suggests that the both species of $BQH^{\cdot}$ and $BQ^{\cdot -}$ exist in E/W (5/5).

6.3 TG signal in Water/Ethanol mixed Solvents.

The time profiles of the TG signals after the excitation of BQ in E/W (10/0~1/9) are shown in figure 6-3. All signals consist of three components; a spike-like signal, a subsequent slow rise component, and slow decay. The TG signal of BQ in ethanol has been analyzed previously [section 3~4 in chapter 3]. The spike-like signal which decays in a few microseconds is originated from the thermal grating. The slower rise and decay components should be the species grating created by the photochemical reaction. In this reaction system, four chemical species (BQ, $BQH^{\cdot}$, ethanol, and hydroxyethyl radical) could contribute to the TG signal. However, since the absorption coefficients of ethanol and the hydroxyethyl radical [27] are smaller than those of BQ and $BQH^{\cdot}$ in the visible and near UV region, [21,23] only two species (BQ and $BQH^{\cdot}$) dominantly contribute to the species grating (Fig. 6-3).

Similar signals were observed for AP. Because the absorption coefficients of AP and $APH^{\cdot}$

[22, 24-25] are larger than those of ethanol and the hydroxyethyl radical, the species grating mainly comes from the AP and $APH^{\cdot}$ contributions.

In these systems, the solute molecules (BQ, $BQH^{\cdot}$, $BQ^{\cdot -}$, AP, $APH^{\cdot}$, and $AP^{\cdot -}$) do not have any absorption bands at the wavelength of the probe light (633nm). [21~25,27] Hence, the square root of the TG signal should be proportional to only the refractive index change. The species grating decays by the mass diffusion process and subsequent reaction process of the radicals, which is mainly the recombination of the radicals. The recombination of $BQH^{\cdot}$ and $APH^{\cdot}$ are reported as the diffusion controlled process. [28] As the excitation laser power for the TG measurement is much weaker (~0.3 mJ/cm^2) than that for the TA experiment, the half life period of the radicals should be much longer than that of the TA measurement (~10ms). The concentrations of the radicals should be almost constant within the time range for the TG measurement (~1ms). Therefore, it is reasonable that the decay profile of the species grating signals can be analyzed by only the diffusion process. The time profile of the TG signal is given by

$$I_{TG}(t)^{1/2} = \delta n_{th}^{\ o} \exp(-D_{th} q^2 t) - \delta n_P^{\ o} \exp(-D_P q^2 t) + \delta n_R^{\ o} \exp(-D_R q^2 t) \qquad (6\text{-}1)$$

where, $\delta n_{th}^{\ o}$, $\delta n_P^{\ o}$, and $\delta n_R^{\ o}$ are the initial refractive index changes of the thermal grating and the species gratings of parent molecules (BQ, AP) and radicals ($BQH^{\cdot}$, $APH^{\cdot}$), respectively [See eq.(3-1) and (3-2)]. Generally, the refractive index change of the thermal grating is negative ($\delta n_{th}^{\ o} < 0$) and the refractive index change of the species grating of all species in this systems is positive ($\delta n_P^{\ o}$, $\delta n_R^{\ o} > 0$). [21~25,27]

The spike-like component of the TG signals is the thermal grating signal. D_{th} from the TG signal agrees well with the calculated one. [29] Comparing the sign of the refractive index in eq (6-1) ($\delta n_P^{\ o}$, $\delta n_R^{\ o} > 0$) with the TG signals (Fig. 6-3), we assigned that the slowly rising component and decay component of the TG signal are due to the species grating of the parent molecules and the radicals, respectively. We fitted the species grating component of the TG signals with double-exponential function and determined D_P and D_R (table 6-1).

The TG signal of BQ in E/W (5/5~1/9)+H_2SO_4 (0.1M) and AP in E/W (10/0~1/9)+NaOH

(0.1M) are similar to the TG signal shown in Fig. 6-3. D of $BQH^{\cdot}$ and $AP^{\cdot -}$ in several mixed solutions are determined by the same analytical method (table 6-1). It is noteworthy that, although the TG signals of BQ in E/W (5/5) can be fitted by a double exponential function, the TREPR spectra (Fig. 6-3) clearly indicate the presence of three species (BQ, $BQH^{\cdot}$, and $BQ^{\cdot -}$). This fact suggests that D of $BQH^{\cdot}$ and $BQ^{\cdot -}$ are similar in ethanol+water. This observation is consistent with the similar diffusion constant of anion radicals and neutral radicals created from ketones in ethanol (chapter 3). D of the anion radicals and that of the neutral radicals of AP are also very close in the mixed solution of ethanol and water. The intensities of the TG signals in pure water are much smaller than that in the water-ethanol mixed solution, because the efficiency of the hydrogen abstraction reaction from water molecule may be smaller than that from the ethanol (next chapter).

Our values of D from the TG method are close to literature values from the TD method [30] (BQ; 1.44×10^{-9}, AP; $1.24 \times 10^{-9} m^2 s^{-1}$ in ethanol) within 10%. The fitting errors of the radicals should be smaller those that of the parent molecules (≤10%).

6.4 Comparison of D of the Parent Molecules and Radicals.

D is plotted against the concentration of water (%) in ethanol in figure 6-4. Figure 6-4a shows that D of mixture of $BQH^{\cdot}$ and $BQ^{\cdot -}$ (white squares) are quite similar to D of $BQH^{\cdot}$ (white circles). Fig. 6-4b shows that D of $APH^{\cdot}$ (white squares) are quite similar to D of $AP^{\cdot -}$ (white circles). Therefore, D of the neutral radicals and the anion radicals are quite close each other in all the mixed solutions.

We compare the obtained D with D_{SE} [eq. (3-4)] and D_{EV} [eq. (3-5), (4-15), or (5-5)]. In previous chapter, we have shown that D of parent molecules agree very well with D_{EV}. On the other hand, D of the neutral or anion radicals are close to D_{SE} with the stick boundary. D_{SE} and D_{EV} in several solutions are also shown in Fig. 6-4. D of the radicals are close to D_{SE} in all the solutions. D of the parent molecules are close to D_{EV} in ethanol rich solutions, but smaller than D_{EV} in the water rich region. The difference becomes larger with increasing the content of water in solution and D becomes closer to D_{SE}.

Figure 6-5 shows the ratio of D between the parent molecules and the radicals against the

concentration of water in ethanol. The ratios of both systems decrease linearly with increasing the concentration of water. The difference in D between the parent molecules and the radicals became smaller by addition of water. In section 3.6, the slow diffusion of radicals was observed regardless of the solvent property (the polarity, the dipole moment and the protic character, etc.). Only in the aqueous solution, the diffusion processes of the radicals are similar to those of the parent molecules. The possible origin of this fact is considered in later sections.

Figure 6-6 shows $D\eta$ against 1/r of the parent molecule (open circle) and the radicals (open square) in ethanol and those of stable molecules in water (open triangle) reported in chapter 3. The curved and straight lines are calculated ones of $D_{SE}\eta$ and $D_{EV}\eta$, respectively. It is evident that $D_P\eta$ and $D_R\eta$ agree with $D_{SE}\eta$ and $D_{EV}\eta$, respectively in ethanol. On the other hand, $D_P\eta$ in water are close to $D_{SE}\eta$ rather than $D_{EV}\eta$. The agreement with $D_{SE}\eta$ could indicate that the water molecules can be treated as a continuous fluid. $D\eta$ of BQ, AP (closed circle) and the radicals ($BQH^{\cdot}$, $BQ^{\cdot -}$ and $APH^{\cdot}$, $AP^{\cdot -}$) (closed square) in E/W (1/9) are also plotted in Fig. 6-6. $D\eta$ of both the radicals and the parent molecules are close to D_{SE} rather than D_{EV}.

6.5 Temperature Dependence of D in Ethanol and in Water.

Temperature dependence of D is examined in ethanol and in water for studying the diffusion processes in these solvents. In many cases, the temperature dependence of neutral stable molecules can be expressed by the Arrhenius-type equation with the diffusion activation energy (E_D) and the pre-exponential factor (D_o) [eq. (3-6)]. We plotted logD against 1/T (Arrhenius plot) in Fig. 6-7 for the samples in ethanol. Although both Arrhenius plots in ethanol show a good liner relationship, the difference in the activation energy is notable. In section 3.8, the different activation energies between the radicals and parent molecules in ethanol and 2-propanol are explained as follows.

If the temperature dependence of the viscosity is written by the following equation [eq. (3-7)]

$$\eta = \eta_o T \exp\left(\frac{E_\eta}{k_B T}\right) \qquad (6\text{-}2)$$

where E_η (= 3.96 kcal/mol in ethanol) is the activation energy of viscosity, [31] we obtain E_D = E_η from the hydrodynamic theory. On the other hand, if D is well expressed by the equation of Evans et al., E_D is given by

$$E_D = E_\eta \left(\frac{c}{r} + d \right) \tag{6-3}$$

where c abd d are the constant, which determined c=-o.86365Å^3 and d=1.0741. In this case, since c is negative, E_D is slightly smaller than E_η and depends on the molecular size. Indeed, if we plot D_{SE} and D_{EV} (Fig. 6-7), it is evident that the temperature dependence of D of the radicals is expressed well with D_{SE}, while, that of the parent molecules are close to D_{EV} with eq (6-3).

On the other hand, the Arrhenius plots of D of the radicals and the parent molecules in water (+10% ethanol) (Fig. 6-8) are not linear and they resemble each other. We also plot D_{SE} and D_{EV} in Fig. 6-8. D of both the radicals and parent molecules are close to D_{SE} rather than D_{EV} which suggest that the temperature dependence of D is mainly determined by that of η. This nonlinearity of the Arrhenius plot of D in water has been reported by Tominaga et al. for stable molecules in water. [15] This nonlinearity was explained by the fact that the temperature dependence of the viscosity of water cannot be expressed by eq (6-2). Water is strongly hydrogen bonded and builds a steric structure. The hydrogen bonding and becomes stronger with decreasing T. Therefore, the slope of the Arrhenius plot becomes steeper with decreasing T. Our results are similar to their results. This result suggests that the hydrodynamic approximation of diffusion is reasonable. We conclude that D of the radicals and the parent molecules are similar in a wide range of temperature in water.

6.6 Similar D of the Radicals and Parent Molecules in Water.

In previous chapter, we reported D of the radicals and the parent molecules in various organic solvents, and founds that D_R is always smaller than D_P. In this chapter, we for the first time find a solvent in which D_R is similar to D_P. In this section, we consider a possible origin of the similarity of D_P and D_R. This unique property of water could be explained by the hydration.

In the case of hydrophilic solutes (e.g. ionic, polar, or hydrogen bonded molecule), the hydrogen bonds of water are destroyed and/or complex-like hydration structures are constructed (hydrophilic hydration).[32] On the other hand, in the case of hydrophobic solute, the solute molecules aggregate (hydrophobic bonded)[4] or the hydrogen bonds of water are reconstructed around the solute (hydrophobic hydration).[5~8] The hydrophobic hydration are sensitive not only to the polarity but also to the size and the shape of the solute molecules. The hydrophobic hydration has been observed for inert gas atoms, small alkanes, and also benzene.[6] Using the X-ray diffraction, Nishikawa et al. reported that tert-buthyl alcohol solvated by the hydrophobic hydration in spite of the hydrophilic part (-OH), while ethanol and propanol are not solvated by the hydrophobic hydration.[7] Moreover, the hydrophobic hydration was observed for the tetraalkylammmonium ions although it has a charge which could interact with water strongly.[8] These facts suggest that the hydrophobic property should be more effective than the hydrophilic properties (hydrogen bonding or charge) of the solutes to the hydration mechanism. Tominaga et al. reported that the diffusion process of toluene, ethylbenzene, hexafluorobenzene, n-buthylbenzene, biphenyl, naphthalene, and ethylnaphtalene are very similar to that of benzene in water (D of these molecules are close to D_{SE} with stick boundary).[15] This fact suggests that these molecules are solvated by the hydrophobic hydration as in the case of benzene. Therefore, it is very plausible that BQ and AP are solvated by the hydrophobic hydration in a water rich solvent. Under this condition, D should be described by the SE equation with stick boundary (f=6). Indeed, D of AP and BQ are close to D_{SE} rather than D_{EV}.

As we have described in previous chapter, D of the transient radicals are close to D_{SE} with stick boundary condition in many organic solutions. The different D_R from D_P in these organic solvents have been explained by an attractive interaction between the radicals and solvents, which was recently supported by a theoretical calculation by Morita and Kato.[33] We found, in this study, that D of the radicals in water rich solutions are still close to D_{SE} with the stick boundary condition. This observation can be interpreted in two ways; the radicals diffuse under the influence of the attractive intermolecular interaction in aqueous solution as in the organic solvents or the diffusion is governed by the hydrophobic hydration as those of the parent molecules. We think that

the hydrophobic hydration is more important in aqueous solution because even tetraalkilammonium ions, which has an electric charge and should interact with solvent significantly, is solvated by the hydrophobic hydration.[8] We plot the reported D of the tetraalkylammonium ions in Fig. 6-6.[8c] D of the radicals in water (+10% ethanol) are close to those of the tetraalkylammonium ions and both D are close to D_{SE} with stick boundary (Fig. 6-4 and 6-6). This fact may indicate that the both species (radicals and tetraalkylammonium ions) are solvated by similar hydrophobic hydration. The solute molecules are surrounded by similar solvent structures of strong hydrophobic hydration, regardless the special solute-solvent interaction exist or not. As the solvation structure of both the parent molecules and the radicals should be quite similar, D_P and D_R are close in water rich solutions. Moreover, the weaker hydrogen bonding effect in an aqueous solution reported by Tominaga et al.[15] have the same origin as the slow diffusion of the radicals (the magnitude of the intermolecular interactions of hydrogen bonding may be similar to that of the radicals in ethanol).

The steric structure of water is gradually constructed by increasing the amount of water in ethanol as revealed by several means.[7, 34] Therefore D of the parent molecules gradually change from D_{EV} in ethanol to D_{SE} in water. On the other hand, D of the radicals can be expressed by D_{SE} in ethanol because of the attractive intermolecular interaction and also by D_{SE} in water because of the hydrophobic hydration. Therefore, D of the radicals are close to D in the entire region of the mixed solutions.

6.7 Conclusion.

The diffusion constants (D) of the parent molecules, the neutral radicals, and anion radicals of benzoquinone and acetophenone in ethanol-water mixed solvents were measured by using the transient grating (TG) method. The neutral radicals and the anion radicals are created selectively by addition of the sodium hydroxide and sulfuric acid in water-ethanol mixed solution. D of the radicals are smaller than those of the parent molecules in ethanol as we have reported. D of the neutral radicals and the anion radicals are similar in any mixtures of ethanol and water. We found that the difference between D_R and D_P becomes smaller with increasing the water content in the

solution. We compare the obtained D with those from the Stokes-Einstein equation (D_{SE}) and D proposed by Evans et al. (D_{EV}). D_R are close to D_{SE} in any solutions we investigated. On the other hand, D_P are close to D_{EV} in ethanol and become smaller than D_{EV} and approach D_{SE} with increasing the water content. In E/W (1/9) solution, D_R and D_P are similar and close to D_{SE}. We consider that both the parent molecules and the radicals are solvated by the hydrophobic hydration. When the solvation structure of the hydrophobic hydration is constructed, the special intermolecular interaction of radicals may be reduced by the strong solvent structures. Therefore, in the water rich region, D_P are close to D_R. We also measured the temperature dependence of D. D of the both radicals and parent molecules can be expressed by the Arrhenius type relationship with a single activation energy (E_D) in ethanol. E_D of the radicals are close to the activation energies of viscosities (E_η), though E_D of the parent molecules are slightly smaller than E_η. These features can be explained on the expressions of D_{SE} and D_{EV}. On the other hand, temperature dependence of D in water (+10% ethanol) cannot be expressed by a single activation energy. The temperature dependence of both the radicals and the parent molecules in water are reproduced well by that of D_{SE}. This result is also attributed to the hydrophobic hydration of the radicals and the parent molecules in water.

References to Chapter 6

1. Okamoto, K.; Terazima, M.; Hirota, N. submitted for publication.

2. Barclay, I. M.; Butler, J. A. V. *Trans. Faraday Soc.* **1938**, 34, 1445.

3. Frank, H. S.; Evans, M. W. *J. Chem. Phys.* **1945**, 13, 507.

4. Kauzmann, W. *Adv. Prot. Chem.* **1959**, 14, 1.

5. (a) Ben-Naim, A. *J. Chem. Phys.* **1972**, 57, 5257, *ibid* **1972**, 57, 5266.; (b) Ben-Naim, A.; Yaacobi, M. *J. Phys. Chem.* **1973**, 77, 95.; (c) Ben-Naim, A. *Hydrophobic interactions* (Plenum Press, New York, **1980**)

6. Nakahara, M.; Wakai, C.; Yoshimoto, Y.; Matsubayashi, N. *J. Phys. Chem.* **1996**, 100, 1345.

7. (a) Nishikawa, K.; Hayashi, H.; Iijima, T. *J. Phys. Chem.* **1989**, 93, 6559.; (b) Nishikawa, K.; Iijima, T. *J. Phys. Chem.* **1993**, 97, 10824.; (c) Nishikawa, K.; Kodera, Y.; Iijima, T. *J. Phys. Chem.* **1987**, 91, 3694.

8. (a) Wen, W-Y.; Hung, J. H. *J. Phys. Chem.* **1970**, 74, 170.; (b) Narten, A. H.; Lindenbaum, S. *J. Chem. Phys.* **1969**, 51, 1108.; (c) Ueno, M.; Tsuchihashi, N.; Yoshida, K.; Ibuki, K. *J. Chem. Phys.* **1996**, 105, 3662.

9. (a) Geiger, A.; Rahman, A.; Stillinger, F. H. *J. Chem. Phys.* **1979**, 70, 263.; (b) Owicki, J. C.;Scheraga, H. A. *J. Am. Chem. Soc.* **1977**, 99, 7413.; (c) Okazaki, K.; Touhara, H.; Adachi, Y. *J. Phys. Chem.* **1979**, 71, 2421.; (d) Mancera, R. L. *J. Chem. Soc. Faraday Trans.* **1996**, 92, 2547.

10. (a) Gorbaty, Y. E.; Demianets, Y. N. *Mol. Phys.* **1985**, 55, 571.; (b) Narten, A. H.;Levy, H. A. *J. Chem. Phys.* **1971**, 55, 2263.; (c) Narten, A. H.; Vaslow, F.; Levy, H. A. *J. Chem. Phys.* **1973**, 58, 5017.; (d) Narten, A. H. *ibid.* **1972**, 56, 5681.

11. (a) Narten, A. H. *J. Chem. Phys.* **1972**, 56, 5681.; (b) Thiessen, W.E.; Narten, A. H. *J. Chem. Phys.* **1982**, 77, 2656.; (c) Ichikawa, K.; Kameda, Y.; Yamaguchi, T.; Wakita, H.; Misawa, M. *Mol. Phys.* **1991**, 73, 79.

12. (a) Rahman, A.; Stillinger, F. H. *J. Chem. Phys.* **1971**, 55, 3336.; (b) Stillinger, F. H.; Rahman, A. *J. Chem. Phys.* **1974**, 60, 1514.; (c) Patey, G. N.; Carnie, S. L. *J. Chem. Phys.*

1983, 79, 4468.; (d) Pettitt, B. M.; Rossky, P. J. *J. Chem. Phys.* **1982**, 77, 1452.

13. (a) Witherspoon, P. A.; Saraf, D. N. J. Phys. Chem. 1965, 69, 3752.; (b) Bonoli, L.; Witherspoon, P. A. *J. Phys. Chem.* **1968**, 72, 2532.

14. (a) Cussler, E. L. *Diffusion* (Cambridge University, Cambridge, **1984**).; (b) Tyrrell, H. J. V; Harris, K. R. *Diffusion in Liquid* (Butterworths, London, **1984**).; (c) *Landolt-Bornstein Tabellen* (Springer, Berlin, **1961**), 6 Aufl., Bd. II.

15. (a) Tominaga, T.; Yamamoto, S.; Takanaka, J. *J. Chem. Soc. Faraday Trans.* **1984**, 80, 1984.; (b) Tominaga, T.; Matsumoto, S.; Ishii, T. *J. Phys. Chem.* **1986**, 90, 139.; (c) Tominaga, T.; Matsumoto, S. *Bull. Chem. Soc. Jpn.* **1990**, 63, 533.

16. Tominaga, T.; Tenma, S.; Watanabe, H. *J. Chem. Soc. Faraday Trans.* **1996**, 92, 1863.

17. (a) Onori, G. *J. Chem. Phys.* **1988**, 89, 4325.; (b) Donkersloot, M. C. A. *J. Solution Chem.* **1979**, 8, 293.; (c) Ben-Naim, A. *J. Chem. Phys.* **1977**, 67, 4884.

18. (a) Mashimo, S.; Umehara, T. *J. Chem. Phys.* **1991**, 95, 6257.; (b) D'Arrigo, G.; Teixeira, J. *J. Chem. Soc. Faraday Trans.* **1990**, 86, 1503.; (c) Coccia, A.; Indovina, P.; Podo, F.; Viti, V. *Chem. Phys.* **1977**, 7, 30.

19. Bingham, E. C.; Hatfield, J. E.; Jackson, R. F. *Bur. Stand. J. Res. Scie.* **1917**, 298.

20. Cadogan, J. I. G. *Principles of Free Radical Chemistry* (The Chemical Society Monographs For Teachers No. 24, **1973**).

21. Kimura, K.; Yoshinaga, K.; Tsubomura, H. *J. Phys. Chem.* **1967**, 71, 4485.

22. Lutz, H.; Breheret, E.; Lindquist, L. *J. Phys. Chem.* **1973**, 77, 1753.

23. Adams, G. E.; Michel, B. D. *Trans. Faraday Soc.* **1967**, 63, 1171.

24. (a) Hayon, E.; Ibata, T.; Lichtin, N.N.; Simic, M. *J. Phys. Chem.* **1972**, 76, 2072.; (b) Beckett, A.; Osborne, A. D.; Porter, G. *Trans. Faraday. Soc.* **1964**, 60, 873.

25. Ononye, A. I.; Bolton, J. R. *J. Phys. Chem.* **1986**, 90, 6270.

26. Pedersen, J. B.; Hansen, C. E. M.; Parbo, H.; Muus, L. T. *J. Chem. Phys.* **1975**, 63, 2398.

27. Simic, M.; Neta, P.; Hayon, E. *J. Phys. Chem.* **1969**, 73, 3794.

28. Khudyakov, I. V.; Koroli, L. L. *Chem. Phys. Lett.* **1984**, 103, 383.

29. (a) Touloukian, Y. S. *Thermophysical Properties of Matter* (Plenum, New York, **1970**), vol III.; (b) *International Critical Tables* (McGraw-Hill, New York, **1928**), vol. III.; (c) *Landolt-Bornstein Tabellen* (Springer, Berlin, **1972**), 6 Aufl., Bd. IV.

30. Donkers, L. R.; Leaist, G. *J. Phys. Chem. B* **1997**, 101, 304.

31. (a) Mizushima, S. Bull. Chem. Soc., (Japan) **1926**, 1, 143.; (b) Phillips, T. W.; Murphy, K. P. *J. Chem. Eng. Data* **1970**, 15, 304.; (c) Rauf, M. A.; Stewart, G. H.; Farhataziz *J. Chem. Eng. Data* **1983**, 28, 324.

32. (a) Samoilov, O. Y. *Discuss. Faraday. Soc.* **1957**, 24, 141.; (b) Frank, H. S.; Wen, W. Y. *ibid.* **1933**, 44, 133.

33. Morita, A.; Kato, S. *J. Am. Chem. Soc.* **1997**, 119, 4021.

34. (a) Nishi, N. *Z. Phys. D* **1990**, 15, 239.; (b) Nishi, N.; Yamamoto, K. *J. Am. Chem. Soc.* **1987**, 109, 7535.; (c) Nishi, N.; Koga, K.; Ohshima, C.; Yamamoto, K.; Nagashima, U.; Nagami, K. *J. Am. Chem. Soc.* **1988**, 110, 5246.

Table 6-1 Diffusion constants (D) of the parent molecules, neutral radicals, and the anion radicals of benzoquinone (BQ) and acetophenone (AP) in ethanol-water mixed solutions.

Content of water (%)	viscosity [a] (cP)	Diffusion constants (10^{-9} m^2s^{-1})							
		BQ		$BQ + H_2SO_4$		AP		AP + NaOH	
		parent	radical [b]	parent	radical [c]	parent	radical [d]	parent	radical [e]
0	1.20	1.6	0.57			1.3	0.61	1.3	0.45
10	1.61	1.2	0.44			0.89	0.44	1.0	0.39
20	2.01	0.85	0.34			0.72	0.38	0.75	0.34
30	2.37	0.72	0.36			0.55	0.33	0.61	0.31
40	2.67	0.64	0.32			0.48	0.28	0.61	0.31
50	2.87	0.58	0.32	0.58	0.31	0.42	0.27	0.43	0.29
60	2.91	0.56	0.35	0.60	0.37	0.39	0.26	0.38	0.22
70	2.71	0.62	0.42	0.65	0.39	0.42	0.30	0.41	0.28
80	2.18	0.77	0.50	0.79	0.48	0.49	0.40	0.49	0.32
90	1.54	0.76	0.61	0.76	0.57	0.55	0.46	0.57	0.45

a) ref. 19
b) neutral radical and anion radical of BQ are created
c) BQ neutral radical are created
d) AP neutral radical are created
e) AP anion radical are created

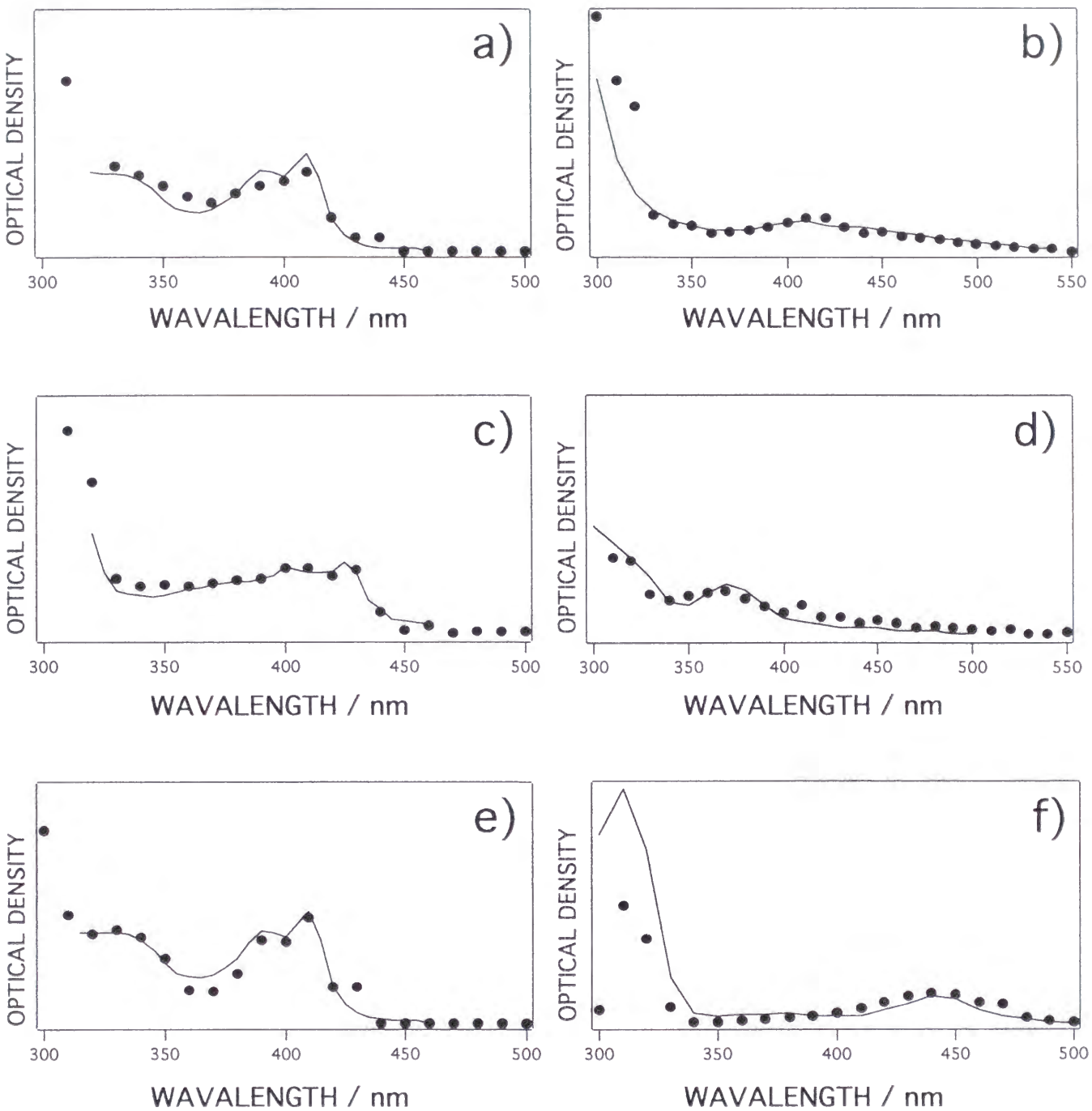

Fig. 6-1 Transient absorption spectra at a 10μs time delay after the excitation of (a) BQ in ethanol, (b) AP in ethanol, (c) BQ in E/W (1/9), (d) AP in E/W (1/9), (e) BQ + H_2SO_4 in E/W (1/9), and (f) AP + NaOH in E/W (1/9). Closed circles are observed TA spectra in this study and solid lines are reported spectra of, ((a) and (e)) BQ anion radical in ethanol from ref.23, (b) AP neutral radical in ethanol from ref. 22, (c) BQ neutral radical in ethanol from ref. 23, (d) AP neutral radical in water from ref. 24, and (f) AP anion radical in water from ref. 24.

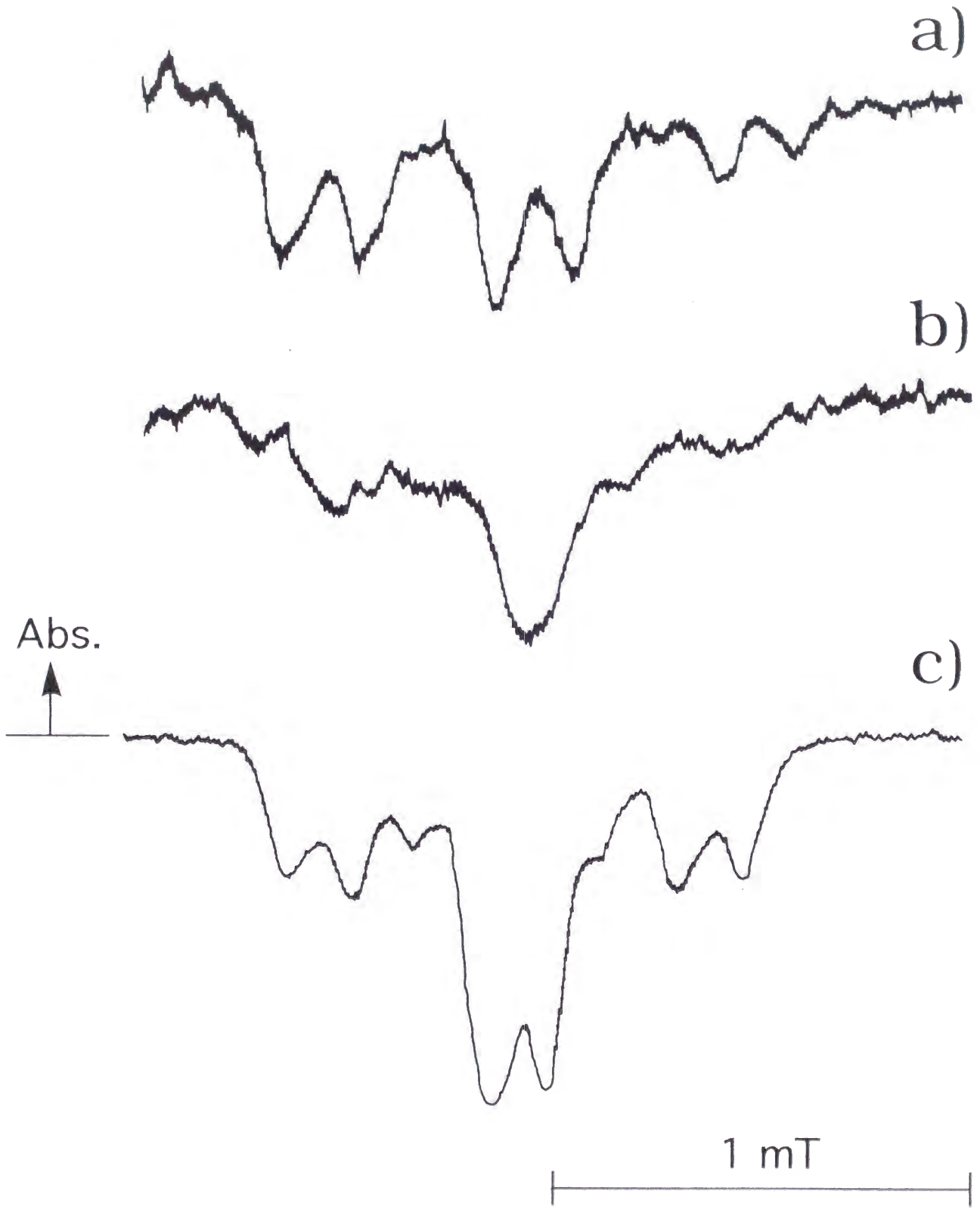

Fig. 6-2 The time resolved EPR spectra at a 1μs time delay after the excitation of BQ (a) in ethanol, (b) in E/W (1/9), and (c) in E/W (5/5).

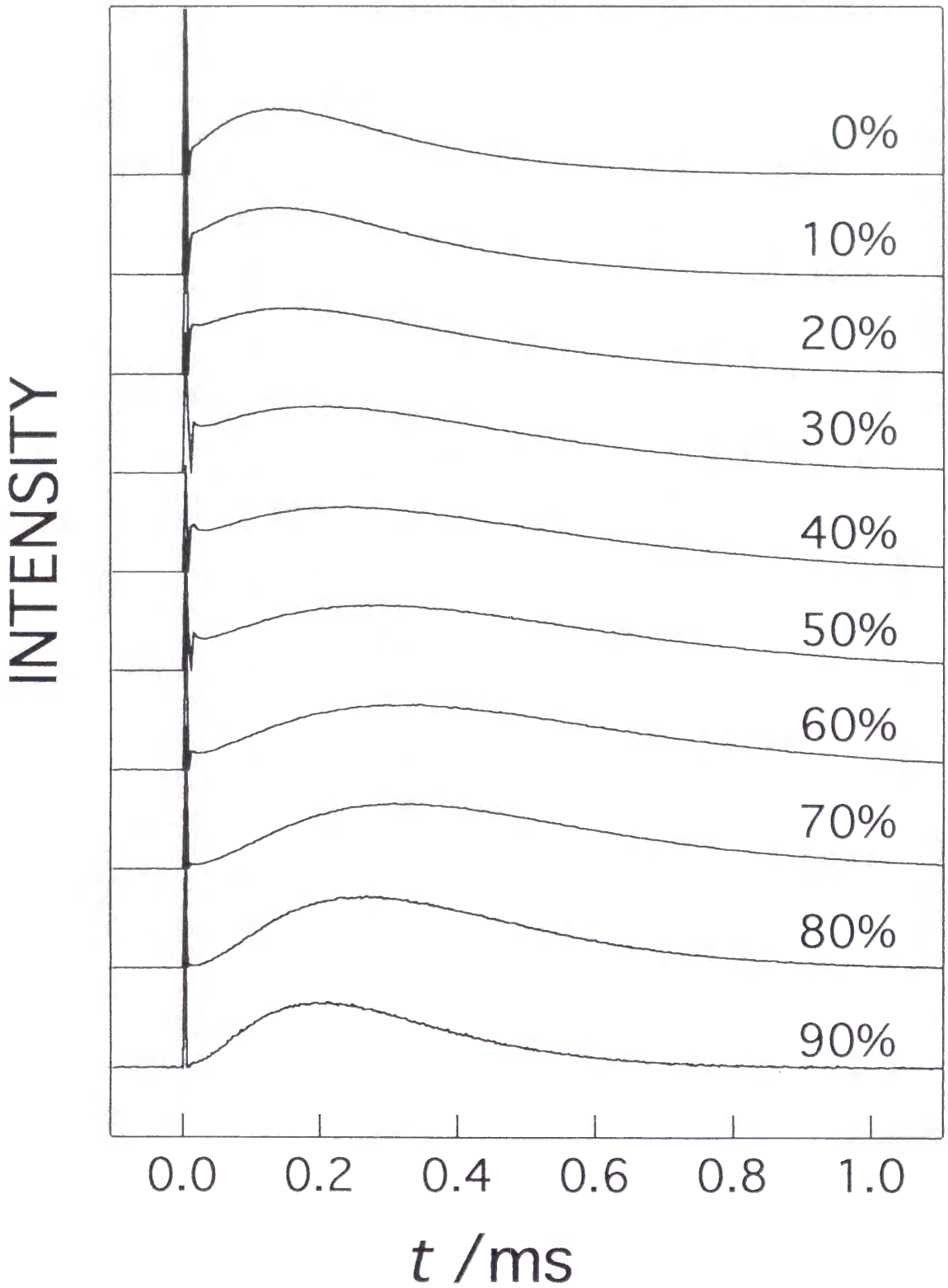

Fig. 6-3 Time profile of the TG signal after the photoexcitation of benzoquinone in ethanol-water mixed solvents at room temperature (~20°C). Volume % of water is indicated in the figure.

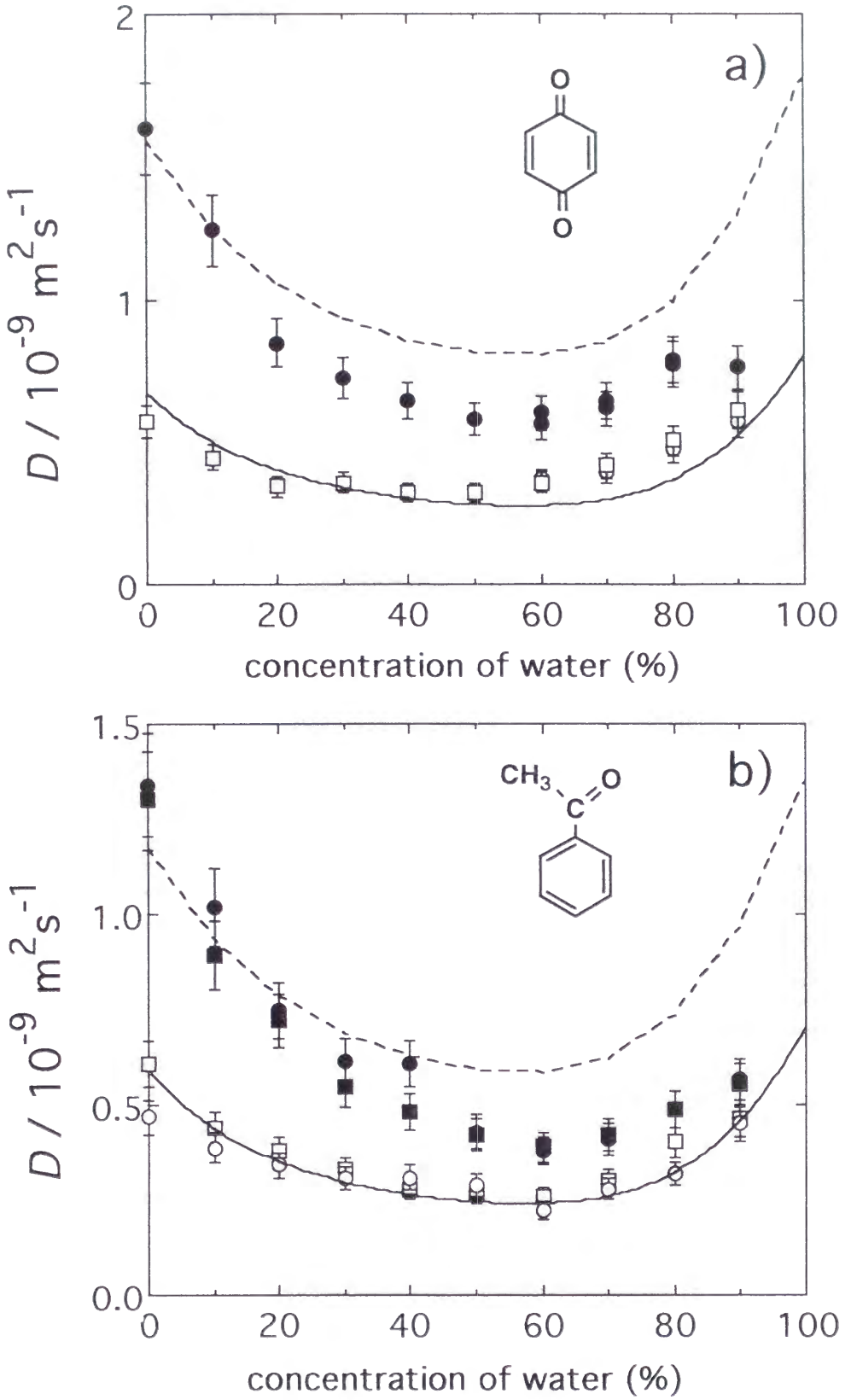

Fig. 6-4 (a) Water concentration dependence of D of the parent molecules (■) and the radicals (□) of BQ and (b) AP, (a) D of the parent molecules (●) and the radicals (○) of BQ + 0.1M H_2SO_4 and (b) AP + 0.1M NaOH. The broken line and the solid line are calculated values of D_{SE} and D_{EV}, respectively.

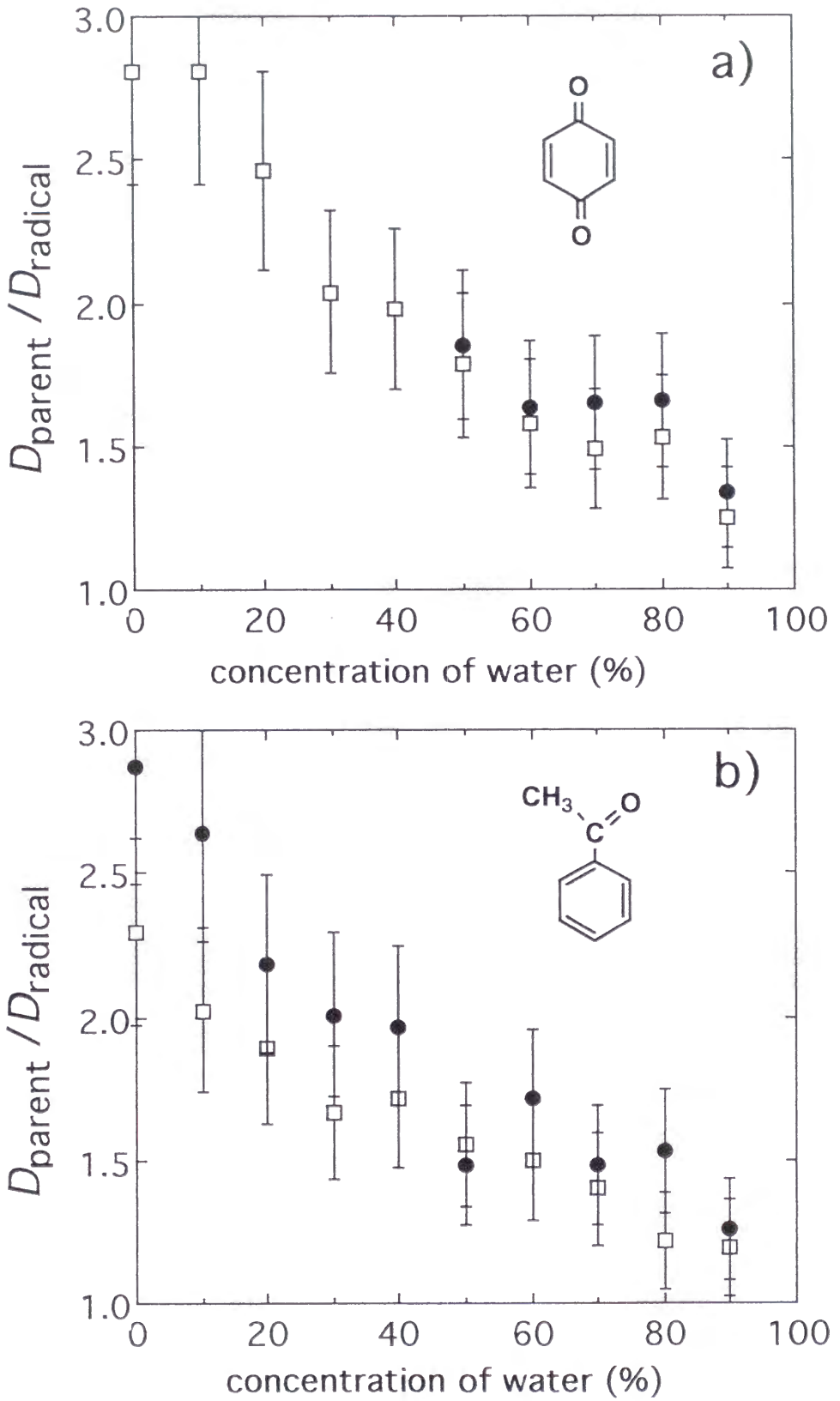

Fig. 6-5 (a) Water concentration dependence of the ratio of parent molecule's D to radical's D of BQ (□) and BQ + 0.1M H_2SO_4 (●), and (b) the ratio of D of the radicals of AP (□) and AP + 0.1M NaOH (●).

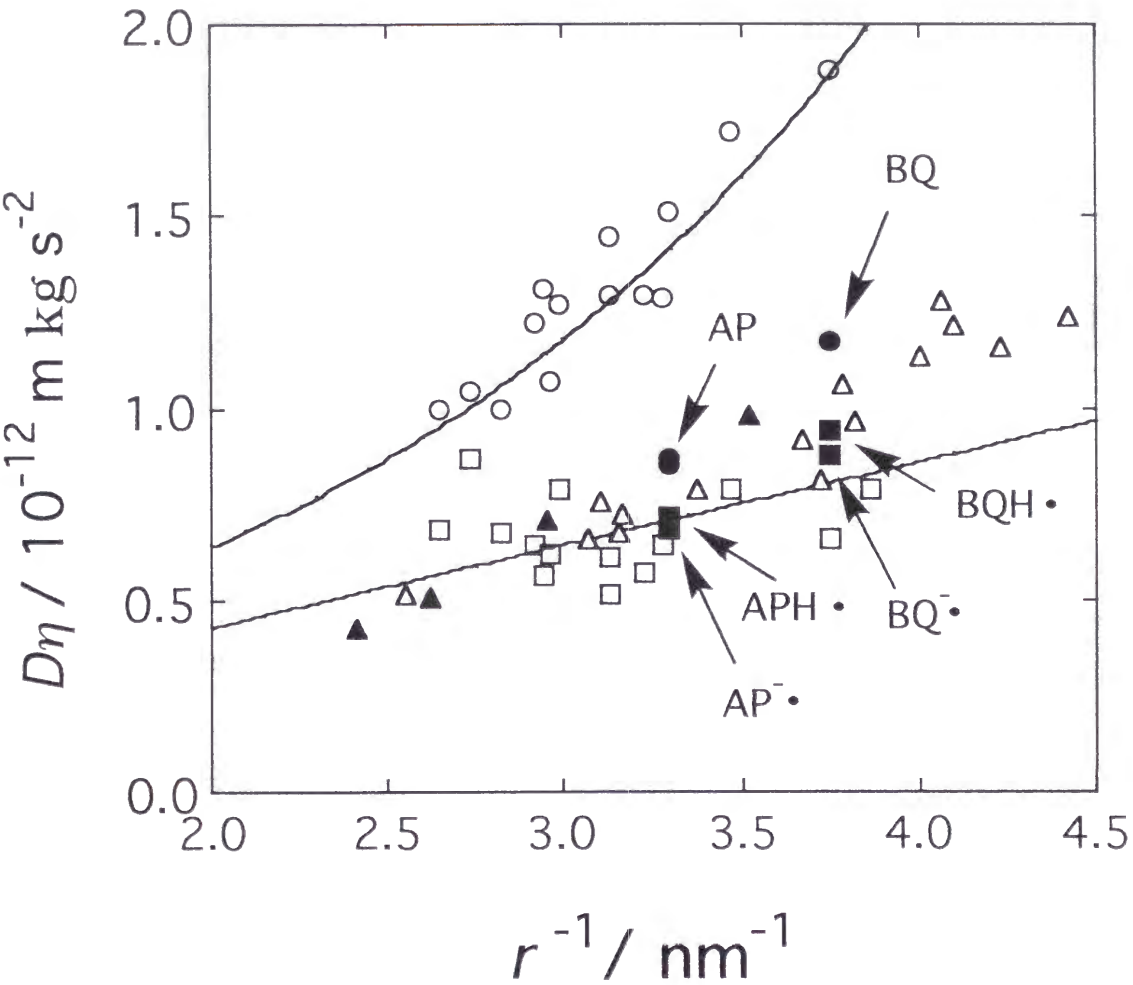

Fig. 6-6 The solute size dependence of Dη of the parent molecules (●) and the radicals (■) in E/W (1/9) solution. The reported values by the TG method (chapter 3) of the parent molecules (○) and the radicals (□) in ethanol are also plotted. The literature values of several molecules (△) (ref. 14) and the tetraalkylammonium ions (▲) (ref. 8c) in water are also plotted. The broken line and the solid line are calculated values of D_{SE} and D_{EV}, respectively.

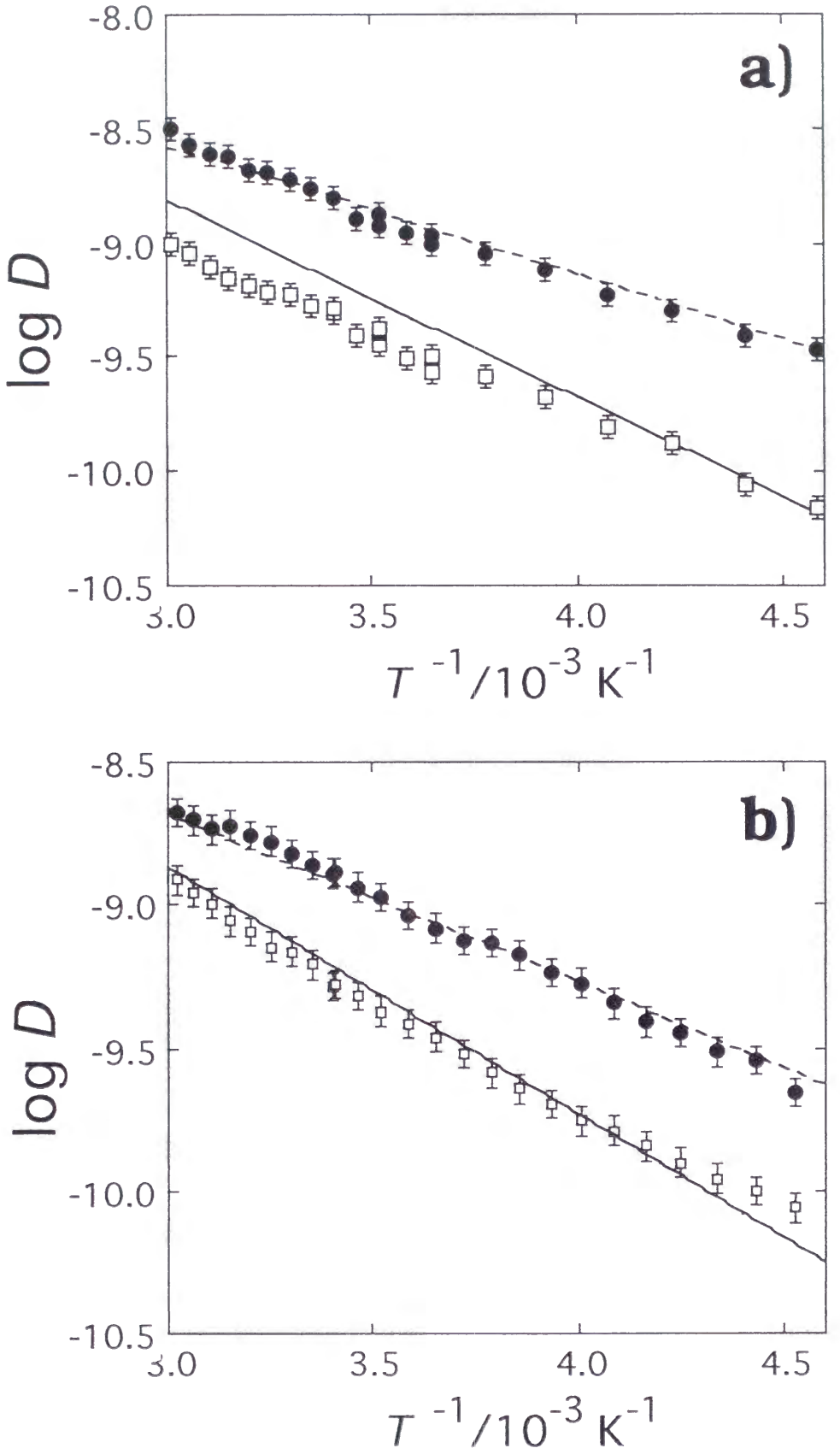

Fig. 6-7 (a) The temperature dependence (Arrhenius plots) of D of BQ and (b) AP in ethanol (50 °C ~ -50 °C). Closed circles and open squares indicate D of the parent molecules and the radicals, respectively.

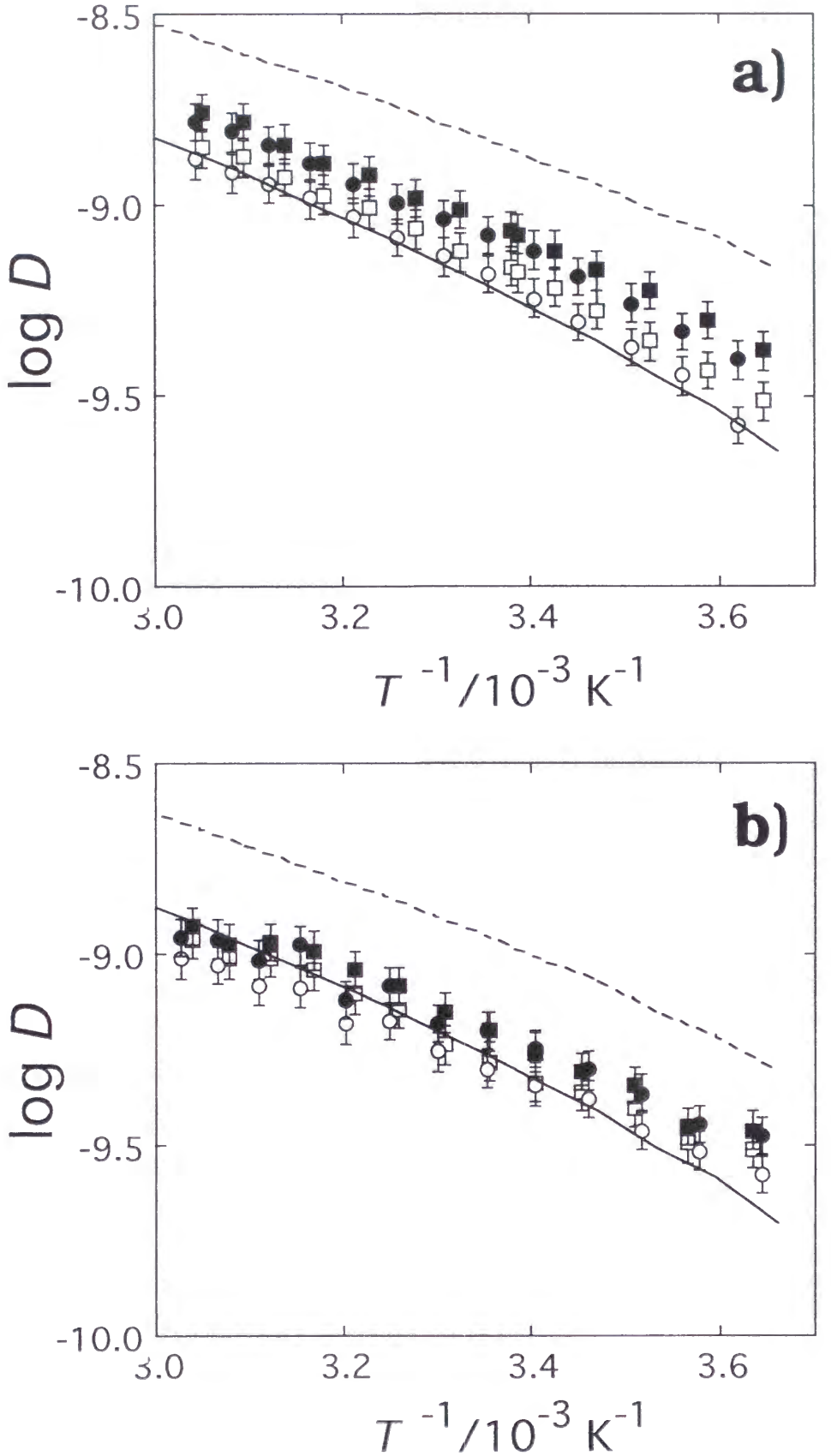

Fig. 6-8 The tempemrature dependence (Arrhenius plots) of D in E/W (1/9) (50 °C ~ 0 °C) of the parent molecules (■) and the radicals (□) of BQ (a) and AP (b), D of the parent molecules (●) and the radicals (○) of BQ + 0.1M H_2SO_4 (a) and AP + 0.1M NaOH (b) in ethanol-water mixed solutions are also shown. The broken line and the solid line represent the calculated values of D_{SE} and D_{EV}, respectively.

Chapter 7

RADICAL DIFFUSION IN MICELLAR SOLUTIONS

7.1 Properties of Micelles.

Because micelles prepare local hydrophobic environments in polar aqueous solution inhomogeneously, they can present a special reaction field and chemical reactions in micelles can be very different from those in homogeneous solutions. [1] So far, many chemical reactions in various micellar systems have been investigated extensively. [2-9] The reaction dynamics shall be greatly influenced by the molecular dynamics in the system such as, how do the solute and chemically active (intermediate) molecules distribute in the micellar phase and the bulk phase? How does the distribution depend on the molecular size, shape, and polarity? How are the diffusion processes affected by the presence of the micelles? For characterizing such properties, the micellar surface, the Stern layer, which has a few Å width plays an important role because in the many cases, the trapped solute molecules may exist in the micellar surface rather than in the micellar core. [10] The strong electric field (~10^3 V/m) is one of the remarkable property of the micelles when one regards it as the reaction field. For example, the micellar electric field may manifest itself in the charge separation or electron transfer reaction. In the homogeneous solutions, the created radicals are frequency quenched immediately by the fast reverse electron transfer processes. However, in the micellar surface, one of the pairs of the ion radicals are thrown out to the bulk phase by the electronic repulsion. Hence, the charge separation efficiency and the lifetimes of the ion radicals increase remarkably. Such effect has been actually observed by using the transient absorption (TA) method [3-6] and the time resolved EPR spectra [7-8] in ionic micellar solutions. For example,

Wallace and co-workers reported that the biphotonic ionization processes of pyrene, triphenylene, and perylene in anionic micellar solution of Sodium dodecyl sulfate (SDS) probed by the TA method. [3] They observed the TA spectra of the hydrated electron and the solute cation radicals with high yields, and interpreted that the photoelectron should be thrown out to the bulk phase by the electric repulsion between the electron and the charge of the micellar surface. [3] Alkaitis et al. reported that the monophotonic ionization yields of phenothiazine and N,N,N',N'-tetramethylbenzidine in SDS micelles are much higher than that in methanol by using the TA method. [4] The micellar effect to the electron transfer of pyrene to N,N-dimethylaniline (DMA) have been investigated by the time-resolved TA signals of the created ion radicals in the anionic micelle of SDS and in the cationic micelle of cetyl trimethyl ammonium bromide (CTAB). [5] They found that the lifetime of the pyrene cation radical became longer in CTAB because the DMA anion radical are separated from the micellar phase to the bulk phase by the electric repulsion. [5] Similarly, efficient charge separation in ionic micellar solutions have been reported about Zinc porphyrin systems by TA [6], EPR [7], and florescence [8] measurements. Moreover, an effect of the micellar charge was investigated for a benzophenone-aniline system probed by the line width of the CIDEP spectra of the created ion radicals. [9]

However, in spite of these many reports on reactions in micellar solutions, there has been no direct observation which shows that how many percentages of the created ion radicals are trapped in the Stern layer and how many percentages exist in the bulk phase. To reveal the molecular dynamics or the distribution in the micellar solution, diffusion constant (D) should be certainly a direct and good quantity. Although, D of stable ions or neutral molecules in micellar solutions have been reported by several methods, [11] direct measurement of D of any transient ion radical, which plays an important role in chemical reactions has never been reported in any micellar solution as far as we know.

In this chapter, we report D of a transient anion radical and a cation radical created by the electron transfer reaction and also D of the neutral parent molecules simultaneously in anionic and cationic micellar solutions by using the transient grating (TG) method. We focused our attention on the electric charge effect between the transient ionic radicals and the micelles.

7.2 Photochemical Reactions in Micellar Solutions.

In this study, we use benzoquinone (BQ) and aniline (AN) as the solutes. The photochemical reaction processes of BQ [12-14] and AN [15-16] in water have been reported as scheme 1. Benzosemiquinone radical ($BQH^{\cdot}$) and anion radical ($BQ^{\cdot -}$) are created from the lowest excited triplet state of BQ by the hydrogen abstraction reaction (process a) and the electron transfer (process b) with the solvent (RH). The neutral radical ($BQH^{\cdot}$) and the anion radical ($BQ^{\cdot -}$) are in equilibrium (process c). This equilibrium completes within 1μs after the creation of the radical. Adams and Michel reported that pKa=4.0. [12] Therefore, in an aqueous solution (pH=7), $BQ^{\cdot -}$ is created dominantly. On the other hand, the cation radical of AN ($AN^{\cdot +}$) is directly created by the one photon ionization in water (process d). [15] The created cation radical ($AN^{\cdot +}$) and the neutral radical ($AN^{\cdot}$) are in equilibrium (process e). Land and Porter reported pKa=7.0 for this equilibrium. [16] Therefore, in aqueous solution (pH=7), both $AN^{\cdot +}$ and $AN^{\cdot}$ are produced.

In this study, we use sodium dodecyl sulfate (SDS; anionic micelles) and cetyl trimethyl ammonium bromide (CTAB; cationic micelles). The photochemical reactions of BQ and AN in SDS and CTAB micellar solutions were studied by the transient absorption (TA) method. Fig. 7-1a shows the observed TA spectra at a 100μs time delay after the excitation of BQ in SDS and CTAB micellar solutions. A similar TA signal was observed for BQ in pure water. Reported spectra of $BQ^{\cdot -}$ [13] in water are also shown in Fig. 7-1. The observed TA spectrum is similar to the reported one of $BQ^{\cdot -}$ in water. Therefore, we conclude that $BQ^{\cdot -}$ is created mainly from BQ not only in water but also in both SDS and CTAB micellar solutions. Fig. 7-1b shows the observed TA spectra at a 100μs time delay after the excitation of AN in SDS and CTAB micellar solutions. Reported spectra of $AN^{\cdot +}$ and $AN^{\cdot}$ in water are also shown in this figure. [15] In this systems, both $AN^{\cdot +}$, and $AN^{\cdot}$ are exist in micellar solutions. Decays of all these TA signals are well described by the second order kinetics and the half-lifes of the TA signals are few milliseconds. This fact suggests that the termination processes are mainly the radical recombination of these radicals. As the excitation laser power for the TG measurement (~0.3 mJ/cm^2) is weaker than that of the TA measurement (~5 mJ/cm^2), the half-life of the radicals for the TG measurement

should be much longer than that for the TA measurement.

7.3 TG signal in Neat Aqueous Solution.

Before examining the molecular diffusion in the micellar solutions, the TG signal of BQ in water is analyzed. The time profile of the TG signals of BQ in water is shown in Fig. 7-2. The square root of the TG signal ($I_{TG}^{1/2}$) can be fitted by a sum of four exponential functions.

$$I_{TG}(t)^{1/2} = \left| - a_1 \exp(-k_1 t) + a_2 \exp(-k_2 t) - a_3 \exp(-k_3 t) + a_4 \exp(-k_4 t) \right| \qquad (7\text{-}1)$$

where, $k_1 > k_2 > k_3 > k_4$ are the decay constants and $a_1 \sim a_4 > 0$ are the pre-exponential factors. The solid line in Fig. 7-2a is the calculated line fitted by the non-linear least-squares method with eq. (7-1) and the time profiles of the four components are shown separately in Fig. 7-2b. If the termination of the radical follows the first order kinetics, the time profile of the TG signal is given by

$$I_{TG}(t)^{1/2} = \delta n_{th}^{\,o} \exp(-D_{th} q^2 t) - \sum_P \delta n_P^{\,o} \exp(-D_P q^2 t) + \sum_R \delta n_R^{\,o} \exp(-D_R q^2 t - 1/\tau_R) \qquad (7\text{-}2)$$

where, τ_R is the lifetime of the radicals when the termination of the radical follows the first order kinetics. From the rate constant, it is apparent that $a_1 \exp(-k_1 t)$ term in eq. (7-1) represents the thermal grating term.

Using the TA method, Ononye and Bolton found that photoexcited BQ abstracts the hydrogen atom from water and $BQ^{\cdot -}$ is created immediately by the proton dissociation.[12] Therefore, the TG signal due to BQ and $BQ^{\cdot -}$ shall be observed in neat water. By the same way to our previous reports in the homogeneous solvents, we can assign $a_3 \exp(-k_3 t)$ and $a_4 \exp(-k_4 t)$ terms to the species gratings of the parent molecule (BQ) and the radical ($BQ^{\cdot -}$), respectively. The origin of the component 2 is unknown. If the sample was not deoxygenated, the relative intensity of a_2 becomes

larger while those of a_3 and a_4 become smaller. Probably, component 2 may be due to the reaction between radical and oxygen dissolved in the solution. On the basis of these assignments, k_3 and k_4 in eq (7-2) are given by

$$k_3 = D_P q^2 \tag{7-3a}$$

$$k_4 = D_R q^2 + 1/\tau_R \tag{7-3b}$$

Since k_1 is much larger than k_3 and k_4, k_1 can be determined accurately by the fitting. On the other hand, because k_3 and k_4 are rather close, there is a larger ambiguity for k_3 and k_4. We estimated that the fitting accuracies for k_3 and k_4 are within 20% and 10%, respectively. We confirmed that the determined values of k_3 and k_4 are stable for varying the initial values for the least-squares fitting.

The results of the TA measurements suggest that the subsequence reaction should be second order reaction. If the decay of the TG signal due to the diffusion process is much faster than that of the subsequence reaction, τ_R in eq. (7-3b) could be approximately replaced by the half-lifetime of the concentration of the ion radicals. On the other hand, if the decay due to the subsequence reaction are much faster than that of the diffusion process, eq. (7-3b) is no longer satisfied and k vs. q^2 plot should not be linear. The relationship between k and q^2 are shown in Fig. 7-3a. The small intercepts with the ordinate and good linearity of these plots suggest that the decay of the TG signal should be faster than that of the reaction processes and eq. (7-3b) should be satisfied. This fact is consistent with the long lifetime of the radicals observed by the TA measurement. Therefore, D can be determined from the slopes of the plots of Fig. 7-3a. The obtained D are listed in table 7-1. Apparently, D of BQ and $BQ^{\cdot -}$ are very similar each other ($D_P/D_R \sim 1.22$). This similarity between D_P and D_R in water is very different from what we obtained in other organic solutions [e.g. D_P/D_R ~2.8 in ethanol (chapter 3)] but closed to what we obtained in 90% water - 10% ethanol mixed solution [$D_P/D_R \sim 1.3$ (chapter 6)].

7.4 TG signal in Micellar Solution.

The time profile of the TG signals of BQ in SDS (0.1M) micellar solution is shown in Fig. 7-4. The component 2, observed in water, did not appear in this system. This fact may indicate that $BQ^{\cdot -}$ is rather stable to oxygenation than $BQH^{\cdot}$. Under this situation, most of $BQH^{\cdot}$ created in micelles should change immediately to $BQ^{\cdot -}$. The TG signals can be fitted by a sum of the three exponential function [eq. (7-1) with a_2=0]. The fitted line and the time profile of each three component are shown in Fig. 7-4 a and b. Obviously, the fastest component (a_1) should be attributed to the thermal grating. It should be noted that the decay of the negative contribution ($-a_3$) is now slower than that of the positive contribution (a_4) and that the ratio of (a_3/a_4) is similar to that in water. The assignment of the chemical species for 3 and 4 should be the same as those in water. The plot of the rate constants (k) against q^2 of BQ and $BQ^{\cdot -}$ in SDS is shown in Fig. 7-3b. This plot shows a good linear relationship. We determined D_P and D_R in SDS from the slopes of this plot and listed in table 7-1. The ratio of D (D_P/D_R~ 11) in SDS micellar solutions is quite different from that in water, while a_3/a_4 is similar to that in water.

The time profile of the TG signal of BQ in CTAB (0.1M) micellar solution is shown in Fig. 7-5. This TG signal consists of two components; thermal grating and species grating signals. Considering the sign of δn (<0), we should attribute the chemical species of the species grating signal to $BQ^{\cdot -}$. The fitted line with a two-exponential function is shown in this figure. Although the intensity of the TA signal, which is proportional to the concentration of $BQ^{\cdot -}$ is close to that of BQ/SDS, the root square of the TG signal intensity, which is also proportional to the concentration of $BQ^{\cdot -}$ is much smaller than that of BQ/SDS. This weaker intensity of the species grating is interpreted by a similar decay rate constant of the TG signals due to BQ and $BQ^{\cdot -}$. Both signals are superposed each other, and the most part of the signal is cancelled by the opposite sign of these contributions. The remaining signal is due to $BQ^{\cdot -}$ because the pre-exponential factors of the TG signal of $BQ^{\cdot -}$ is larger than that of the BQ. Assuming that the TG intensity ratio of $BQ^{\cdot -}$ to BQ is the same as that in SDS micelle (Fig. 7-4b), we can separate the species grating signal as shown in Fig. 7-5b [by using eq. (1) with a_2=0 and k_3=k_4]. The plot of k vs q^2 in CTAB is shown in Fig. 7-3c and determined D_P (= D_R) are listed in Table 7-1.

Fig. 7-7 shows the time profiles of the TG signals of (a) AN / SDS (0.1M) micellar solution and (b) AN / CTAB (0.1M) micellar solution. Since the absorption band of $AN^{\cdot+}$ are larger and closer to the probe wavelength (633nm) than those of $AN^{\cdot}$, the species which mainly contribute to the TG signal should be $AN^{\cdot+}$ (Fig. 7-1b). The TG signal of AN / SDS is quite similar to that of BQ / CTAB, while the TG signal of AN / CTAB is quite similar to that of BQ / SDS. Those signals in SDS and CTAB can be also fitted by a sum of two and three exponential functions, respectively. The k vs. q^2 plots of AN and $AN^{\cdot+}$ are shown in Fig. 7-7, and obtained D are listed in table 7-1.

D of $BQ^{\cdot-}$ in SDS and $AN^{\cdot+}$ in CTAB are similar to D of $BQ^{\cdot-}$ in neat water, while D of $BQ^{\cdot-}$ in CTAB, $AN^{\cdot+}$ in SDS, and the parent molecules in both micellar solutions are much smaller than D in neat water. This fact suggests that the diffusion process of the ion radicals in ionic micellar solutions are very sensitive to the electric charge of the ion radicals and micelles.

7.5 Interaction between the Ion Radicals and the Micellar Surface.

If the solute molecules exist only in the bulk phase, D in the micellar solution should be equal to D in water. On the other hand, if the solute molecules exist in the micelles, D should be close to D of the micelles. D of BQ and $BQ^{\cdot-}$ in water were already shown in the above section as 1.1 and $0.9 \times 10^{-9} m^2 s^{-1}$, respectively (Table 7-1). We could not obtain D of AN and $AN^{\cdot+}$ in water because the TG signal is too weak to be analyzed. However, in chapter 6, we found that D in aqueous solutions are mostly controlled by the molecular size and shape, and the electric characters of the solute are not important for the speed of the diffusion. Therefore we can safely assume that D of AN and $AN^{\cdot+}$ are close to D of BQ or $BQ^{\cdot-}$ c.a. $1 \pm 0.1 \times 10^{-9} m^2 s^{-1}$ in neat water.

When the charge of ion radicals and micellar surface are the same sign ($BQ^{\cdot-}$ / SDS, $AN^{\cdot+}$ / CTAB), D of the ion radicals are larger than that of the parent molecules and close to D in aqueous solutions. The large D imply that the most part of the ion radicals exist in the bulk phase. We considered that the created ion radicals throw out to the bulk phase by the electric repulsion even though the parent molecules stays in the micelles and the photochemical reaction take place inside the micelles. On the other hand, when the charge of the ion radicals and the micellar surface are

opposite ($BQ^{\cdot -}$ / CTAB, $AN^{\cdot +}$ / SDS), D of the ion radicals are close to D of the parent molecules and also D of the micelles. (The self diffusion constants of the micelles are reported as 0.07×10^{-9} and 0.04×10^{-9} $m^2 s^{-1}$ for SDS [17] and CTAB, [18] respectively.) This fact suggests that the large amount of the ion radicals and the parent molecules exist in the micellar phase (on the micellar surface). The dominant presence of BQ and AN in micelles may be due to the hydrophobic nature. The equilibrium constant of the distribution will be described latter. It was reported that aromatic hydrocarbons such as benzene and toluen are in the micellar core by the strong hydrophobic character, but the hydrophobic solute which have the hydrophilic group (-OH, =O, or $-NH_2$) are trapped on the micellar surface (Stern layer) rather than in the micellar core. [10] Considering these facts, we think that BQ and AN are located on the Stern layer rather than in the micellar core. This location might be one of causes of the efficient releasing and trapping of the photochemically created ion radicals.

Because of the electric charge of the ion radicals, we may think that the ion radical could be located in water rather than in the non-polar micelles. However, D measured in this study strongly suggests that the created ion radicals are trapped on the micellar surface by the Coulomb force between the charges of ion radicals and the Stern layer.

So far, many groups studied the electric interaction between ionic radicals and micelles indirectly. [2-9] For example, Kautusin-Razem et al [5] measured the lifetimes of the ion radicals created by the electron transfer between pyrene and N,N-dimethylaniline (DMA) in methanol (6μs), CTAB cationic micelle (500μs), SDS anionic micelle (66.6μs), and Igepal neutral micelle (13.1μs). They interpreted the long lifetime in the CTAB micellar solution by the hindrance of the reverse electron transfer due to the electronic repulsion between the cation radical of dimethyl aniline and cationic micellar surface of CTAB. (As pyrene is a large molecule, it hardly exists in water than DMA regardless of the micellar charge.) As another example, the line width of the EPR spectra of the benzophenone (BP) anion radical was found to be sharpe in the SDS micellar solution, while it was broad in the CTAB micellar solution. [9] The different line width was interpreted in terms of the different environment of the radical; that is, the anion radical trapped on the cationic micelle (CTAB) gives the broader spectrum by the motional restriction. In this study,

we obtain much more direct evidence for the trapping of the ion radicals from the D measurements.

7.6 Micellar concentration dependence of D.

To study the dynamics of the ion radicals in more detail, the micellar concentration dependence of D is measured. D at various micellar concentrations for BQ and $BQ^{\cdot -}$ are listed in Table 7-2 and plotted in figure 7-8. Micellar concentrations [M] are estimated by the following equation.

$$[M] = \frac{[Det] - cmc.}{\overline{n}} \qquad (7\text{-}4)$$

where, [Det] is the concentration of detergent (SDS or CTAB) and $\overline{n}$ is the mean micelle aggregation number. $\overline{n}$ of SDS and CTAB are ~60 [19] and ~70, [20] respectively. The critical micellar concentration (cmc) of SDS and CTAB are 8.2mM and 0.92mM, respectively. [21] D of $BQ^{\cdot -}$ in the SDS solution does not depend on the micellar concentration and always close to D in the aqueous solution (broken line in Fig. 7-8). This fact implies that most of $BQ^{\cdot -}$ exist in the bulk phase in the SDS solution at any concentration of the micelle.

On the other hand, D of $BQ^{\cdot -}$ in the CTAB solution and D of BQ in the SDS and CTAB solutions depend on the micellar concentration. D of $BQ^{\cdot -}$ and BQ become smaller with increasing the micellar concentration and closer to D of the micelle (solid line in Fig. 7-8). It suggests that the relative amount of the solute molecules in the micellar phase compared with that in the bulk phase increases with increasing the micellar concentration. If the micellar concentration is high (≥0.1M), almost of all solute molecules are trapped in the micellar phase. In the following, we quantitatively explain the observed micellar concentration dependence of D by taking into account the equilibrium between the bulk phase and the micelles.

The solubilization of a solute molecule in the micellar solution may be expressed by the equilibrium between the micellar phase and the bulk phase as [22]

$$[S] + [M] \leftrightarrows [SM] \qquad (7\text{-}5)$$

where [S] and [SM] are the concentrations of the solute in the bulk phase and in the micellar phase, respectively. [M] is the concentration of the micelles obtained by eq (7-4). Generally, the equilibrium constant (K_s) is given by

$$K_s = \frac{[SM]}{[S]\,[M]} \tag{7-6}$$

If we assume that D of the solute (D_s) can be described by the average between D in the bulk phase (D_b) and in the micellar phase (D_m), D_s is given by the following equation.[23]

$$D_s = \frac{D_m\,[MS] + D_b\,[S]}{[MS] + [S]} \tag{7-7}$$

From eqs (7-6) and (7-7), we obtained the following relationship.

$$D_s = D_m \left[1 + \frac{1}{1 + K_s\,[M]} \left(\frac{D_b}{D_m} - 1 \right) \right] \tag{7-8}$$

D_s calculated with eq. (7-8) is plotted in Fig. 7-9. The calculated D_s reproduce the observed micellar concentration dependence of D fairly well with $K_s = 1.1X10^4\ M^{-1}$ (BQ/SDS) and $K_s = 4.3X10^3\ M^{-1}$ (BQ/CTAB). This fact supports our diffusion model; that the solute diffuse in the micellar solution in equilibrium between the bulk phase and the micellar phase. It should be note that D of $BQ^{\cdot -}$ are close to D of BQ at any micellar concentration (Fig. 7-8). This suggests that the equilibrium constant (K_s) of $BQ^{\cdot -}$ is close to that of BQ. This similar K_s may be due to a competition between the hydrophobic nature of $BQ^{\cdot -}$, which tends to be stabilized in water and the electric interaction with the micelles.

7.7 Conclusion.

Diffusion constants (D) of the photochemical intermediate anion radicals of BQ ($BQ^{\cdot -}$) and the

cation radical of AN ($AN^{\cdot +}$) in the anionic micellar solution of SDS and the cationic micellar solution of CTAB were measured by using the transient grating (TG) method. It is found that D of $BQ^{\cdot -}$ in the SDS solution and $AN^{\cdot +}$ in the CTAB solution are larger than those of the parent molecules, while in BQ/CTAB and AN/SDS cases, D of both the ion radicals and the parent molecules are similar. These observations are consistently explained in term of the Coulomb interaction between the ion radicals and the charge in the Stern layer of the micelles. The ion radical with the like charge as the micelle exists in the bulk phase by the electric repulsion. On the other hand, the ion radical with the opposite charge to that of the micelle exists on the micellar surface rather than in the bulk phase. The micellar concentration dependence of D is also investigated by BQ in the SDS and the CTAB solutions. D of $BQ^{\cdot -}$ in the SDS solution are insensitive to the micellar concentration and similar to D of $BQ^{\cdot -}$ in neat water. However, D of BQ in the SDS solution and D of BQ and $BQ^{\cdot -}$in the CTAB solution are sensitive to the concentration of the micelle. The observed micellar concentration dependence of D can be reproduced by using a diffusion model, which takes into account the equilibrium between the micellar surface and bulk phase. Therefore if we measure the diffusion constant in the photochemical reaction system, we can determine the equilibrium constant.

References to Chapter 7

(1) (a) Gebicki, J. M.; Hicks, M. *Nature* **1973**, 243, 232. (b) Gebicki, J. M.; Hicks, M. *Chem. Phys. Liqid* **1976**, 16, 142. (c) Hicks, M.; Gebicki, J. M. *Chem. Phys. Liqid* **1976**, 16, 142. (d) Fromhertz, P. *Chem. Phys. Lett.* **1980**, 77, 460. (e) Menger, F. M.; Jerknnica, J. M.; Johnston, J. C. *J. Am. Chem. Soc.* **1978**, 100, 4676. (f) Menger, F. M.; Boyer, B. J. *J. Am. Chem. Soc.* **1980**, 102, 5936.

(2) (a) Menger, F. M. *Accounts Chem. Res.* **1979**, 12, 111. (b) Menger, F. M.; Portnoy, C. E. *J. Am. Chem. Soc.* **1967**, 90, 4404. (c) Lindquist, R. N.; Cordes, E. H. *J. Am. Chem. Soc.* **1968**, 90, 1269.

(3) Wallace, S. C.; Gratzel, M.; Thomas, J. K. *Chem. Phys. Lett.* **1973**, 23, 359.

(4) (a) Alkaitis, S. A.; Beck, G.; Gratzel, M. J. Am. Chem. Soc. 1975, 97, 5723. (b) Alkaitis, S. A.; Gratzel, M. *J. Am. Chem. Soc.* **1976**, 98, 3549.

(5) Katusin-Razem, B.; Wong, M.; Thomas, J. K. *J. Am. Chem. Soc.* **1978**, 100, 1679.

(6) (a) Brugger, P. -A.; Infelta, P. P.; Braun, A. M.; Gratzel, M. *J. Am. Chem. Soc.* **1981**, 103, 320. (b) Darwent, J. R. *J. Chem. Soc., Chem. Commun.* **1980**, 805.

(7) (a) Levstein, P. R.; van Willigen, H. *Chem. Phys. Lett.* **1991**, 184, 415. (b) Hanaishi, R.; Ohba, Y.; Yamauchi, S.; Iwaizumi, M. *Bull. Chem. Soc. Jpn.* **1996**, 69, 1533.

(8) Costa, S. M. B.; Brookfield, R. L. *J. Chem. Soc. Faraday Trans. 2* **1986**, 82, 991.

(9) Hirata, T.; Miyagawa, K.; I'Haya, Y.; Murai, H. *Nippon Kagaku Kaishi* **1992**, 12, 1423.

(10) Hirose C.; Sepulveda, L. *J. Phys. Chem.* **1981**, 85, 3689.

(11) (a) Corti, M.; Degiorgio, V. *J. Phys. Chem.* **1981**, 85, 711. (b)Rohde, A.; Sackmann, E. *J. Phys. Chem.* **1980**, 84, 1598. (c) Missel, P. J.; Mazer, N. A.; Benedek, G. B.; Carey, M. C. *J. Phys. Chem.* **1983**, 87, 1264. (d) Lindman, B.; Puyal, M-C.; Kamenka, N.; Rymden, R.; Stilbs, P. *J. Phys. Chem.* **1984**, 88, 5048.

(12) (a) Ononye, A. I.; Bolton, J. R. *J. Phys. Chem.* **1986**, 90, 6270. (b) Adams, G. E.; Michel, B. D. *Trans. Faraday Soc.* **1967**, 63, 1171.

(13) Kimura, K.; Yoshinaga, K.; Tsubomura, H. *J. Phys. Chem.* **1967**, 71, 4485.

(14) Scheerer, R.; Gratzel, M. *J. Am. Chem. Soc.* **1977**, 99, 865.

(**15**) (a) Saito, F.; Tobita, S.; Shizuka, H. *J. Chem. Soc. Faraday Trans.* **1996**, 92, 4177. (b) Yoshihara, T.; Yamaji, M.; Shizuka, H. *Chem. Phys. Lett.* **1996**, 261, 431.

(**16**) Land, E. J.; Porter, G. *Trans. Faraday. Soc.* **1963**, 59, 2027.

(**17**) Clifford, J.; Pethica, B. A. *J. Phys. Chem.* **1966**, 70, 3345.

(**18**) (a) Tominaga, T.; Nishinaka, M. *J. Chem. Soc. Faraday Trans.* **1993**, 89, 3459. (b) Tominaga, T.; Nakamura, T.; Saiki, H. *Chem. Lett.* **1997**, 979.; (c) Leaist, D. G.; Hao, L. *J. Phys. Chem.* **1993**, 97, 7763.

(**19**) (a) Rassing, J. E.; Sams, P. J.; Wyn-jones, E. *J. Chem. Soc., Faraday II* **1974**, 70, 1247. (b) Yekta, A.; Aikawa, M.; Turro, N. J. *Chem. Phys. Lett.* **1979**, 63, 543.

(**20**) Rosen, M. J. *Surfactants and Interfacial Phenomena,* 2nd Ed., (Wiley-Interscience, **1989**).

(**21**) (a) Dorrance, R. C.; Hunter, T. F. *J. Chem. Soc. Faraday Trans. I* **1972**, 68, 1312.; (b) Dorrance, R. C.; Hunter, T. F. *J. Chem. Soc. Faraday Trans. I* **1974**, 70, 1572.

(**22**) (a) Turro, N. J.; Yekta, A. *J. Am. Chem. Soc.* **1978**, 100, 5951. (b) Coll, H. *J. Phys. Chem.* **1970**, 74, 520. (c) Granath, K. *Acta Chem. Scand.* **1953**, 7, 297.

(**23**) Stigter, B. D.; Williams, R. J.; Mysels, K. *J. J. Phys. Chem.* **1955**, 59, 330.

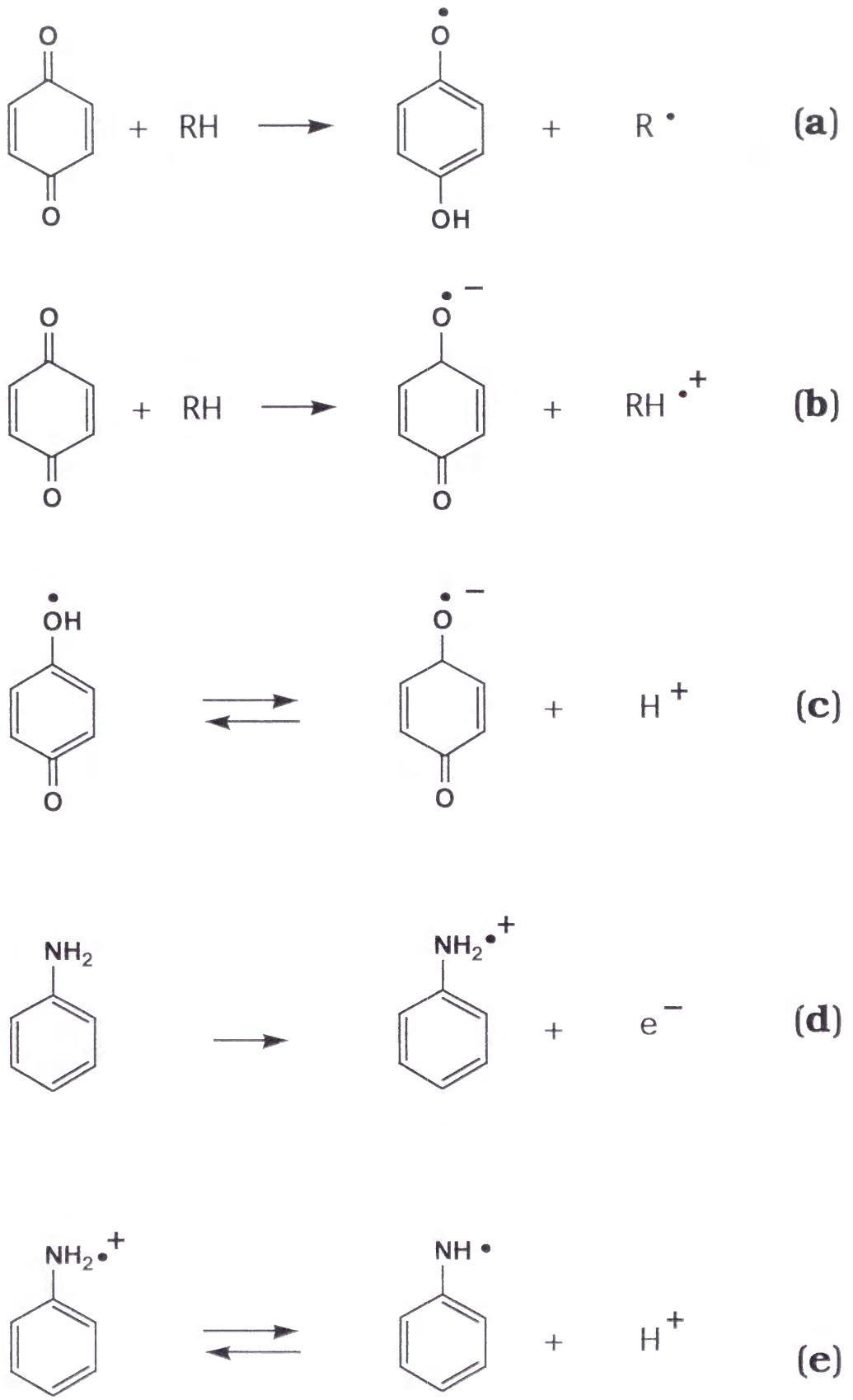

Scheme 7-1

Table 7-1; Diffusion constants of the ion radicals (D_R) and parent molecules (D_P) in water, SDS and CTAB (0.1M) micellar solutions.

	Benzoquinone		Aniline	
	$D_p/10^{-9}m^2s^{-1}$	$D_r/10^{-9}m^2s^{-1}$	$D_p/10^{-9}m^2s^{-1}$	$D_r/10^{-9}m^2s^{-1}$
water	1.1±0.2	0.90±0.05		
SDS (0.1M)	0.10±0.06	1.1±0.1	0.11±0.05	0.11±0.05
CTAB (0.1M)	0.19±0.06	0.19±0.06	0.08±0.01	1.0 ±0.2

Table 7-2; Micellar concentration dependence of diffusion constants of the ion radicals and parent molecules of the parent molecules of benzoquinone in SDS and CTAB micellar solutions.

[SDS] or [CTAB]/M	$D/10^{-9}m^2s^{-1}$ in SDS		$D/10^{-9}m^2s^{-1}$ in CTAB
	BQ	$BQ^{\cdot-}$	BQ and $BQ^{\cdot-}$
0.01	1.2±0.2	0.56±0.05	0.83±0.08
0.02	1.0±0.2	0.32±0.03	0.68±0.06
0.04	1.1±0.2	0.26±0.03	0.40±0.04
0.06	1.1±0.1	0.15±0.02	0.28±0.04
0.08	1.0±0.1	0.14±0.02	0.26±0.04
0.10	1.1±0.1	0.10±0.06	0.09±0.06

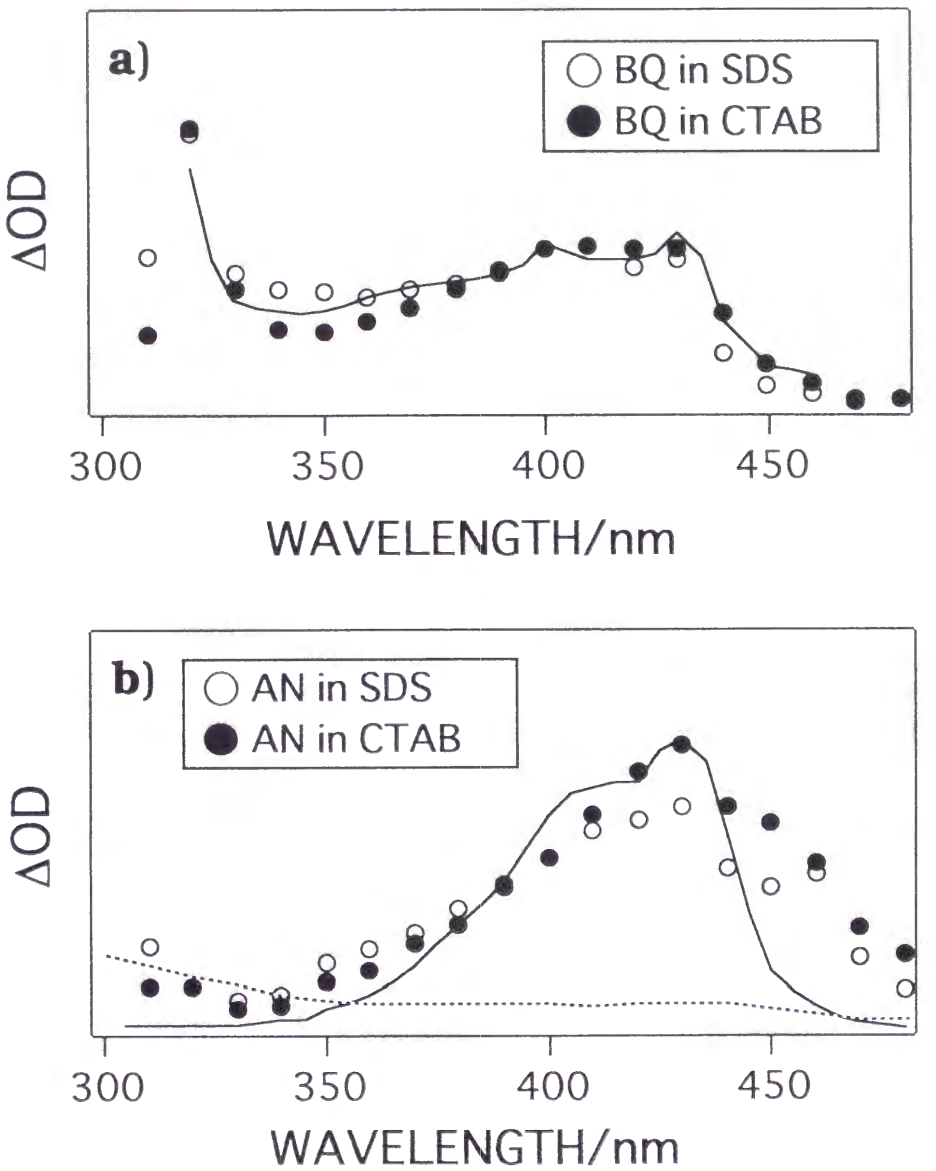

Fig. 7-1 (a) Transient absorption spectra at a 100μs delay after the excitation of BQ in SDS aqueous solution (○) and BQ in CTAB aqueous solution (●). Solid line is the reported spectrum of BQ anion radical in water (Ref. 19). (b) Transient absorption spectra at a 100μs delay after the excitation of AN in SDS aqueous solution (○) and AN in CTAB aqueous solution (●). Solid line and broken line are the reported spectrum of AN cation radical and neutral radical in water (Ref. 14)

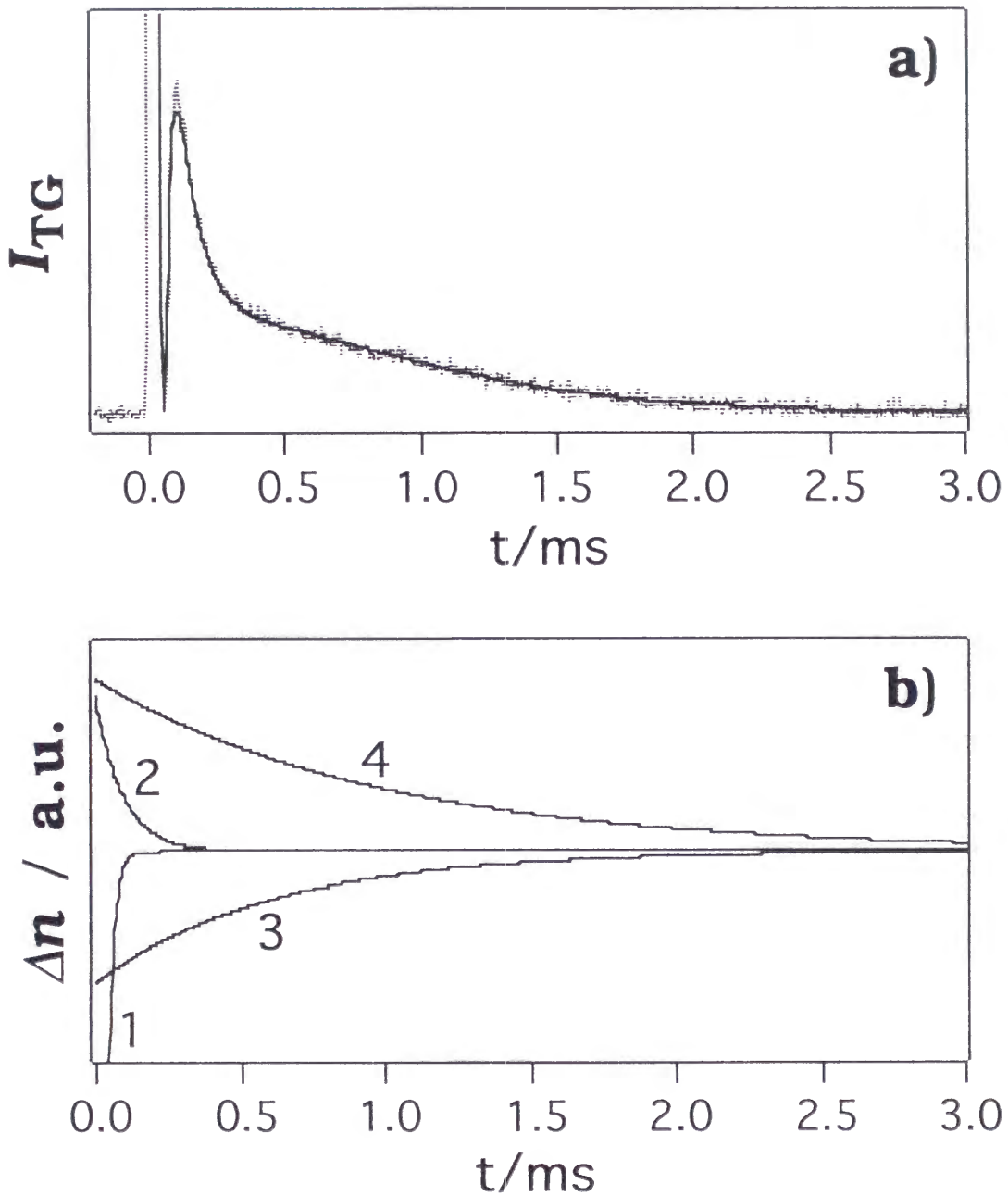

Fig. 7-2 (a) Time profile of the TG signal after the photoexcitation of BQ in water at 23°C (dotted line) and the best fitted curve (solid line) by eq (7-1). (b) Four components for the fitting in (a) are shown separately. The assignments of these components are 1; thermal grating, 3 and 4; species grating of BQ and that of the anion radical of BQ, respectively. Component 2 is unknown.

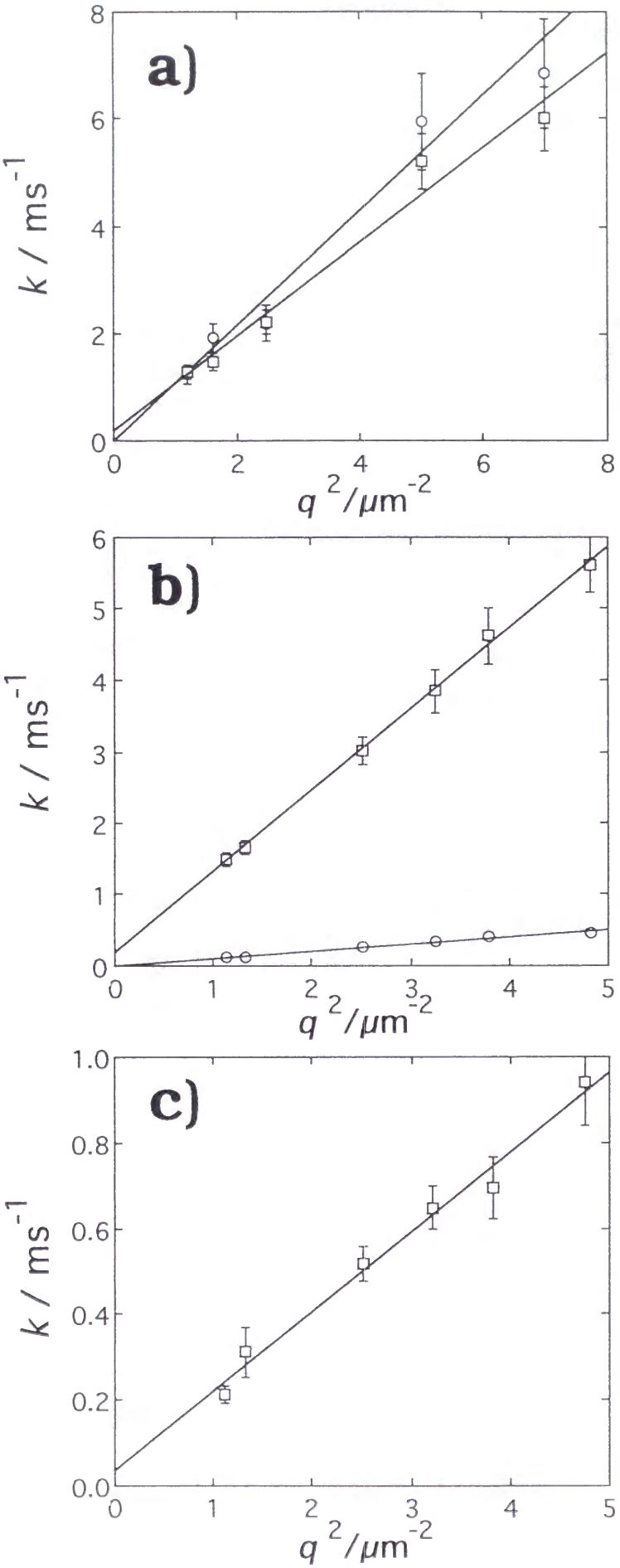

Fig. 7-3 Relationship between the decay rate constants (k) of the TG signal and q^2 of BQ (○) and $BQ^{\cdot -}$ (□) (a) in water, (b) in SDS, and (c) in CTAB. The straight lines are fitting line by the least square method.

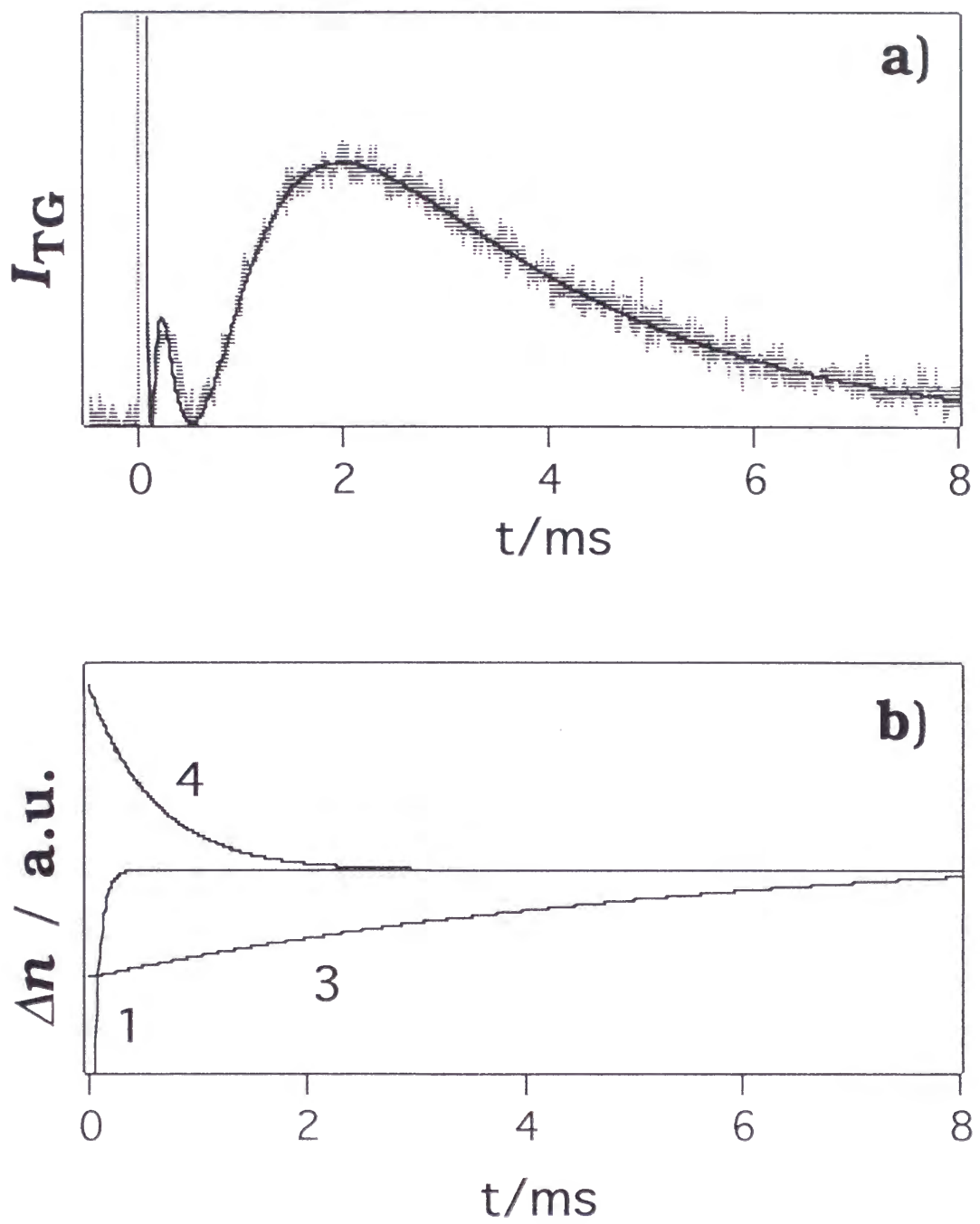

Fig. 7-4 (a) Time profile of the TG signal after the photoexcitation of BQ in SDS solution at 23°C (dotted line) and the best fitted curve (solid line) by eq (7-1) with a_4=0. (b) Three components for the fitting in (a) are shown separately. The assignments of these components are 1; thermal grating, 2 and 3; species grating of BQ and that of the anion radical of BQ, respectively.

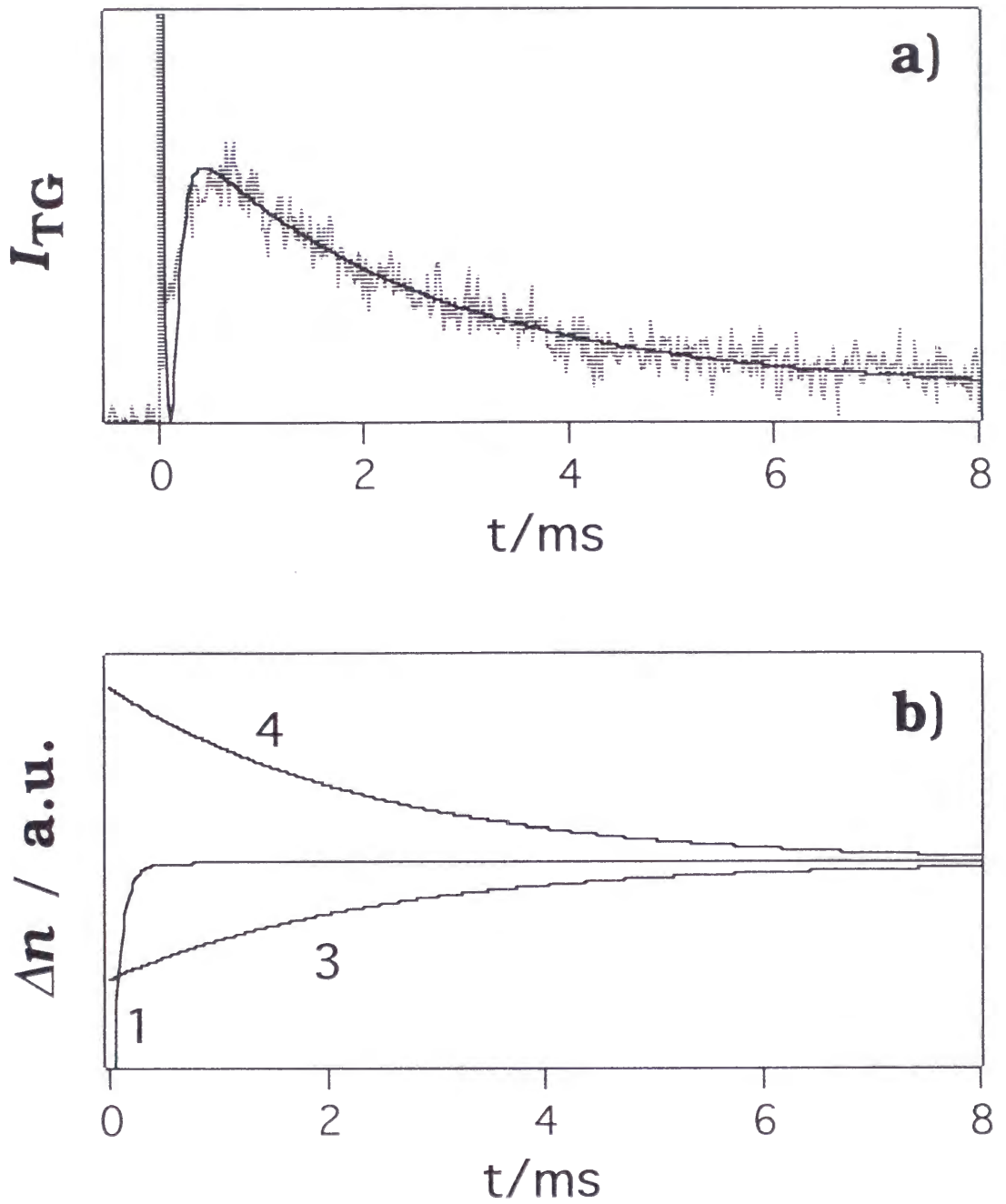

Fig. 7-5 (a) Time profile of the TG signal after the photoexcitation of BQ in CTAB solution at 23°C (dotted line) and the best fitted curve (solid line) by eq (7-1). (b) Three components in the grating signal are shown separately (text). The assignments of these components are 1; thermal grating, 2 and 3; species grating of BQ and that of the anion radical of BQ, respectively.

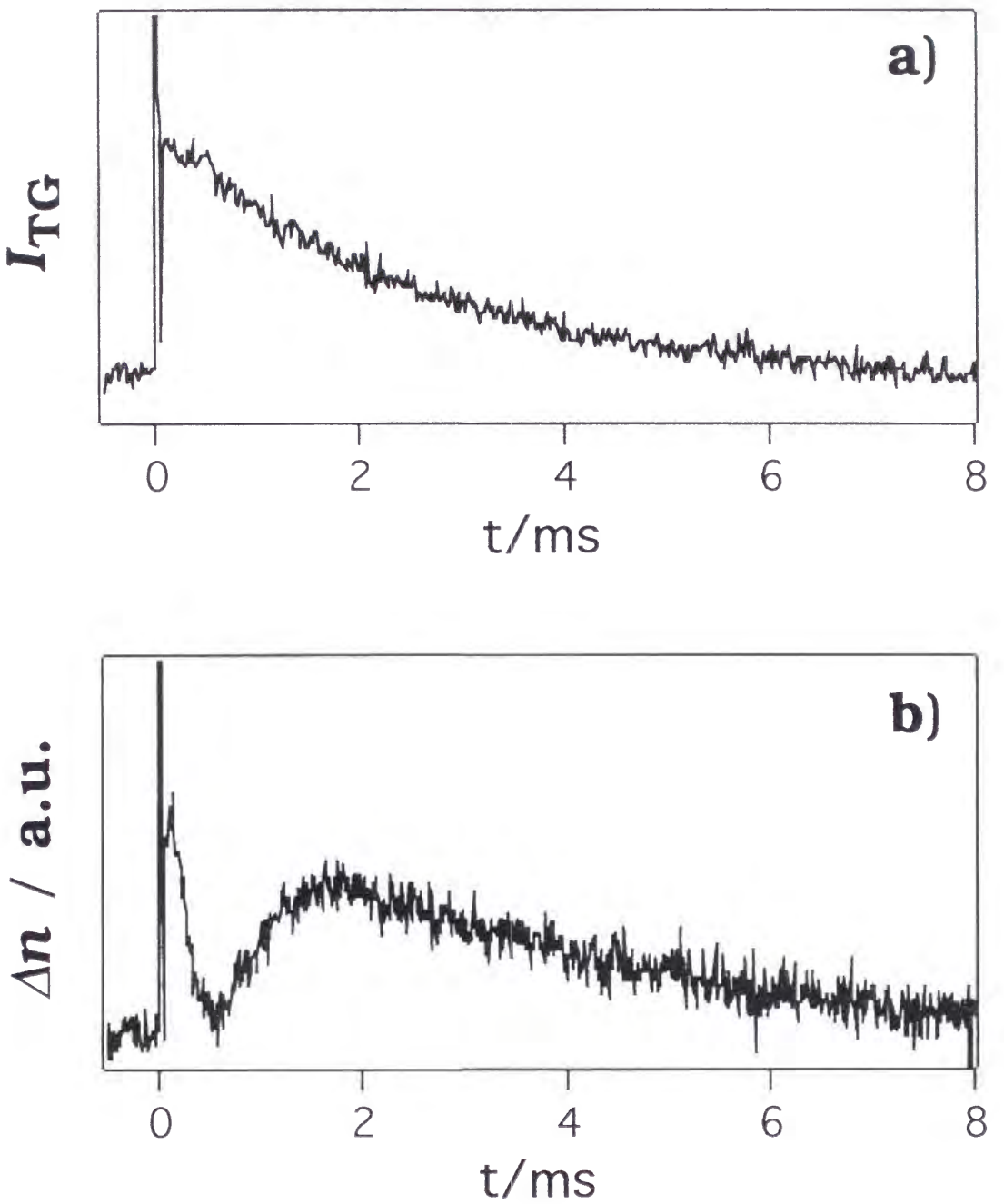

Fig. 7-6 Time profile of the TG signal after the photoexcitation of (a) AN in SDS solution and (b) that of AN in CTAB solution at 23°C.

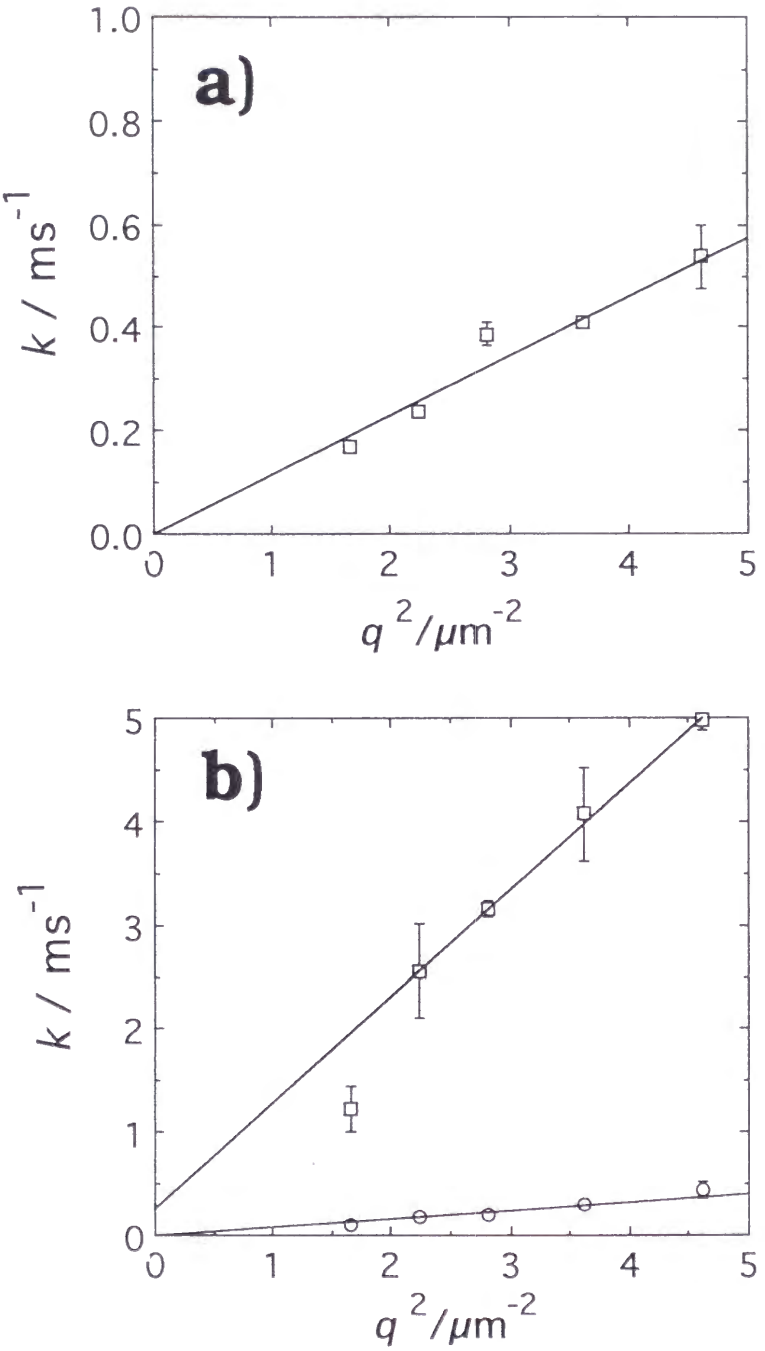

Fig. 7-7 Relationship between the decay rate constants (k) of AN(○) and $AN^{\cdot+}$(□) of the TG signal and q^2 (a) in SDS and (b) in CTAB. The straight lines are fitting line by the least square method.

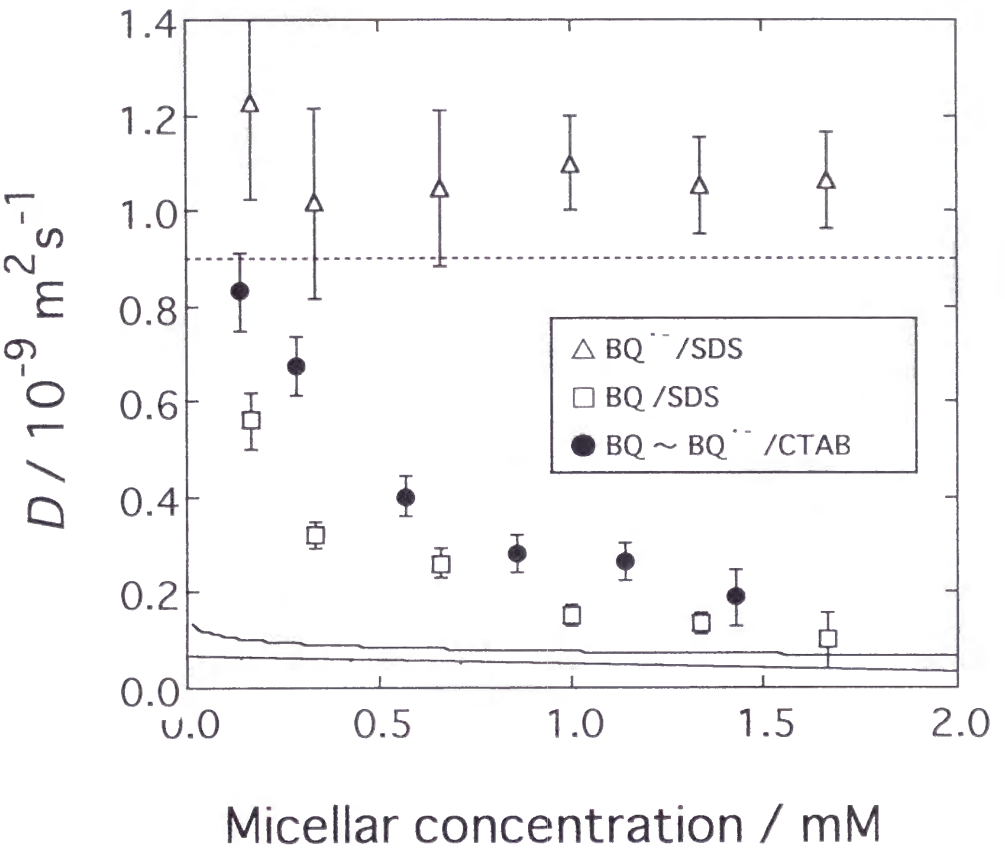

Fig. 7-8 Micellar concentration dependence of D of $BQ^{\cdot -}$ in SDS solution (△), D of BQ in SDS micellar solution (□), and both BQ and $BQ^{\cdot -}$ in in CTAB solution (●). The dotted line is D of BQ in water. The solid lines are reported self diffusion constant of SDS (up) and CTAB (down) (Ref. 17, 18).

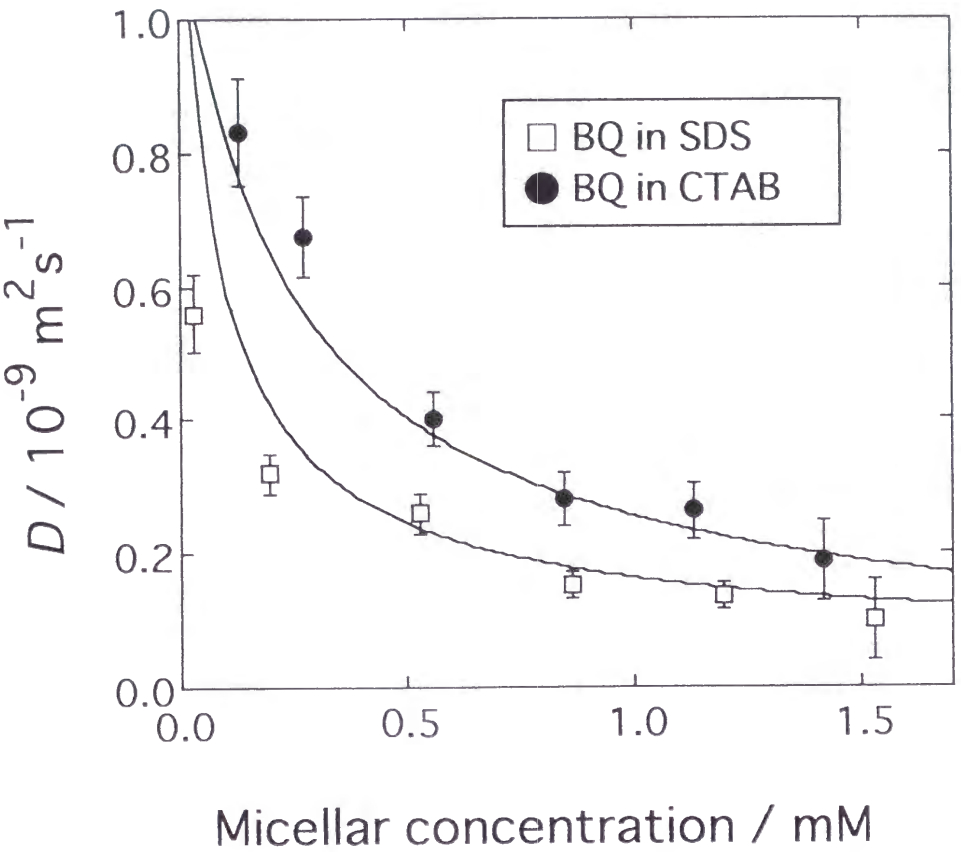

Fig. 7-9 Micellar concentration dependence of D of the parent molecule of BQ in SDS solution (□), in CTAB solution (●). The curved lines are calculation D values by eq. (7-8) with K_s= 1.1X10^4 M^{-1} (SDS), 4.3X10^3 M^{-1} (CTAB).

Chapter 8

SUMMARY

In this thesis, it was demonstrated that the laser induced transient grating (TG) method is a very useful and convenient technique to measure the diffusion coefficients (D) of short-lived radicals accurately. As a result, the following interesting facts were found.

(1) The photo reaction intermediate radicals created by the photoinduced hydrogen abstraction ($HR^{\cdot}$) diffuse much more slowly than the stable parent molecules in organic solvents though the radical and the parent molecule possess nearly the same size and the same shape.

(2) On the other hand, D of the benzyl radical ($BR^{\cdot}$) created by the photodissociation is similar to that of the parent molecule.

(3) The diffusions of the anion radicals created from $HR^{\cdot}$ are similar to those of the electric neutral $HR^{\cdot}$ in organic solution.

(4) The differences in D between $HR^{\cdot}$ and the parent molecules become larger with increasing the viscosities of solvent (η), decreasing the solute radii (r), and the temperature (T).

(5) Diffusion of $HR^{\cdot}$ are anomalously slow in a variety of solvents regardless of the solvent properties, such as the polarity, the dipole moment and the protic (or aprotic) character of the solvent.

(6) The radical diffusion may be influenced by the solvent structure. For example, in aqueous solution, which has a very strong structure by the hydrogen bonding, D of $HR^{\cdot}$ close to that of the parent molecule.

(7) The diffusion of the ion radicals in the micellar solutions are influenced by the electric interaction between the ion radicals and the micellar surface.

Especially, discovery of the anomalous slow diffusion phenomenon of $HR^{\cdot}$ is very important because it points out that D of a transient radical should not be simply substituted by that of a stable

molecule with a similar molecular volume in an analysis of chemical reaction. Such the different behaviors of the similar molecules can not be explained by the simple hydrodynamic model. The anomalous slow diffusion of the radicals suggests the existence of the strong intermolecular interaction between the radicals and the surround molecules. To explain the origin and the mechanism of the anomalous slow diffusion of radicals is very important and interesting.

Possible origin of the slow diffusion of $HR^{\cdot}$ was proposed by Morita and Kato from a study of an ab initio molecular orbital (MO) theory. [1] They found that the intramolecular charge polarization of pyrazinyl radical ($PyH^{\cdot}$) and benzophenone ketyl radical ($BPK^{\cdot}$) are much enhanced than those of the parent molecules by the partial external electric field. On the other hand, such the enhancement was not observed for the benzyl radical. These facts suggest that the enhanced intramolecular charge polarization may be the origin of the anomalous slow diffusion of radicals. Quite recently, Morita and Kato demonstrated the molecular dynamics (MD) simulation which was taken care of the intramolecular charge polarization to represent the anomalous slow diffusion of radicals. [2] They found that the calculated value of D of $PyH^{\cdot}$ are about three times smaller than that of the parent molecule (pyrazine) in methanol. These facts are very consistent to our experimental result (1) and (2). The result (3) can be also explained by the intramolecular charge polarization as follows. According to their analysis, the charge sensitivity depends on the molecular structure. When a charge is attached to the neutral radical ($HR^{\cdot}$) used in this work, the molecular structure could be altered and it becomes similar to that of the parent molecules. Then the enhanced intramolecular charge polarization could diminish. In that case, only the intermolecular interaction by the electric charge (not the charge sensitivity) causes the slow diffusion of the ionic radicals like the stable ion's case. Morita and Kato described that the enhanced intramolecular charge polarization of radicals are induced by the partial external electric field on each site of the solute molecules, which is prepared by the fluctuation of the solvent molecules. However, some questions remain, for example, which properties of the solvent (dipole moment, polarizability, dielectric constant, or relaxation time, etc.) govern the partial external electric field on each site of radicals? How are the solvation structure of radicals? Therefore, it is unclear whether the detail properties of the radical diffusion obtained by the TG experiment [(4); r, η, and T dependence and

(5); solvent property dependence] can be reproduce by the their theory. Such questions would be solved by both the experiment and the calculation in the future. At least now, there is no discrepancy between the result of the TG method and that of the calculation by Morita and Kato, qualititively.

On the other hand, D of the radicals can be reproduced quantitatively by the equation based on the hydrodynamic theory. In the wide range of the solvent viscosity, the solute radius, or the temperature, D of the radicals are very close to D of the Stokes-Einstein equation, while D of the parent molecules are very close to D of the equation of Evans et al. It should be important to consider about that agreement between experimental D and calculated D by the hydrodynamic theory. In spite of this agreement, the origin or mechanism of the anomalous slow diffusion can not be explained by only the hydrodynamic theory. Therefore, both interpretation form the hydrodynamic theory and the statistical theory must be needed for further investigation to understand more closely about the molecular diffusion in solution.

1. A. Morita and S. Kato, J. Am. Chem. Soc., 119, 4021 (1997).

2. A. Morita and S. Kato, J. Phys. Chem., *in press*.

Chapter 9

ACKNOWLEDGMENT

The present thesis is the summary of my studies of Graduate School of Science of Kyoto University during 1992～1997. This work could never come into existence without a lot of support and help of many people. I would first like to thank to express my sincere acknowledge to Professor Noboru Hirota for giving the warm encouragement, continuing kind guidance, and valuable suggestion. I wish to expresses my heartfelt appreciation to Assistant Professor Masahide Terazima for his many help and persevering teaching to me throughout the course of this work. Without his help, this work could not have been accomplished. I am deeply indebted to Dr. Yoshifumi Kimura for giving helpful advice and offering his computer programs for analysis. I wish to thank Dr. A. Morita and Prof. S. Kato for the discussion on the origin of the anomalous slow diffusion of the radicals and showing us the results of the ab initio MO calculation before the publication. I would like to thank Prof. M. Nakahara and Mr. Saito for the measurement of D of the parent molecules by the PGSE method. I would like to thank Prof. T. Tominaga for helpful discussion about comparison of the TG method with the Taylar dispersion method. I am indebted to Dr. K. Ohara for the measurement by the cw and time-resolved EPR method. I wish to thank Prof. J. Yamauchi and Assistant Prof. M. BaBa for their encouragement and helpful advice. I am very grateful to all the past and present members of the laboratory for their useful comment and so kind cooperation. I am very happy to meat them. I would like to appreciate my family for their warm understanding and hearty consideration. Finally, I wish to express my gratitude to my fiancee for devoted support.

December 1997, Kyoto

Koichi Okamoto

Koichi Okamoto

岡本晃一